EMBRACING NOVEL TECHNOLOGIES IN DENTISTRY AND ORTHODONTICS

This volume includes the proceedings of the
Forty-sixth Annual Moyers Symposium and the Forty-fourth
Annual International Conference on Craniofacial Research
March 1-3, 2019
Ann Arbor, Michigan

Editor-in-Chief
Burcu Bayirli

Associate Editors
Hera Kim-Berman
Anthony Puntillo

Copy Editor
Dawn Bielawski

Volume 56
Craniofacial Growth Series

Department of Orthodontics and Pediatric Dentistry
School of Dentistry

The University of Michigan
Ann Arbor, Michigan

Publisher's Cataloguing in Publication Data

Department of Orthodontics and Pediatric Dentistry
Craniofacial Growth Series
Embracing Novel Technologies
In Dentistry and Orthodontics
Volume 56

ISSN 0162 7279
ISBN 0-929921-00-3
ISBN 0-929921-51-8

CONTRIBUTORS

SERCAN AKYALCIN, Associate Professor, Program Director, Department of Orthodontics, Tufts University School of Dental Medicine, Boston, MA.

J. MOODY ALEXANDER, Orthodontist, Private Practice, Arlington, TX.

WICK G. ALEXANDER, Clinical Professor, Department of Orthodontics, School of Dentistry, University of Texas Health Science Center, Houston, TX.

BURCU BAYIRLI, Clinical Associate Professor, Department of Orthodontics, University of Washington, Seattle, WA.

ROLF G. BEHRENTS, Professor of Orthodontics and Director of the Orthodontic Program at the Center for Advanced Dental Education of Saint Louis University, Saint Louis, MO.

CHRISTINA BONEBREAK JACKSON, Orthodontist, Director of Clinical Affairs, SOVE Inc., Chapel Hill, NC.

LUCIA CEVIDANES, Associate Professor, Department of Orthodontics and Pediatric Dentistry, School of Dentistry, University of Michigan, Ann Arbor, MI.

JERYL D. ENGLISH, Professor, Chair, Department of Orthodontics, School of Dentistry, University of Texas Health Science Center, Houston.

DENNIS J. FASBINDER, Clinical Professor, Cariology, Restorative Sciences, and Endodontics, University of Michigan, Ann Arbor, MI.

DANIELA GARIB, Associate Professor, Department of Orthodontics, Bauru Dental School and Hospital for Rehabilitation of Craniofacial Anomalies, University of São Paulo, Bauru, SP, Brazil.

AHMED A. GHONEIMA, Associate Professor and Program Director, Department of Orthodontics, Hamdan Bin Mohammed College of Dental Medicine, Mohammed Bin Rashid University of Medicine and Health Sciences, Dubai, UAE; Adjunct Faculty, Department of Orthodontics and Oral Facial Genetics, Indiana University School of Dentistry, Indianapolis, IN.

PRESTON GREER, Orthodontist, Private Practice, Waco, TX.

GUILHERME JANSON, Professor, Department of Orthodontics, Bauru Dental School, University of São Paulo, Bauru, SP, Brazil.

F. KURTIS KASPER, Associate Professor and Director of Orthodontic Research, The University of Texas Health Science Center at Houston, School of Dentistry, Department of Orthodontics, TX.

HERA KIM-BERMAN, Program Director, Graduate Orthodontics and Clinical Assistant Professor, Department of Orthodontics and Pediatric Dentistry, School of Dentistry, University of Michigan, Ann Arbor, MI.

JOSH KNOWLES, Orthodontist, Private Practice, Temple, TX.

CHING-CHANG KO, Professor and Vig/William Endowed Chair, Division of Orthodontics, The Ohio State University College of Dentistry, Columbus, OH.

JANE JUNGEUN KWON, Research Assistant, Oral and Craniofacial Health Sciences Research, Adams School of Dentistry, University of North Carolina, Chapel Hill, NC.

YAN-TING LEE, Research Assistant, Oral and Craniofacial Health Sciences Research, Adams School of Dentistry, University of North Carolina, Chapel Hill, NC.

CHUNFENG LIAN, Postdoctoral Researcher, Department of Radiology and Biomedical Research Imaging Center, University of North Carolina, Chapel Hill, NC.

CAMILA MASSARO, Doctoral Student, Department of Orthodontics, Bauru Dental School, University of São Paulo, Bauru, SP, Brazil.

JAMES A. MCNAMARA JR., Professor Emeritus, Department of Orthodontics and Pediatric Dentistry, School of Dentistry, University of Michigan, Ann Arbor, MI.

FELICIA MIRANDA, Doctoral Student, Department of Orthodontics, Bauru Dental School, University of São Paulo, Bauru, SP, Brazil.

PRITI MULIMANI, Doctoral Student, Oral Health Sciences, University of Washington, Seattle, WA.

MATTHEW PASTEWAIT, Resident, Division of Craniofacial and Surgical Science, Adams School of Dentistry, University of North Carolina, Chapel Hill, NC.

TRACY E. POPOWICS, Associate Professor, Department of Oral Health Sciences, University of Washington, Seattle, WA.

ANTHONY M. PUNTILLO, Private Practice, Crown Point, IN.

CHRISTOPHER S. RIOLO, Affiliate Associate Professor, Department of Orthodontics, University of Washington, Seattle, WA.

ANTONIO CARLOS RUELLAS, Associate Professor, Department of Orthodontics and Pediatric Dentistry, School of Dentistry, University of Michigan, Ann Arbor, MI; Professor, Department of Orthodontics and Pediatric Dentistry, School of Dentistry, Federal University of Rio de Janeiro, Rio de Janeiro, RJ, Brazil.

DINGGANG SHEN, Professor, Department of Radiology and Biomedical Research Imaging Center, University of North Carolina, Chapel Hill, NC.

STEPHEN J. STERLITZ, Assistant Clinical Professor, Cariology, Restorative Sciences, and Endodontics, University of Michigan, Ann Arbor, MI.

ESTHER SUH, Dental Student, School of Dentistry, University of Michigan, Ann Arbor, MI.

SAMEH M. TALAAT, Assistant Lecturer, Department of Orthodontics, College of Dentistry, Future University in Egypt, Cairo, Egypt; Research Associate, Department of Oral Technology, Bonn University, Germany.

CHIHIRO TANIKAWA, Associate Professor, Department of Orthodontics and Dentofacial Orthopedics, Graduate School of Dentistry, Global Center for Medical Engineering and Informatics, Osaka University, Japan.

LI WANG, Assistant Professor, Department of Radiology and Biomedical Research Imaging Center, University of North Carolina, Chapel Hill, NC.

TAI-HSIEN WU, Postdoctoral Research Associate, Division of Orthodontics, Ohio State University College of Dentistry, OH.

MARILIA SAYAKO YATABE, Clinical Assistant Professor, Department of Orthodontics and Pediatric Dentistry, School of Dentistry, University of Michigan, Ann Arbor, MI.

PREFACE

It is an exciting time for our profession. The availability of digital advances is improving the personalized care we provide to our patients. An orthodontist is not dependent on a separate entity to produce aligners anymore. We can stage and produce aligners on our computers in our offices. Quality of research will increase as these new technologies enable us to be more precise in our findings as well as open new horizons to explore and investigate. Virtual and augmented reality will change how we teach our students and educate our patients. As orthodontists and critical thinkers, we have to persevere to learn the new technologies in dentistry and orthodontics. Most importantly, we have to find the best way to incorporate these new methods into our practices, research, and teaching. The collection of articles in this volume is a great start, but it is up to us to be life-long learners to keep up with these changes in our specialty never forgetting that the sole beneficiaries of these advances should be our patients.

The topic of novel technologies in dentistry and orthodontics was addressed during the *46th Annual Moyers Symposium* and the *44rd Annual International Conference on Craniofacial Research (Presymposium)* held at the University of Michigan on Friday, March 1, 2019 through Sunday, March 3, 2019. This meeting was sponsored by the Department of Orthodontics and Pediatric Dentistry, School of Dentistry, University of Michigan. The proceeding of this annual meeting is memorialized in the 56th volume of the Craniofacial Growth Series and contains reports, original research and review articles from internationally renowned experts, scientists and clinicians. The 56th volume and the entire Craniofacial Growth Series is made available to the public through the University of Michigan Deep Blue Repository https://deepblue.lib.umich.edu/handle/2027.42/146667 .

As in previous years, the *Symposium* honored the late Dr. Robert Moyers, Professor Emeritus of Dentistry and Fellow Emeritus and Founding Director of the Center for Human Growth and Development at the University of Michigan.

We thank Michelle Jones of the Office of Continuing Dental Education for coordinating and managing the *Presymposium* and the *Symposium*. We also thank Dawn Bielawski for her invaluable work as Copy Editor and Jade Cook for verifying all citations and references.

We acknowledge Dr. Nan Hatch, the Chair of the Department of Orthodontics and Pediatric Dentistry for her support of the meeting and this publication.

Finally, we thank the speakers and participants of the *Symposium* and the *Presymposium* and appreciate their attendance and support throughout the 46 years of history of the meeting.

Burcu Bayirli
Editor-in-Chief

Hera Kim-Berman
University Liaison
January, 2020

TABLE OF CONTENTS

WHAT IS "BIG DATA" AND WHY IS IT IMPORTANT TO THE PRACTICE OF ORTHODONTICS?

Anthony M. Puntillo

ABSTRACT

Electronic medical data is said to account for 30% of the world's data production. The control and analysis of this "Big Data" will dramatically shape the future of health care. Compared to our medical counterparts, orthodontists have been slow to recognize the intrinsic value of the digital data we are collecting in our practices. To date there have been relatively few instances where orthodontic researchers or corporate entities have utilized the analysis of electronic patient records for the advancement of patient outcomes and experiences. The ability to collect and analyze large quantities of complex information using artificial intelligence (AI) is essential to the future of our profession. We must recognize the significance of Big Data and seek ways to use it for the betterment of our patients' care.

KEY WORDS: Big Data; Orthodontics; Electronic Health Records; Artificial Intelligence

INTRODUCTION

"Big Data" is defined as an accumulation of data that is too large and complex for processing by traditional database management tools [1]. Ubiquitous internet connectivity is quickly driving the electronic collection of large and extremely complex volumes of information associated with nearly every aspect of our lives. The analysis of this pooled data allows major corporations such as Facebook, Amazon, Google, Twitter, and many others to know and understand everything from our travel, sleep, and purchasing patterns to our political inclinations. Data creation and collection in today's society is not simply limited to finance and consumer related functions. In fact, the National Institutes of Health (NIH) estimates that by 2025 genomic information alone will "equal or exceed" the quantity of data produced by YouTube and Twitter [2]. Furthermore, medical data is said to be accumulating on the order of 750 quadrillion bytes every day – or some 30% of the world's data production [3]. The mining and analysis of vast quantities of digital medical data will dramatically shape the future of healthcare. If the specialty of orthodontics is to remain based in science, our profession needs to harness the power of the data we are accumulating in our practices to improve our clinical decision making and deliver more personalized orthodontic care to our patients.

The collection of large, diverse quantities of patient data holds great promise for improved future healthcare outcomes and experiences. However, Big Data is not without its controversies or challenges. In April 2019, Facebook announced that it is expecting to be fined by the Federal Trade Commission (FTC) a record $3 billion to $5 billion. The penalty stems from claims that the company has not fulfilled promises to protect its users' privacy [4]. Hospitals, teaching institutions, and healthcare providers have amassed multi-million-dollar HIPAA fines. In fact, recently a suit was filed against the University of Chicago Hospital by a former patient of the University and Google for what is alleged to be improper sharing of patients'

protected health data [5]. In late 2018, Apple CEO Tim Cook told the U.S. Congress that, "Consumers shouldn't have to tolerate another year of companies irresponsibly amassing huge user profiles, data breaches that seem out of control and the vanishing ability to control our own digital lives" [6]. It may be virtually impossible in today's digital world to completely secure all data; however, security measures must be at the forefront of any data collection and all efforts to completely "scrub" individual identifying information should be implemented. While developing technologies to benefit patients, healthcare providers have an obligation to prioritize the protection of our patients' private information.

BACKGROUND

The practice of medicine has traditionally centered around the collection of data; however, that information was historically gathered and stored in an analog format, making it extremely difficult and time intensive to analyze. In 2009, the United States Congress passed into law the American Recovery and Reinvestment Act (ARRA) [7]. A portion of that law included the Health Information and Technology for Economic and Clinical Health Act (HITECH). HITECH's goal was to improve the manner in which healthcare was delivered to patients by investing in progressive health information systems. By 2016, HITECH mandated the full implementation of Electronic Health Records or Electronic Medical Records (EHRs/EMRs) for healthcare providers participating in Medicare and Medicaid. It is important to recognize that EHRs are not simply limited to provider notes, but also include lab tests, medical imaging, genetic profiles, prescriptions, insurance claims, and data generated from personal monitoring devices. To assist hospitals and doctors in this digital transformation, the government allocated nineteen billion dollars of stimulus money for conversion subsidies. The initial stages of health information digitization are now under way and we are just beginning to realize some of the expected benefits. Those benefits include increased transparencies and efficiencies, empowered patients, more robust research data, and better clinical outcomes. It is expected that these advances will ultimately lead to better overall population health outcomes.

While government stimulated the digitization of medical data collection, the true value of that collected information can only be understood through scientific analysis. Because the volume of data is so large and complex it is impossible to analyze without the assistance of AI. The NIH has recognized that Big Data analytics offers the potential for significant scientific advancements. Consequently, the NIH announced in February (2019) that it was recruiting for a new position of "Chief Data Science Strategist." The NIH noted the importance of this new position and indicated that the strategist would have a significant impact on the direction of biomedical research over the next decade [2].

Government is not alone in its recognition of the value contained within digital healthcare data. Corporate and healthcare entities, including all of the largest technology companies, also appreciate the importance of fully participating in the analytics of healthcare data. In 2014, the American Academy of Ophthalmology invested in the creation and maintenance of the nation's first electronic health record-based comprehensive eye disease and condition registry, IRIS®. By 2019, the IRIS® registry had recorded more than 230 million patient visits from 53 million patients. To date, the estimated total avoided compliance penalties to registry participants is more than $186 million [8]. Additionally, in January of 2018, JPMorgan Chase and Berkshire Hathaway announced a joint venture with Amazon (Haven) that is aimed at using data to reduce health care costs and improve outcomes for their employees [9]. Later that same year (November 2018), Amazon launched a new service called Amazon Comprehend Medical [10]. This service processes natural language and uses AI to extract relevant medical information from unstructured text such as medical notes, prescriptions, and radiology reports. Tech behemoth Alphabet/Google has also joined the healthcare data rush through its life sciences arm, Verily. Verily is focused on developing tools to collect and organize health data. One of their current projects involves

tracking biometric information from 10,000 volunteers with the ultimate goal of establishing a baseline of human health [11]. The future of IBM is significantly linked to its Watson AI computer intelligence. It has used this computing platform to create Watson Health. Watson Health uses data, analytics and AI to help solve pressing medical challenges, including the treatment of cancers [12]. These technology companies, and others that have not been traditionally associated with the delivery of healthcare, will shape the future of medicine.

The first orthodontic Big Data studies might actually be attributed to the works of Drs. T. Wingate Todd and B. Holly Broadbent Sr. Almost a century ahead of Verily's modern day efforts, the Bolton-Brush Growth Studies were initiated in Cleveland to establish a baseline for normal human growth and development [13]. Their studies, which originated in the 1920s, collected more than 200,000 serial radiographs on more than 6,000 subjects and sought to determine a baseline for the normal human growth and development process. Their radiographic records were supplemented with handwritten notes on the patients' nutritional, medical, and dental health status. As the data and subsequent studies from the projects predated the digital revolution by decades, the manual work was labor intensive and took years to complete. Nevertheless, the insights gained from their efforts continue to be of immeasurable value to the profession of orthodontics and our patients.

The potential for digital Big Data to be efficiently mined and provide answers to medical questions is immense. In fact, for the orthodontic specialty, the analysis of electronic health records has already provided valuable clarity regarding the poor correlation between premolar extractions and obstructive sleep apnea. Larsen et al. retrospectively examined thousands of electronic medical and dental records for patients participating in a Minnesota health insurance plan [14]. Half of the subjects (n=2,792) in their study had one missing premolar in each quadrant. The other half of the sample (n=2,792) had no missing premolars. The groups were paired in a 1:1 match on age range, gender, and body mass index (BMI) range. They ultimately found that the diagnosis of obstructive sleep apnea, confirmed by polysomnography, was nearly identical (p=0.16) between the groups. Subsequently, their study of more than 5,000 patients concluded that the absence of four premolars, one from each quadrant, was not a significant factor in the cause of obstructive sleep apnea.

DISCUSSION

Individual orthodontic practices began digitally collecting clinical records in the 1990s. Initially, the conversion from analog to digital records in orthodontics began with the capturing of two-dimensional information such as treatment notes, photographs, and radiographs. Eventually, practices transitioned to three-dimensional data such as dental models and cone beam computed tomographic (CBCT) radiographs. Most of the early electronic records, however, were stored in individual practice silos and lacked the standardization necessary for the records to be of much scientific value.

The era of orthodontic Big Data in a digital world largely began in 1999. It was at this time that Align Technology began marketing digitally designed plastic tooth aligners to orthodontists. The creation of their product required a digital three-dimensional dental model. Initially, these models were generated from traditional analog intraoral impressions. The impressions were shipped to Align and, then, digitally scanned to convert the impression image into an electronic format. Additionally, digital photographs and radiographs were collected by Align for these patients. Thus began the pooling of large quantities of electronic orthodontic treatment records. In 2011, Align moved further to completely digitize the model creation process by acquiring Cadent, a company which had developed one of the first intra-oral three-dimensional optical scanners [15]. According to the company's reports, over the last two decades, Align has generated plastic aligners for more than six million patients [16]. The electronic treatment data from all of those patients has and continues to be collected and analyzed by the company. Align has gained

valuable insights from the clinical data that orthodontists have shared with them. By combining the principles of engineering with their analysis of the collected electronic records, Align has been able to drive multiple product improvements, thereby, creating more predictable outcomes and increased treatment efficiencies. Ultimately, the data from the shared Invisalign user experience has helped to produce a better patient experience and increased orthodontic aligner usage.

Align Technology may have been the first to start collecting orthodontic patient data, but it is no longer alone. Gaidge (2011) is an orthodontic management tool that uses the digital "Cloud" to automatically collect large quantities of practice data daily from individual orthodontic practices [17]. The Gaidge collection process works seamlessly with several practice management software systems. They currently have more than 1,000 orthodontists and more than 1,500 practice locations sharing data within the system. In 2017 alone, the Gaidge system tracked 400,000 new patient exams and 280,000 orthodontic treatment starts. Once collected, the individual practice performance information can be digitally analyzed through the Gaidge platform to provide users with useful practice management statistics. Their platform, which is accessed over the internet, allows practitioners to gain valuable insights into their practice operations. The ability to compare practice metrics such as average treatment times, average number of appointments, appliance usage, and many other data points to regional and national peer averages can help to drive practice improvements. The Gaidge platform continues to evolve and has the potential, in the future, to eventually include the incorporation of more clinic-based data (i.e. malocclusion type, specific appliance type, etc.). Efficiently managed practices will ultimately lead to an enhanced overall orthodontic patient experience.

Orthoscience is another corporate newcomer to the collection of orthodontic Big Data companies [18]. Founded by Dr. Sean Carlson, Orthoscience provides an online digital platform for the storage and sharing of electronic orthodontic treatment data, including 3D models and radiographs. Once the treatment records are manually uploaded to the system, users have the ability to view, analyze, and compare treatment time-points. Comprehensive patient treatment records (CaseCards™) can be shared and used as valuable teaching tools. The system aims to create a large database of highly documented case reports that will improve the orthodontic educational process. Currently, however, the system is in limited release. Furthermore, the case selection bias associated with the required manual upload of the records may ultimately limit the platform's scientific strength.

Finally, it is important to also recognize that electronic orthodontic treatment data is not limited to the information doctors record and collect in our offices. Just as in medicine, personal monitoring devices, specifically those associated with smart phone apps, have the ability to collect and compare orthodontic treatment data. Most people are familiar with Google Maps and Waze. These apps combine Global Positioning System (GPS) data and a shared user experience to help us navigate to our destinations in the most efficient manner (i.e. shortest route while avoiding traffic slowdowns). Similarly, orthodontists and patients can now use a dental digital tracking system, Dental Monitoring (2015) [19]. This system allows patients to use smart phone cameras to capture intra-oral photographs at different time points during the course of their orthodontic care. AI is then utilized to assess the actual dental position compared to the planned digital movements at a specific timepoint. This tracking information can then be shared through the app with the treating doctor and can be used to direct mid-treatment course adjustments, thus assuring the most efficient individualized path of care for each patient.

CONCLUSIONS

Without the government subsidies and a minimal threat of lost Medicare and Medicaid reimbursements, orthodontists have been slower in our conversion to EHRs than our medical

counterparts. This has delayed our recognition of the immense value and importance of pooled electronic case records, Big Data. The majority of scientific research published in orthodontic journals today is performed on sample sizes of less than 1,000 individuals. Smaller sample sizes ultimately weaken the validity of the research and can lead to contradictory published conclusions. The Larsen et al. study clearly demonstrates that large data bases can provide clarity to important orthodontic treatment questions [14]. We must join our medical counterparts in completely transitioning to EHRs and understanding that the electronic treatment data we are collecting is essential to the future advancement of our profession. Government, corporate, and health care entities alike have recognized the value of this data and it is time we do so as well.

REFERENCES

1. Merriam-Webster. https://www.merriam-webster.com/dictionary/big%20data. Accessed January 2019.

2. Roussi, A. The NIH makes a big push for big data. Healthcare Analytics News 2018. (https://www.idigitalhealth.com/news/the-nih-makes-a-big-push-for-big-data). Accessed January 2019.

3. Fry E, Mukherjee S. Tech's Next Big Wave: Big Data Meets Biology. Fortune 2018. (https://fortune.com/2018/03/19/big-data-digital-health-tech/). Accessed December 2018.

4. Issac M, Kang C. Facebook expects to be fined up to $5 Billion by F.T.C. over privacy Issues. The New York Times 2019. 24 April 2019.

5. Wakabayashi D. Google and the University of Chicago are sued over data sharing. The New York Times 2019. https://www.nytimes.com/2019/04/24/technology/facebook-ftc-fine-privacy.html. Accessed June 2019.

6. Cohen, JK. Apple CEO to Congress: it is time to step in, protect our privacy. https://www.beckershospitalreview.com/cybersecurity/apple-ceo-to-congress-it-s-time-to-step-in-protect-our-privacy.html. Becker's Hospital Review 2019. Accessed June 2019.

7. United States of America Congress. American Recovery and Reinvestment Act of 2009. https://www.congress.gov/bill/111th-congress/house-bill/1/text. Accessed June 2019.

8. Mid-Year Forum 2019 Report. American Academy of Ophthamology 2019. https://www.aao.org/about/governance/academy-blog/post/mid-year-forum-2019-report. Accessed June 2019.

9. Business Wire. Amazon, Berkshire Hathaway, and JPMorgan Chase & Co. to partner on U.S. employee health care [Press release]. 30 January 2018.

10. https://www.havenhealthcare.com/media/abj-partner-health-care. Accessed June 2019.

11. Amazon Comprehend Medical. Amazon Web Services 2019. https://aws.amazon.com/comprehend/medical/. Accessed June 2019.

12. Verily. Introducing Verily. YouTube 2015. https://www.youtube.com/watch?v=Lyv0_GIGSbY. Accessed June 2019.

13. Watson Health: Get the facts. IBM (2019). https://www.ibm.com/blogs/watson-health/watson-health-get-facts/. Accessed July 2019.

14. Behrents RG, Broadbent HB Jr. A chronological account of the Bolton-Brush Growth Studies: In search of truth of the greater good of man. Case Western Reserve University 1984. https://case.edu/dental/sites/case.edu.dental/files/2018-04/Chronological_Account_BoltonBrush.pdf. Accessed February 2019.

15. Larsen AJ, Rindal DB, Hatch JP, Kane S, Asche SE, Carvalho C, Rugh J. Evidence supports no relationship between sleep apnea and premolar extraction: an electronic records review. *J Clin Sleep Med* 2015;12(11):1443-1448.

16. Globe Newswire. Align Technology [Press release]. 29 March 2011. http://investor.aligntech.com/news-releases/news-release-details/align-technology-acquire-intra-oral-scanning-leader-cadent-190. Accessed June 2019.

17. Globe Newswire. Align Technology [Press release]. 17 December 2018. http://investor.aligntech.com/news-releases/news-release-details/align-technology-reaches-6-millionth-invisalignr-patient. Accessed June 2019.

18. Lund, B. You Should Know: Gaidge Practice Metrics. Orthotown 2013: April.

19. Orthoscience website. https://www.orthoscience.com. Accessed June 2019.

20. Moylan HB, Carrico CK, Lindauer, SJ, Tüfekçi E. Accuracy of a smartphone-based orthodontic treatment-monitoring application: A pilot study. *Angle Orthod* 2019;89(5):727-733.

3D PRINTING APPLICATIONS IN CLEAR ALIGNER FABRICATION

F. Kurtis Kasper

ABSTRACT

Advances in digital imaging and 3D printing technologies have enabled orthodontic tooth movement with a series of positioning appliances in the form of clear aligner therapy. Current methods for clear aligner fabrication apply 3D printed models to support thermoforming of the appliances, and various factors can affect the efficiency of the workflow and the potential clinical utility of the aligners. Accordingly, effective application of 3D printing in clear aligner fabrication depends upon appropriate consideration of these factors in the context of the requirements of clear aligner therapy and the operational demands of the practice. This article will provide an overview of the principal components of the workflow for clear aligner fabrication, review considerations involved in the 3D printing of models to support clear aligner fabrication, and discuss emerging applications of 3D printing in clear aligner therapy.

KEY WORDS: Three-dimensional Printing, Orthodontics, Dental Models, Clear Aligner Therapy, Removable Orthodontic Appliances

INTRODUCTION

Clear aligner therapy involves a series of minor tooth movements achieved through application of a corresponding series of individual aligners, which are changed in sequence over the duration of treatment. Interestingly, the concept of applying a series of positioners to accomplish major tooth movements through small sequential movements was first proposed in 1945 by Dr. Harold Kesling, who concluded “at present, this type of treatment does not seem to be practical…its practical application might be developed in the future [1].” Indeed, Kesling’s prediction was realized with the release of the Invisalign® system by Align Technology, Inc. in 1999, which leverages digital scanning, computer-aided design, and additive manufacturing technology to produce a series of aligners from a single impression [2, 3]. The Invisalign® system and comparable clear aligner systems generally involve digital manipulation of a digital impression of the dentition of the patient to develop a series of small sequential tooth movements from the initial condition to the desired final outcome. Physical models of the arches corresponding with each step then are fabricated via 3D printing (see Figure 1). The series of physical models support the fabrication of a corresponding series of clear aligners through a thermoforming process and subsequent trimming. Given the prominent role of 3D printing in the current workflow for clear aligner production, this article will review the basic components of the workflow for aligner fabrication, highlight considerations in the 3D printing of models to support fabrication of clear aligners, and offer discussion of challenges and future directions in 3D printing applications in clear aligner fabrication.

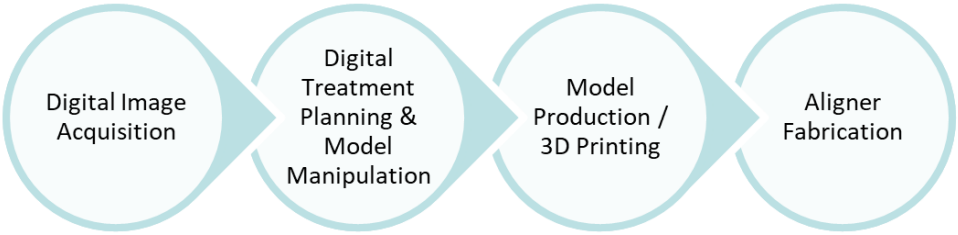

Figure 1. Workflow for clear aligner fabrication harnessing digital and 3D printing technologies.

TRADITIONAL WORKFLOW FOR CLEAR ALIGNER FABRICATION

Digital Image Acquisition

The modern workflow for clear aligner fabrication begins with acquisition of a digital representation of the dental anatomy of the patient, using either a direct or an indirect approach. Indirect workflows involve application of traditional impression materials, such as alginate or vinyl polysiloxane, with standard techniques to register the patient anatomy. Plaster models cast from the impressions enable acquisition of a digital representation of the model surfaces through use of a variety of scanning technologies, which currently include optical and computed tomography scanners. In some cases, scanners and associated software allow generation of a digital model directly from a scan of the impression, bypassing the need to cast a plaster model for scanning. Alternatively, intraoral scanning devices facilitate digital registration of the patient anatomy directly without taking a physical impression. Each pathway culminates in the generation of a digital representation of the initial presentation of the patient dentition that supports planning orthodontic tooth movement with clear aligners.

Treatment Planning and Model Manipulation

Various software platforms allow a clinician to plan a series of sequential tooth movements from the initial positions to desired final positions in the treatment of the patient. An early step in the digital planning involves segmentation to isolate the crown of each tooth on the digital model. Some software platforms support importation and overlay of data from computed tomography scans, if available, on the intraoral scan data to provide visualization of the root structures when planning treatment. The clinician then manipulates the positions of the teeth to desired positions and plans sequential movements of the teeth within reasonable limits for each stage. Some tooth movements warrant the use of auxiliaries such as attachments, and many software platforms support the design and application of attachments in the digital set-up. The digital workflow results in the development of a series of virtual models with teeth in the planned positions associated with each stage, and the software exports files corresponding to the arches at each virtually planned stage to drive model production (usually in a standard tessellation language or .stl file format).

Model Production

The virtually planned tooth movements presently require generation of tangible models to support fabrication of clear aligner appliances. A variety of computer-aided manufacturing technologies

exists in the orthodontic space for production of physical orthodontic models from digital design files and generally involves additive or subtractive manufacturing approaches. Subtractive manufacturing technologies, such as milling, apply computer-controlled tool bits to remove material selectively from a starting block of material to realize the desired model. Alternatively, additive manufacturing techniques, such as 3D printing, build a part layer-by-layer from a precursor material. While orthodontic models produced by milling and 3D printing support thermoforming of clear aligners for clinical application [4], 3D printing presently stands as the dominant technology for orthodontic model production in clear aligner therapy, due in part to the decreasing cost of 3D printers.

Aligner Fabrication

The final phase in clear aligner fabrication involves thermoforming aligners on the physical copies of the digital models developed for each stage during the virtual planning. Some clinicians prefer to outsource model production and/or aligner fabrication to companies or orthodontic laboratories, while others engage in aligner fabrication in-house. Each path applies a thermoforming process to conform a polymeric film selected from a variety of available materials and thicknesses on the contours of each physical model to generate each aligner. Once trimmed and polished, the clinician delivers the aligners to the patient in the appropriate sequence. As production of orthodontic models by 3D printing typically involves non-recyclable materials now, production lines generally destroy or discard the models used to support aligner fabrication. In some cases, clinicians deliver the final-stage models to the patient for keeping, in the event they are needed in the future to make replacement retainers. While increasing numbers of orthodontists embrace 3D printing technologies in their offices, various factors and preferences influence when in-house model production may be appropriate. For example, some orthodontists may fabricate aligners for all of their clear aligner cases in-house, while others might prefer to apply in-house production in limited movement cases that involve a lesser number of stages. In all cases, a range of considerations in the 3D printing process influence the efficiency of model production and the potential clinical utility of the models produced.

3D PRINTING CONSIDERATIONS IN CLEAR ALIGNER FABRICATION

3D Printing Technologies

From the many 3D printing technologies available for manufacturing applications, the dominant technologies currently marketed in the orthodontic space for model production include stereolithograpy (SLA), digital light processing (DLP), PolyJet photopolymerization (PJP), and fused deposition modeling (FDM). While the technologies differ in terms of the details underlying part production, each ultimately builds a part layer-by-layer from a precursor material. Accordingly, the 3D model must be prepared for printing using software that slices the model into the various layers to be printed in sequence to build the whole part. The fidelity of the printed model depends on each step of the workflow, from acquisition of the digital model of the patient anatomy to post-print processing of the printed part. The following sections will focus on considerations associated with the 3D printing phase of the workflow in clear aligner production and the potential impacts on workflow efficiency and clinical utility of the fabricated appliances.

Model Design and Preparation for Printing

The preparation of a digital model for 3D printing involves a number of factors that may influence the efficiency of the workflow and the dimensional fidelity of the printed part. As previously mentioned, the model must be processed into a series of slices to drive the building of the part layer-by-layer. The

slice thicknesses must correspond with print layer heights supported by the 3D printing technology to be used, which can range from approximately 0.016 mm for PJP printers to 0.35 mm for FDM printers [5, 6]. The layer heights can be selected from options available to the user with some printing technologies, and the options available may depend on the particular material to be printed. Print layer height selection influences the temporal efficiency of the printing workflow, as decreasing the layer height increases the number of layers and time required to print a given model [5]. The print layer height also affects the surface quality of the printed model, with smaller layer heights resulting in smoother model surfaces (see Figure 2) [4, 5, 7]. Interestingly, the smaller layer heights might not always translate to greater dimensional fidelity of the printed models, and the effect of print layer height on model accuracy can differ across printers [5, 7, 8]. Accordingly, selection of appropriate print layer heights requires consideration of several factors, including the accuracy and surface smoothness requirements of the model for clear aligner fabrication and the workflow efficiency requirements of the practice.

Figure 2. Palatal views of the incisors of 3D printed models showing increasing surface smoothness with decreasing layer heights of 0.100 mm, 0.050 mm, and 0.025 mm.

Although 3D printers presently require selection of a single print layer height, future development of printers capable of supporting multiple layer heights within a given print may enable application of adaptive slicing approaches, in which larger layer heights are applied to less important areas, such as the model base, and smaller layer heights are applied to the critical areas of the model, such as the dentition, to balance efficiency and dimensional fidelity [4].

Preparation of digital model files for printing also requires selection of an appropriate part orientation with respect to the printer platform and design of supporting structures, if needed, to enable realization of the virtual design. As 3D printers build parts layer-by-layer, the part should be oriented such that regions of each layer connect with the previously printed layer, otherwise unsupported regions may fail to incorporate into the model [9]. Printer-specific software packages typically facilitate selection of a print orientation and incorporation of supporting structures, if needed, in appropriate regions of the part to assist printing. One should avoid inclusion of supporting structures in contact with critical regions of the model, such as the dentition, as removal of the supports may impart dimensional deviations in these regions. Incorporation of supporting structures requires additional material in production of the model and may require additional time in the printing and processing of the model. However, some print orientations support production of a model of an appropriate design without addition of supporting structures. For example, orthodontic models may be oriented with the model base in contact with the build platform of the printer, such that the occlusal surfaces of the teeth are approximately parallel with the build platform (i.e., “flat orientation”), or oriented with the occlusal surfaces approximately perpendicular to the platform and the posterior region of the model in contact with the platform (i.e., “perpendicular orientation”) (see Figure 3) [9]. Depending upon the model design and the anatomy

present on the particular model, the flat and perpendicular orientations commonly support printing of models without inclusion of supporting structures, as the model supports itself.

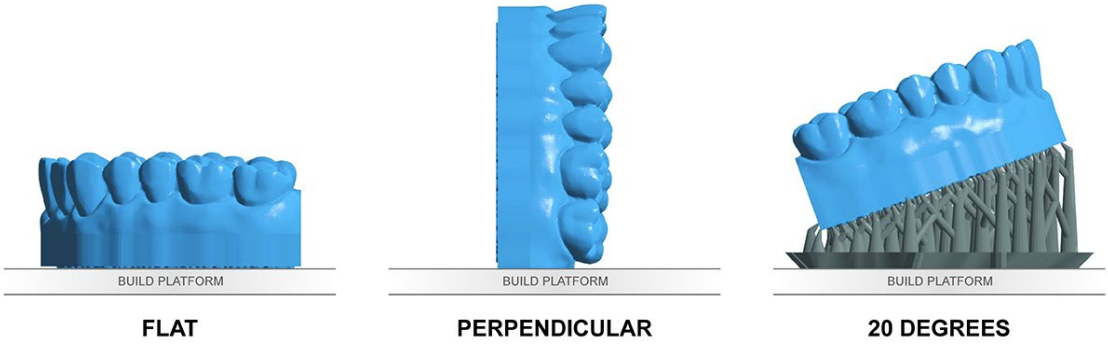

Figure 3. Examples of model orientations with respect to the build platform for 3D printing, with an occlusal plane approximately parallel with the build platform ("flat"), an occlusal plane approximately perpendicular to the build platform ("perpendicular"), and offset at a 20-degree angle with inclusion of supporting structures to facilitate printing ("20 degrees"). Reprinted from [9] with permission from JCO, Inc.

A recent study demonstrated that the orientation of the model during printing can affect the dimensional accuracy of the model, with perpendicularly oriented models under the conditions investigated demonstrating underbuilding of the facial surfaces of anterior dentition and underbuilding of distal surfaces of the most posterior dentition, which might be associated with print error propagation and unsupported model regions, respectively [9]. The selected model orientation affects the efficiency of the printing workflow, as flat models will require less print layers than the same models with a perpendicular orientation (and in turn less time), but more models can be accommodated on a build platform at a time with a perpendicular orientation relative to a flat orientation. Print layout describes the arrangement of models on the build platform for printing, and the layout can affect the efficiency of the workflow with some printing technologies. For example, SLA and PJP printers involve movement of physical parts and/or scanning of a polymerization-initiating light source in the printing of each layer. The travel time of the moving parts across the platform often depends upon the layout of the parts for the print job, which can affect the total time required for printing.

Aspects of the design of the model can also be tuned to influence the efficiency of the 3D printing workflow. For instance, the base of the model to be used in clear aligner fabrication can be trimmed digitally to a "horseshoe" shape corresponding with the alveolar arch to reduce the amount of material and time required to print the model [10-12]. Although the efficiency of the printing workflow may be increased with the use of a horseshoe base design, transverse dimensional deviations at the posterior region of such models were reported in some cases, which may be reduced through incorporation of a transverse bar for stability in the region [11, 13]. Hollowing of the interior of models presents an additional design approach to reduce the material and time required for model production. Specifically, the model can be manipulated digitally to produce a hollow shell-like structure, minimizing the material in the interior of the model while maintaining the shape and dimensions of the model surface (see Figure 4). However, the effect of hollowing on the dimensional accuracy of the printed models remains to be investigated [10]. Although hollowing can increase operational efficiency in printing models, it is essential that the printed model present sufficient structural stability to support fabrication of a clear aligner via

thermoforming without deformation that might have an impact on the fit and clinical utility of the aligner [14].

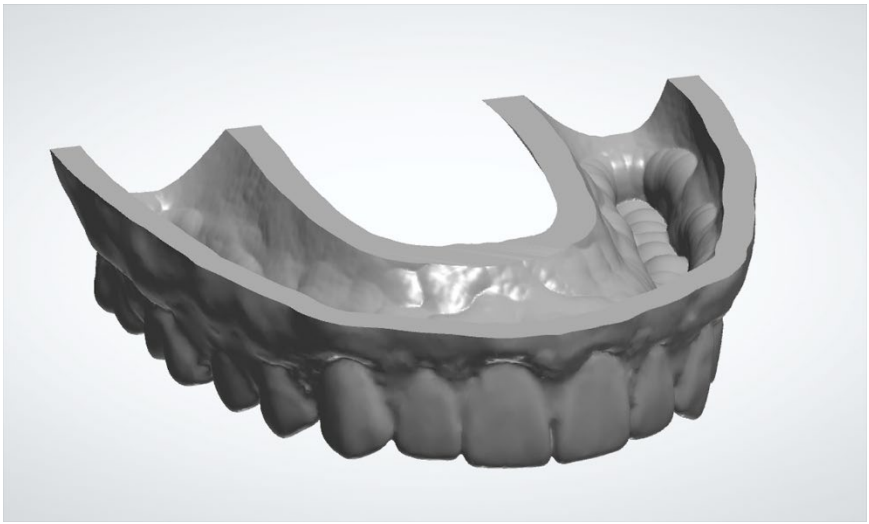

Figure 4. Digital orthodontic model illustrating “hollowing” or digital removal of structure from the base of the model prior to 3D printing to increase workflow efficiency.

The material applied in 3D printed model production must also be considered in the workflow for clear aligner fabrication. Currently, orthodontic model production by 3D printing generally involves acrylic resins, although alterative materials such as ceramics and composites have been used [15-17]. The optimal printing parameters for a given material typically require the use of specific printers capable of achieving those conditions, so the material selected must be compatible with the format, make, and model of the 3D printer to be used. Otherwise, the anticipated physical properties, such as mechanical strength, of the printed material might not be achieved. Clear aligner fabrication requires that the 3D printed models present sufficient mechanical strength, structural integrity, and thermal stability to support thermoforming of the aligner without deforming beyond clinically acceptable tolerances. Additionally, potential effects of the materials themselves on patients and personnel should be considered, as residual resin monomer might present toxicity to patients if transferred with the appliance, and patients and personnel may develop allergies to acrylics with exposure [18, 19].

Post-print Processing

Workflows for 3D printed model production typically involve post-print processing steps before application of the model in thermoforming of clear aligners. For instance, models printed using SLA and DLP printers generally require washing in a solvent such as isopropyl alcohol to remove excess resin followed by drying in air to allow residual solvent to evaporate from the model surface. The parts then generally undergo post-print exposure to ultraviolet light and/or heat under controlled conditions to facilitate continued polymerization of the resin, which may be necessary to achieve optimal physical properties of the model. Post-print processing also may be warranted for some ceramic-based models, as post-print processing in the form of heat exposure was found to improve significantly the compressive mechanical properties of 3D printed calcium sulfate-based models [16]. The post-print processing of 3D printed models involves additional materials, personnel time, and the associated costs, which collectively affect the operational efficiency of the workflow and should be considered. Post-print processing may

also affect the dimensional accuracy of the printed model under certain conditions. Some studies suggest that polymerization shrinkage associated with the 3D printing and post-print curing of resin models can contribute to negative deviation of the model relative to the digital design file [10, 11, 13, 20, 21]. Additionally, insufficient removal of residual resin prior to post-print curing may result in incorporation of excess material into the part, especially in areas where it may tend to settle, such as central grooves, gingival margins, and interproximal spaces, which may manifest as a positive deviation of the part in these regions [7]. Similarly, insufficient evaporation of solvent from the models prior to post-print curing could result in solvent swelling artifacts at the model surface.

Dimensional Accuracy of 3D Printed Models

Clear aligner fabrication demands suitable dimensional accuracy of the 3D printed orthodontic model on which the aligner is thermoformed to enable appropriate fit and clinical utility. The dimensional fidelity of 3D printed models has been a popular subject of investigation in the literature in recent years, with many studies concluding that 3D printed models are acceptable alternatives to plaster models for orthodontic applications [6, 10, 12, 15, 22-24]. However, some studies suggest that 3D printed models are not acceptable under the conditions investigated [13, 17, 21, 25]. The differences in the findings among the articles tend to reflect differences in the conditions and workflows applied in the studies. Indeed, comparison of the results from various studies requires consideration of the workflow applied and the potential contributions of error within the individual steps to the overall error observed [20].

Recognizing the influence of workflow on model production, some studies have investigated the dimensional fidelity of 3D printed models derived from different workflows. One study assessed the accuracy and reproducibility of linear measures taken on typodonts, plaster duplicates made from alginate impressions of the typodonts, digital models obtained from a laboratory scan of the typodonts, and 3D printed duplicates [24]. The authors reported no statistically significant differences in the measures between the various models, indicating an equivalence of the plaster, digital, and 3D printed models. 3D printed models produced from intraoral scans of 28 volunteers were compared to plaster models derived from alginate impressions of the same volunteers in another study [13]. The study found statistically significantly smaller intermolar distances on the 3D printed models, which the authors attributed to potential polymerization shrinkage of the horseshoe shaped model design applied. The study concluded that the 3D printed models were not acceptable for diagnosis and treatment planning, and that the dimensional differences likely would have negative implications for fabrication of clear aligners and retainers. A different study compared linear transverse measurements between plaster models from alginate impressions and 3D printed models from intraoral scans of 40 patients, reporting statistically significant differences between plaster and 3D printed models [26]. While the 3D printed models were found to be smaller than the plaster models in the intercanine and intermolar measures, the authors deemed the differences to not be clinically significant. Wesemann et al. also investigated indirect and direct digitalization workflows for 3D printed model production, and recommended a traditional workflow involving conventional impressions, cast plaster models, and desktop scans of the plaster to generate digital models for orthodontic applications [27]. However, the authors suggested that intraoral scanners are acceptable for use in workflows for manufacturing orthodontic appliances.

Just as the method with which a digital model is obtained can influence the outcomes of the 3D printing workflow, the type of 3D printer used for model production can also affect the outcomes. Several studies have investigated application of various 3D printers in orthodontic model production. A report by Hazeveld et al. applied DLP, PJP, and powder-based printers in duplicating models from patients with various malocclusions and evaluated differences in linear measures of crown height and width for each tooth [15]. The authors concluded that the models reproduced by each technology were clinically acceptable for select applications in orthodontics that involve interpretation of the models, such as

diagnosis and treatment planning. Kasparova et al. compared linear measures on 3D printed duplicates of plaster models produced using a PJP printer and a FDM printer, concluding that models from both printers investigated could potentially replace plaster casts [6]. Another study compared SLA and PJP printers in reproducing models from 2 cases using digital superimposition analysis techniques [20]. While statistically significant differences were found between the 2 technologies, the authors concluded that both likely are suitable for diagnosis and treatment planning. However, the article did not discuss potential suitability of the models for appliance fabrication. Favero et al. compared models produced on various SLA, DLP, and PJP printers marked for orthodontic applications, finding statistically significant differences in overall dimensional accuracy between printers [5]. The authors concluded that the requirements of the envisioned application of the models to be printed should guide selection of the appropriate printer. Models from DLP and PJP printers were compared in a study by Brown et al., in which it was concluded that models from both printers were clinically acceptable [10]. Zhang et al. compared 3 DLP printers and 2 SLA printers, finding higher accuracy in DLP prints of models at 0.100 mm layer heights compared to SLA prints at the same layer height [8]. The authors offered that the accuracy requirements of models depend upon the envisioned application. A study by Kim et al. evaluated dental models manufactured with SLA, DLP, fused filament fabrication (FFF), and PJP, finding PJP and DLP outperformed FFF and SLA in terms of precision, with PJP presenting the highest accuracy [23]. Overall, findings vary with the printers applied in the studies, and differences in the applied methods limit comparisons that can be made between studies.

As the literature reflects, evaluation of the dimensional fidelity of 3D printed models can involve a multitude of measures and outcomes. Some studies evaluate accuracy of 3D printed models in terms of "trueness" and "precision," where trueness reflects the closeness of a measured value from a model to a reference value and precision reflects the closeness of measurements of a particular quantity of interest across repeatedly printed models [8, 20, 23, 27]. A variety of linear measurements have been applied in studies of the dimensional fidelity of 3D printed models, and they typically include measurements of landmarks in the x-plane (e.g., intercanine distance), y-plane (e.g., molar-to-molar distances on the same side of the arch), and z-plane (e.g., crown height) [6, 10-13, 15, 17, 20-22, 24, 25]. Discrepancies in measures in the z-plane, particularly in crown height, were reported in several studies, with 3D printed models presenting significantly smaller measures than the reference models [10, 15, 20, 21].

Many studies applied linear measurements made with digital calipers on physical models and/or virtual calipers on digital models. Difficulty in landmark identification presents a common limitation discussed in studies applying linear measures with physical calipers on 3D printed models [7, 15, 17, 21, 25]. Some studies report that a reduction in surface detail on 3D printed models contributes to the difficulty in identifying landmarks [17, 25]. A study characterizing the surfaces of 3D printed models by scanning electron microscopy, profilometry, and stereomicroscopy noted that the surfaces of models from an SLA printer were smoother than those of plaster models, which has been suggested to contribute to difficulty in positioning calipers correctly on the surfaces of acrylic models [24, 28]. Accordingly, some studies incorporated reference markers on the models to facilitate measurements, but inclusion of markers on dentally relevant landmarks may alter the anatomy in those regions and have implications on the printing associated with those areas of the model [23, 27]. The anatomy present on the model can also affect linear measures taken on the models, especially in cases of crowding, where the crowding may sterically interfere with positioning of the calipers or other measurement tools [7, 17, 22]. Crowding may also hinder accurate scanning of the associated dentition, and the anatomy of the crowded teeth may lead to loss of detail in the crowded region of a printed model [7, 17, 22, 25]. Studies comparing linear measures taken from 3D printed models with corresponding measures taken on digital models note that the digital nature of the linear measurements in software and manipulation of the digital model (e.g., magnifying regions of interest) can contribute to differences observed between the two modalities [22, 29]. Other studies have applied computer-controlled coordinate measuring instruments with associated

software to determine differences in measurements of landmarks on 3D printed models with respect to a reference model to minimize operator error [27].

While linear measures can provide insight into the dimensional fidelity of 3D printed models, the complexity of the dental anatomy and the arch form required for clear aligner therapy might not be evaluated adequately with linear measures alone. Some argue that arch dimension measures must also be evaluated for 3D printed models envisioned to support fabrication of clear aligners and other appliances to ensure suitability of fit [10]. Other studies have applied 3D dimensional analysis methods to quantify dimensional deviations between the surfaces of 3D printed models and the corresponding reference models [5, 8, 9, 11, 16, 20, 23, 28]. Many of these studies applied metrology software to superimpose digitally the reference model (e.g., the digital model file used as the input for 3D printing) and a surface scan of the 3D printed model, followed by quantification of the dimensional deviations between the models across the region of interest. The digital 3D comparison software often enables visualization of the regions of the model presenting deviations and the relative magnitudes and directions of the deviations (see Figure 5) [5, 8, 9, 11, 16, 20, 23, 28]. Accordingly, the 3D analysis methods reflect the complexity of the anatomy of the dentition and present greater relevance in the evaluation of the overall dimensional accuracy of 3D printed models for clear aligner fabrication applications than linear measures alone.

While many studies have reported statistically significant differences in linear and/or 3D comparison measurements between 3D printed and reference models, the differences should be considered in the context of the requirements of the envisioned clinical application. Specifically, statistically significant differences may not necessarily be clinically significant. A range of clinical tolerance values has been discussed in the literature in the evaluation of 3D printed orthodontic models, with many studies applying tolerances in a range of 0.10 mm to 0.50 mm for the purposes of study model production [5, 8, 10, 15-17, 26]. However, numerous studies underscore the importance of consideration of the envisioned application of the model in determining appropriate tolerances for clinical acceptability [5, 8-10, 12, 15-17, 21, 23]. While evidence-based tolerances for 3D printed models for clear aligner fabrication remain to be developed, several values have been applied in the literature in this context. For example, Zhang et al. proposed use of a tolerance of less than 0.05 mm for models to be used in clear aligner fabrication, while Kim et al. suggested that the deviations must be less than 0.25 to 0.3 mm for an aligner fabricated on the model to exert an orthodontic force [8, 23]. Alternatively, Wesemann et al. proposed that deviation requirements for orthodontic applications could be described in grades, with deviations less than 0.03 mm being “excellent,” less than 0.14 mm being “very good,” less than 0.25 mm being “acceptable,” and more than 0.25 mm being “unacceptable” [27]. In addition to consideration of the magnitude of dimensional deviations on a 3D printed model, the locations at which deviations occur also should be considered [5, 9, 17, 25]. One study suggested that loss of detail observed on the incisal edges and cusp tips on some 3D printed models may affect the seating of an appliance, such as a clear aligner, on the occlusal surface, while another study suggested that loss of detail at the cervical margins, fissures, fossae, and cusp tips might not be critical for production of appliances [17, 25].

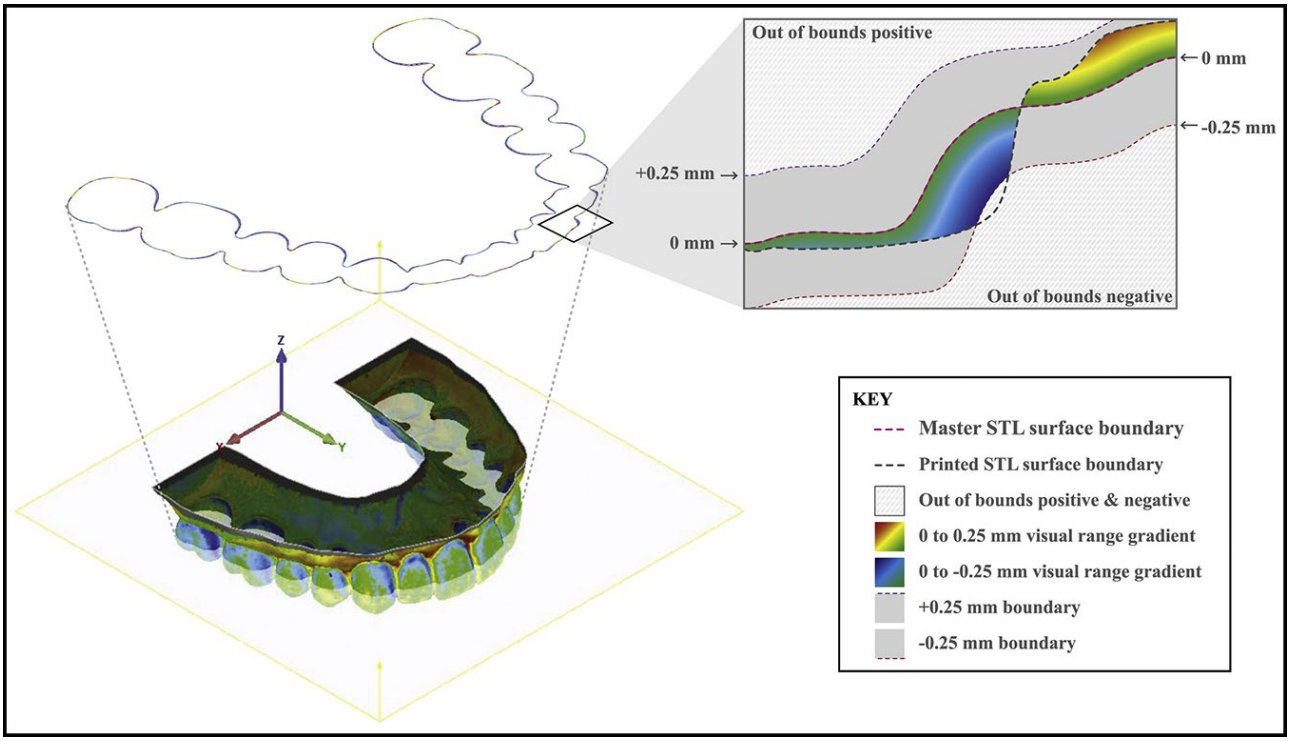

Figure 5. Illustration of 3D comparison data from digital superimposition of a scan of a 3D printed model (Printed STL) and the digital file used as the input for printing (Master STL). Colors represent different magnitudes and directions of dimensional deviation across the model, as depicted in the cross-sectional view and associated inset. Reprinted from [5] with permission from Elsevier.

FUTURE DIRECTIONS IN CLEAR ALIGNER FABRICATION

Technological advances enabled a paradigm shift in orthodontics by making the workflow for production of Kesling-style tooth positioning appliances practical. The next paradigm shift in clear aligner therapy will likely involve 3D printing of the aligners directly from digital designs (see Figure 6) [30, 31]. Direct printing of aligners would bypass the model printing and thermoforming steps of the current workflow, considerably increasing the efficiency and decreasing the environmental impacts of clear aligner production. Recent literature suggests the feasibility of aspects of the workflow, as demonstrated in experimental fabrication of retainers directly by 3D printing [32-34]. Direct printing of clear aligners could enable new horizons in clear aligner mechanics, by enabling spatial control of aligner properties, such as thickness, which is not feasible with current thermoforming methods [30, 35]. Existing software tools could be applied toward design and fabrication of clear aligners directly by 3D printing, but the development of specialized software tools would be warranted to expand capabilities and to simplify workflows. Even with appropriate software tools, aspects of the design of the appliance, such as the appropriate offset from the surface of the dentition, will need to be investigated [19].

Figure 6. Photograph of a clear aligner fabricated directly via 3D printing in a resin cleared for intraoral use for production of occlusal splints. The aligner was designed digitally to fit a scan of a typodont and is shown after removal of the supporting structures.

The major barrier on the pathway to directly printing aligners is the unavailability of a material suitable for the application at present. Although the number of 3D printable resins cleared for intraoral use on the market in the United States continues to increase, none known presently satisfies the requirements for clear aligner fabrication. Among a variety of material design requirements for the application, a resin for printing clear aligners directly must be compatible with 3D printing, esthetic, durable, stable, biocompatible, cost-effective, and present appropriate mechanical properties. While development of a material that satisfies these requirements is not a trivial pursuit, reports suggest that a material for clear aligner production will be available in the near future [36]. Even with a suitable material for the application, the clinical utility of 3D printed aligners will depend upon realization of the digitally designed part dimensions. Tunable aspects of the 3D printing workflow have been shown to affect the dimensional accuracy of 3D printed orthodontic models, and these findings will likely translate to the fabrication of clear aligners by 3D printing. However, the complexity of the aligner design, comprising a thin shell-like structure, and the transparency of the material present additional challenges for 3D printing. For instance, over-penetration of initiating light while 3D printing small patent features in clear materials can present a challenge and may require inclusion of biocompatible photoquenchers [37]. Additionally, analysis of the dimensional accuracy of 3D printed clear aligners will present challenges, as optical scanning of clear materials typically requires application of a spray or powder to facilitate scanning and may affect the measurements [30]. Ultimately, the fit of 3D printed aligners will need to be assessed, and few methods for quantification of the fit of clear aligners have been reported [4, 38, 39]. Moreover, tolerances for the clinical acceptability of 3D printed clear aligners remain to be developed. Considering the many challenges, direct fabrication of clear aligners does not appear to be practical presently, but continued advances in 3D printing and other technologies may soon enable the next paradigm shift in clear aligner therapy.

CONCLUSIONS

Many factors can affect the clinical utility of 3D printed orthodontic models for clear aligner fabrication and the efficiency of the workflow associated with their production. Emerging technologies may enable fabrication of clear aligners directly via 3D printing in the future. In either case, research and the requirements associated with clear aligner therapy should inform evidence-based selection of appropriate 3D printing factors and workflows in clear aligner fabrication.

ACKNOWLEDGEMENTS

This research was funded in part by the American Association of Orthodontists Foundation. I thank Drs. Jeryl English, Alex Edelmann, and Marian McCarty for insightful guidance and constructive feedback in the preparation of this contribution.

REFERENCES

1. Kesling HD. The philosophy of the tooth positioning appliance. *Am J Orthod Oral Surg* 1945;31(6):297-304.

2. Hennessy J, Al-Awadhi EA. Clear aligners generations and orthodontic tooth movement. *J Orthod* 2016;43(1):68-76.

3. Melkos AB. Advances in digital technology and orthodontics: a reference to the Invisalign method. *Med Sci Monit* 2005;11(5):PI39-42.

4. Martorelli M, Gerbino S, Giudice M, Ausiello P. A comparison between customized clear and removable orthodontic appliances manufactured using RP and CNC techniques. *Dent Mater* 2013;29(2):e1-10.

5. Favero CS, English JD, Cozad BE, Wirthlin JO, Short MM, Kasper FK. Effect of print layer height and printer type on the accuracy of 3-dimensional printed orthodontic models. *Am J Orthod Dentofacial Orthop* 2017;152(4):557-565.

6. Kasparova M, Grafova L, Dvorak P, Dostalova T, Prochazka A, Eliasova H, et al. Possibility of reconstruction of dental plaster cast from 3D digital study models. *Biomed Eng Online* 2013;12:49.

7. Loflin WA, English JD, Borders CL, Harris LM, Moon AL, Holland JN, et al. Effect of print layer height on the assessment of 3D-printed models. *Am J Orthod Dentofacial Orthop* 2019;156(2):283-289.

8. Zhang ZC, Li PL, Chu FT, Shen G. Influence of the three-dimensional printing technique and printing layer thickness on model accuracy. *J Orofac Orthop* 2019;80(4):194-204.

9. Short MM, Favero CS, English JD, Kasper FK. Impact of orientation on dimensional accuracy of 3D-printed orthodontic models. *J Clin Orthod* 2018;52(1):13-20.

10. Brown GB, Currier GF, Kadioglu O, Kierl JP. Accuracy of 3-dimensional printed dental models reconstructed from digital intraoral impressions. *Am J Orthod Dentofacial Orthop* 2018;154(5):733-739.

11. Camardella LT, de Vasconcellos Vilella O, Breuning H. Accuracy of printed dental models made with 2 prototype technologies and different designs of model bases. *Am J Orthod Dentofacial Orthop* 2017;151(6):1178-1187.

12. Koretsi V, Kirschbauer C, Proff P, Kirschneck C. Reliability and intra-examiner agreement of orthodontic model analysis with a digital caliper on plaster and printed dental models. *Clin Oral Investig* 2019;23(8):3387-3396.

13. Camardella LT, Vilella OV, van Hezel MM, Breuning KH. Accuracy of stereolithographically printed digital models compared to plaster models. *J Orofac Orthop* 2017;78(5):394-402.

14. Siller J, Villanueva D, Cozad BE, English JD, Kasper FK. Optimization of 3D printed orthodontic models for thermoformed appliance fabrication. *In: 2019 IADR/AADR/CADR General Session & Exhibition*.: June 19-22, 2019; Vancouver, BC, Canada. Abstract 3859.

15. Hazeveld A, Huddleston Slater JJ, Ren Y. Accuracy and reproducibility of dental replica models reconstructed by different rapid prototyping techniques. *Am J Orthod Dentofacial Orthop* 2014;145(1):108-115.

16. Ledingham AD, English JD, Akyalcin S, Cozad BE, Ontiveros JC, Kasper FK. Accuracy and mechanical properties of orthodontic models printed 3-dimensionally from calcium sulfate before and after various postprinting treatments. *Am J Orthod Dentofacial Orthop* 2016;150(6):1056-1062.

17. Wan Hassan WN, Yusoff Y, Mardi NA. Comparison of reconstructed rapid prototyping models produced by 3-dimensional printing and conventional stone models with different degrees of crowding. *Am J Orthod Dentofacial Orthop* 2017;151(1):209-218.

18. Groth C, Kravitz ND, Jones PE, Graham JW, Redmond WR. Three-dimensional printing technology. *J Clin Orthod* 2014;48(8):475-485.

19. Ye N, Wu T, Dong T, Yuan L, Fang B, Xia L. Precision of 3D-printed splints with different dental model offsets. *Am J Orthod Dentofacial Orthop* 2019;155(5):733-738.

20. Dietrich CA, Ender A, Baumgartner S, Mehl A. A validation study of reconstructed rapid prototyping models produced by two technologies. *Angle Orthod* 2017;87(5):782-787.

21. Keating AP, Knox J, Bibb R, Zhurov AI. A comparison of plaster, digital and reconstructed study model accuracy. *J Orthod* 2008;35(3):191-201.

22. Cuperus AM, Harms MC, Rangel FA, Bronkhorst EM, Schols JG, Breuning KH. Dental models made with an intraoral scanner: a validation study. *Am J Orthod Dentofacial Orthop* 2012;142(3):308-313.

23. Kim SY, Shin YS, Jung HD, Hwang CJ, Baik HS, Cha JY. Precision and trueness of dental models manufactured with different 3-dimensional printing techniques. *Am J Orthod Dentofacial Orthop* 2018;153(1):144-153.

24. Saleh WK, Ariffin E, Sherriff M, Bister D. Accuracy and reproducibility of linear measurements of resin, plaster, digital and printed study-models. *J Orthod* 2015;42(4):301-306.

25. Guzmán JFG, Ohara AT. Evaluation of three-dimensional printed virtual setups. *Am J Orthod Dentofacial Orthop* 2019;155(2):288-295.

26. Manuelli M, Huanca LG, Farronato M, Martintoni A, Marcolina M, Lucchese A. Comparison of linear transverse measures between plaster and resin printed digital models*. J Biol Regul Homeost Agents* 2018;32(2 Suppl. 2):81-85.

27. Wesemann C, Muallah J, Mah J, Bumann A. Accuracy and efficiency of full-arch digitalization and 3D printing: A comparison between desktop model scanners, an intraoral scanner, a CBCT model scan, and stereolithographic 3D printing. *Quintessence Int* 2017;48(1):41-50.

28. Dostalova T, Kasparova M, Kriz P, Halamova S, Jelinek M, Bradna P, et al. Intraoral scanner and stereographic 3D print in dentistry—quality and accuracy of model—new laser application in clinical practice. *Laser Physics* 2018;28(12):125602.

29. Scott JD, English JD, Cozad BE, Borders CL, Harris LM, Moon AL, et al. Comparison of automated grading of digital orthodontic models and hand grading of 3-dimensionally printed models. *Am J Orthod Dentofacial Orthop* 2019;155(6):886-890.

30. Edelmann A. Analysis of the thickness of 3D printed orthodontic aligners. Master of Science in Dentistry Thesis. The University of Texas Health Science Center at Houston; 2019.

31. McCarty M. Effect of print orientation and duration of ultraviolet curing on dimensional accuracy of 3-dimensional printed orthodontic clear aligners. Master of Science in Dentistry Thesis. The University of Texas Health Science Center at Houston; 2019.

32. Cole D, Bencharit S, Carrico CK, Arias A, Tüfekçi E. Evaluation of fit for 3D-printed retainers compared with thermoform retainers. *Am J Orthod Dentofacial Orthop* 2019;155(4):592-599.

33. Nasef AA, El-Beialy AR, Eid FHK, Mostafa YA. Accuracy of orthodontic 3D printed retainers versus thermoformed retainers. *Open J Med Imaging* 2017;07(04):169-179.

34. Nasef AA, El-Beialy AR, Mostafa YA. Virtual techniques for designing and fabricating a retainer. *Am J Orthod Dentofacial Orthop* 2014;146(3):394-398.

35. Elkholy F, Schmidt F, Jäger R, Lapatki BG. Forces and moments applied during derotation of a maxillary central incisor with thinner aligners: An in-vitro study. *Am J Orthod Dentofacial Orthop* 2017;151(2):407-415.

36. Saunders S. EnvisionTEC's steady, stealthy rise in orthodontics 3D printing. https://3dprint.com/205403/. Accessed July 1, 2019.

37. Grigoryan B, Paulsen SJ, Corbett DC, Sazer DW, Fortin CL, Zaita AJ, et al. Multivascular networks and functional intravascular topologies within biocompatible hydrogels. *Science* 2019;364(6439):458-464.

38. Mantovani E, Castroflorio E, Rossini G, Garino F, Cugliari G, Deregibus A, et al. Scanning electron microscopy evaluation of aligner fit on teeth. *Angle Orthod* 2018;88(5):596-601.

39. Mantovani E, Castroflorio E, Rossini G, Garino F, Cugliari G, Deregibus A, et al. Scanning electron microscopy analysis of aligner fitting on anchorage attachments. *J Orofac Orthop* 2019;80(2):79-87.

IN-HOUSE ORTHODONTIC WORKFLOW USING 3D PRINTING

Christopher S. Riolo, Burcu Bayirli

ABSTRACT

Innovations in technology are disrupting the orthodontic profession. These changes affect both orthodontic care delivery and the economics of care delivery - the orthodontic marketplace. "Disruptive Innovation in healthcare involves technologies, products, or services that are cheaper, simpler, and more convenient, making it possible for less expensive professionals to provide advanced services in affordable settings, or even for *patients to care for themselves*."[1,2]. This is not the first time that the orthodontic profession has experienced disruptive innovation. The initiation of the direct bonded appliance or the straight wire appliance in the 1970s was also disruptive. Orthodontists were concerned that these changes in technology would result in an increase in the number of general dentists and pediatric dentists doing orthodontics. In reality, these advances in technology provided benefits to patients and the orthodontic profession as a whole.

KEY WORDS: 3D Printing; Lingual; Orthodontics; Hybrid Orthodontic Treatment; In-House Workflow

INTRODUCTION

The advent of Invisalign in 1999 caused orthodontists to believe that general dentists and pediatric dentists would treat more orthodontic patients. It is true that general dentists have treated more orthodontic patients since the introduction of Invisalign, but so have orthodontists! In fact, the "Orthodontic Pie" has increased in size and both general dentists as well as orthodontists are providing more orthodontic treatment. Invisalign, through their enormous advertising budget, is almost certainly probably responsible for the esthetic adult orthodontic market that all of us enjoy today.

Digital technology has advanced at a rapid rate since the introduction of Invisalign and the production of clear aligners is easier now; treatment planning and outcomes of clear aligners has improved immensely. As a result of these recent advances, today, we are experiencing disruption of the orthodontic marketplace by the "direct to patient care" model through corporations such as Smile Direct Club, Candid Co, Byte, etc. due to the appearance of custom orthodontic appliances [1,2]. The same digital technology that makes this corporate direct to patient care model possible offer orthodontists real opportunities to improve the care they offer their patients:

1) Proactive treatment planning;

2) Hybrid orthodontic treatment using two or more custom orthodontic appliances coordinated on a unified digital platform; and

3) Using 3D printing to take control of our workflow to provide our patients true customization of orthodontic treatment at a minimum cost.

Proactive Treatment Planning

Digital orthodontics involves the planning and execution of orthodontic treatment with the use of digital orthodontic records. These digital records include phototographs, radiographic images, and STL models usually acquired through intraoral scanning. This transition to digital orthodontic records has facilitated advances in digital treatment planning and digital orthodontic appliance design; resulting in the development and concomitant rise of "Custom Orthodontic Appliances", such as Invisalign, Incognito, SureSmile and a myriad of direct to patient clear aligner systems.

A "Custom Orthodontic Appliance" is an orthodontic appliance system preprogrammed to a predetermined occlusal outcome resulting in a paradigm shift from "reactive" treatment planning to "proactive" treatment planning. In the traditional reactive treatment planning model, the orthodontist has an extraction or a non-extraction treatment plan in mind. For example, this hypothetical treatment plan may involve Class II mechanics, as well as interproximal reduction (IPR) of tooth material during treatment. In this treatment paradigm, the orthodontist delivers the brackets and begins to level and align. As the treatment progresses we make irreversible treatment decisions sequentially: we may decide to begin Class II elastics and procline the lower incisors; it is difficult or impossible to re-upright these incisors. We may extrude tooth segments; it is very difficult to re-intrude these teeth. If we perform IPR, we certainly cannot replace the enamel. With each of these treatment decisions, we decrease our degrees of freedom. In other words, the universe of possible occlusal outcomes become smaller with each treatment decision. As treatment progresses, we eventually decide that we have achieved the best occlusal result possible; thereby, we remove the brackets and deliver retainers. Is this the best result possible? The answer is we do not know for sure. It may be the best result possible at this point, after making a series of irreversible decisions. Could we have achieved a better treatment outcome, if we could return to the start of the treatment? It would be nice to know the amount of lower incisor proclination leveling and Class II mechanics may cause. The traditional reactive paradigm sometimes works well for our adolescent patients, but this model rarely produces the best clinical outcome for our interdisciplinary patients or our adult patients with highly restored, worn and/or debilitated dentitions. These patients with compromised dentitions require a proactive treatment paradigm in order to achieve an optimal occlusal result. In this "proactive" paradigm, the digital records are employed to produce a treatment setup. The factors that are important in achieving an ideal occlusal result are identified using the treatment setup. A custom appliance can then be fabricated using this same setup in order to maximize the treatment efficiency, maximizing the quality of the treatment outcome.

Hybrid Orthodontic Treatment

Hybrid orthodontic treatment entails the use of two or more appliance systems during orthodontic treatment. Hybrid treatment may be coordinated in a sequential or parallel manner. In the

sequential model, one treatment modality is employed at a time. The parallel model requires the coordination of multiple appliance systems at the same time to achieve a single plan treatment outcome. This coordination is best achieved using custom appliance systems employing a single treatment setup. At this point in time, the software required to achieve this coordination is limited.

Hybrid treatment has started, because there are logistical, biomechanical and aesthetic advantages as well as disadvantages associated with various orthodontic appliance systems, such as buccal fixed appliances, lingual fixed appliances, and clear aligners. Many patients are best treated with a combination of these orthodontic appliances. There are obvious and simple examples of sequential hybrid treatment in all our practices. Fixed appliance systems incorporating bands often result in open contacts. These spaces are easily resolved using a short series of one to three clear aligners. Another simple example includes the correction of small rotations with clear aligners after debond rather than extending treatment time with fixed appliances. It is difficult and frequently expensive to utilize this type of hybrid treatment using commercially produced appliances. The solution is to transition this workflow in-house employing resin 3D printing, staging these small movements, and thermoforming a limited series of aligners in-house.

This transition allows more complex sequential hybrid treatment that is the most beneficial treatment option for some patients. The patient in Figure 1 presented with a Class I molar relationship, moderate lower anterior crowding, history of periodontal disease, and poor oral hygiene. He required extraction of four bicuspids during orthodontic treatment. Minimizing the duration of fixed appliance therapy was desirable due to periodontal disease. In addition, this patient desired aesthetic orthodontic treatment ruling out buccal fixed appliances; therefore, a lingual fixed appliance system was elected. As a result of the lower anterior crowding, the use of lingual fixed appliances was likely to extend treatment time, because it can be very difficult to align lower anterior teeth with lingual fixed appliances in patients presenting with significant lower anterior crowding. Therefore, we decided to start treatment with clear aligners (before lingual fixed appliance treatment) moving selected tooth segments from the first stage, aligning the dentition, and gaining access to the lingual surfaces of the lower anterior teeth. Clear aligners had additional advantages in this case: They are an aesthetic treatment option and facilitate oral hygiene. Not only were clear aligners most efficient to initiate orthodontic treatment, they were also the safest treatment tactic with respect to this patient's periodontal health. Lastly, they satisfied the patient's requirement for aesthetic orthodontic treatment.

Unfortunately, four bicuspid treatment using clear aligners is unpredictable and unlikely to result in an excellent treatment result [3,4,6]. Using clear aligners in four bicuspid extraction treatment tends to result in tipping of the teeth adjacent to the extraction sites. This type of molar tipping in bicuspid extraction treatment using clear aligners is a classic presentation and can be seen in the progress photos shown in Figure 1b. Resolution of molar or bicuspid tipping is very difficult using clear aligners[4]. Resolving this type of tipping is relatively straight forward using a buccal or lingual edgewise fixed appliance system. Using both custom appliance systems (clear aligners and fixed lingual) is the definitive solution for this patient (Figure 1).

Why should we be limited to a single system as a treatment tactic and why should the patient have to compromise his desire for aesthetic orthodontic treatment? Failure to offer our patients aesthetic orthodontic treatment options is one of the reasons patients seek esthetic treatment through the direct to patient care model and forego the benefits of a more comprehensive treatment plan. Many patients have an appreciation for the benefits of aesthetic orthodontic treatment, but frequently do not have an appreciation for the benefits of comprehensive orthodontic treatment resulting in a healthy stable occlusion.

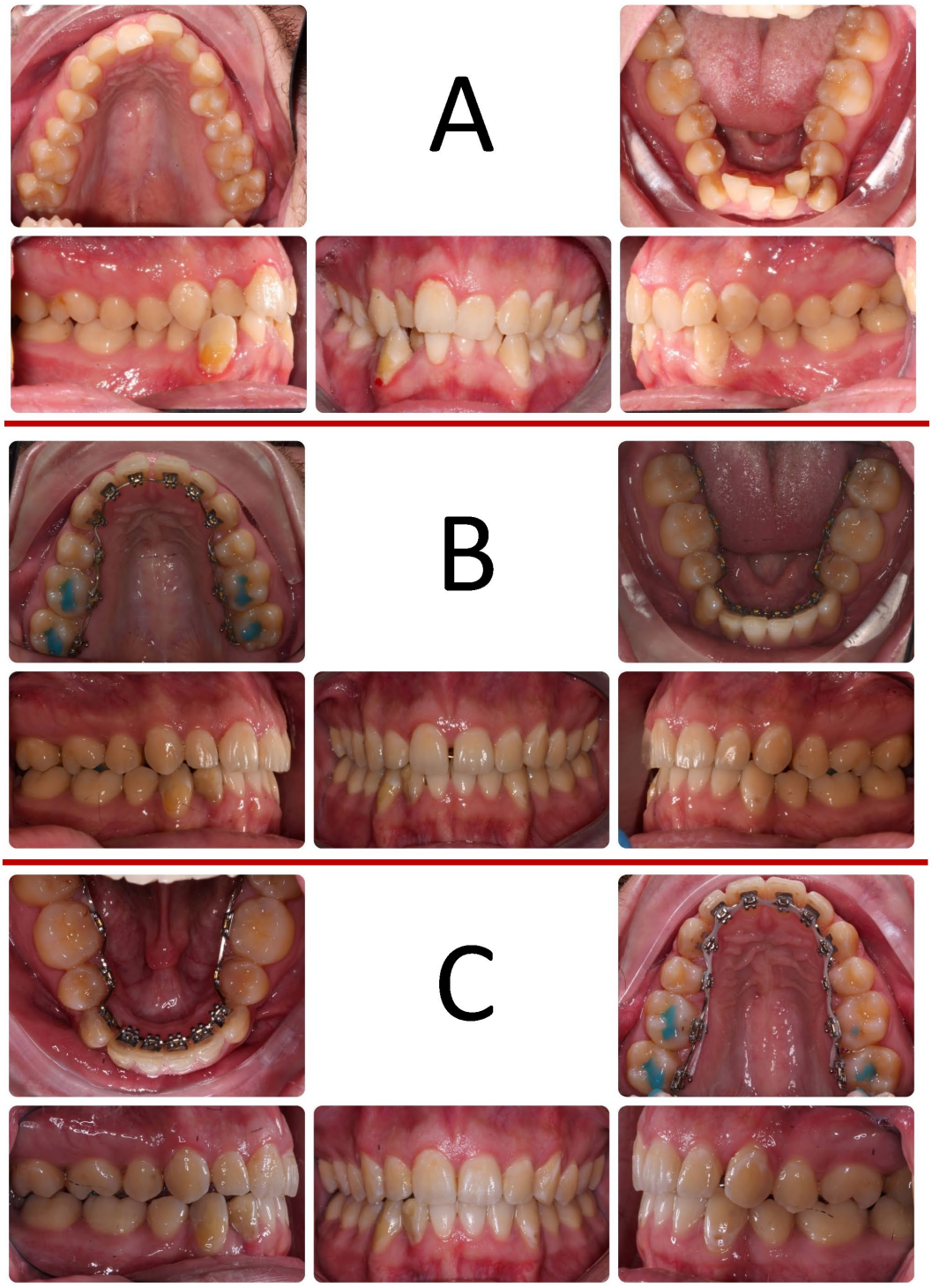

Figure 1: Figure 1A displays the initial presentation of a patient with periodontal disease, severe lower anterior crowding, and a desire for aesthetic orthodontic treatment. Figure 1B displays the intraoral photos the day that lingual fixed appliances were delivered after a first phase of 4 bicuspid extractions, space closure, and alignment using clear aligners. Figure 1c shows the same patient two appointments after initial delivery of lingual fixed appliances.

Hybrid treatment can also be used for both logistical and biomechanical reasons. Patient shown in Figure 2 presented with a deep impinging overbite and a Class II molar relationship. He was interested in efficient and effective treatment; he was willing to wear buccal fixed appliances in order to complete his orthodontic correction. Logistically, buccal fixed appliances in the lower arch are difficult to manage in a patient with deep impinging overbite.

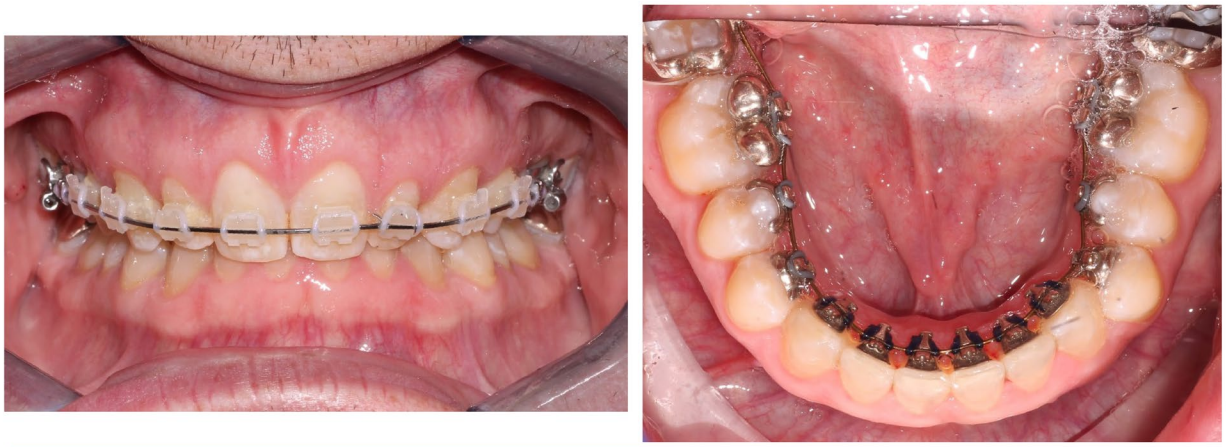

Figure 2: Figure 2 on the left shows the anterior intraoral view of a patient with a Class II malocclusion and a deep impinging overbite. On the right, the same patient is shown from the mandibular occlusal view; the hybrid lower lingual/ upper buccal fixed appliance system providing both biomechanical and logistical efficiency.

On the other hand, there are two primary advantages to using lingual fixed appliances in the lower arch in this situation. First one is logistical as the appliance system is placed out of occlusion. Second advantage is biomechanical due to the location of the point of force application versus the center of resistance (Figure 3). The logistical advantage is obvious, because using a lingual appliance, we can avoid placement of posterior occlusal buildups that tend to deepen the bite over time. Figure 3a shows the point of force application using a buccal fixed appliance versus the center of resistance of the root. There is a significant buccal lingual offset between these two points resulting in a moment and adverse tendency for tooth proclination. This tendency for proclination requires the application of torque in order to resist this proclination tendency. On the other hand, Figure 3b shows the point of force application using a lingual fixed appliance system. The lingual fixed appliance system results in a point of force application over or near the center of resistance of the tooth minimizing or eliminating the need for torque during intrusion.

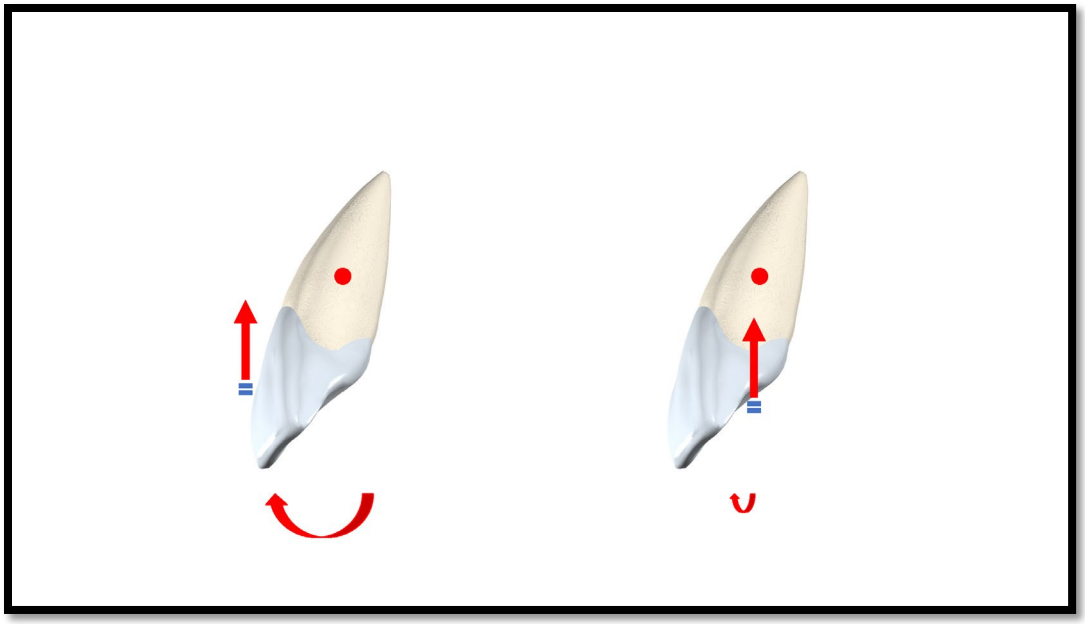

Figure 3: On the left side Figure 3 shows a significant offset from the point of force application using buccal fixed appliances, compared to the center of resistance of the tooth with the application of an intrusive force. This offset results in a moment and a tendency for adverse proclination of the tooth during intrusion. In comparison, on the right side, the point of force application with a lingual fixed appliance system minimizes or eliminates this adverse moment and the concomitant tendency for proclination under an intrusive force.

While it is clear, a hybrid approach is an efficient treatment option, the problems with this treatment approach are twofold:

1) Coordination of the different appliance systems; and

2) The cost of this type of treatment.

The solution is to replace commercial appliance systems with "in-house" custom appliance systems. The workflow for design and fabrication of the clear aligner system is well established at this time [5,7], but the workflow to design and fabricate a fixed orthodontic appliance system in-house is not well established [7,8].

True Customization of Orthodontic Treatment

Clear aligners fabricated in-house employ 3D resin printing. Resin printing in orthodontics involves different types of Stereolithography (SLA) printing. There are three general types of SLA technologies commonly employed in orthodontic clinical care: Laser SLA, Digital Light Processing (DLP) and LCD masking. All these printing technologies have commonalities. They all use: 1) Photo sensitive resin; 2) Light source; 3) Membrane; and 4) Build Plate. The differences between laser SLA, DLP, and LCD technology is mainly the way light is projected to cure the photo sensitive resin (Figure 4). These differences affect the accuracy, speed, and cost associated with printers. The accuracy requirements in orthodontic 3D printing is less than dentistry in general [9]. Each of the printing technologies properly employed can be used for the fabrication of in-house aligners.

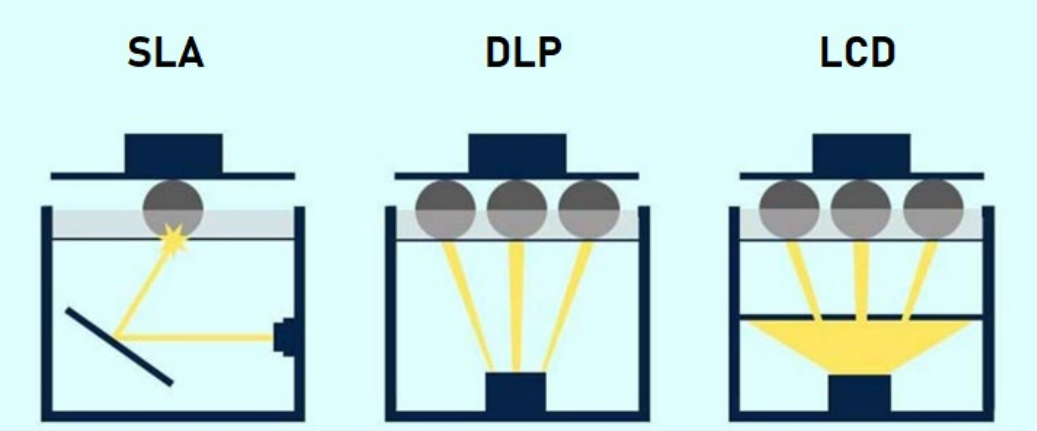

Figure 4: Figure 4 diagrammatically shows Laser SLA (left), DLP (center) and LCD (right) projection used in SLA resin printing. SLA printing uses a laser to cure photo sensitive resin point by point, DLP uses a Digital Micro-mirror Device (DMD) to produce a high-resolution projection and cure photo sensitive resin a whole layer at a time. LCD projection uses LCD light source and a "masking" screen to cure a whole layer of photo sensitive resin at a time.

Designing and printing fixed appliances requires access to software that is not commercially available. Therefore, at this time, the only way to design an in-house custom fixed appliance system is to use "off the shelf" CAD software. The workflow required for the design and fabrication is shown in Figure 5.

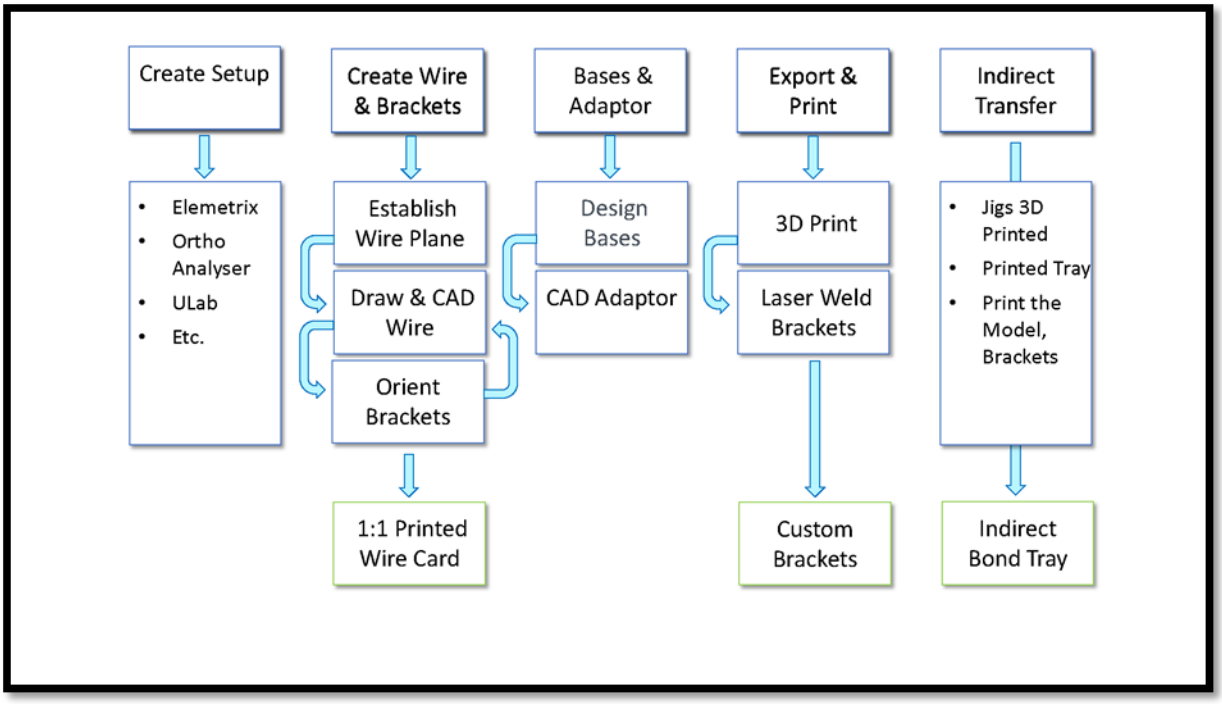

Figure 5: The workflow required for the design and fabrication of an in-house custom fixed appliance system is shown above.

The design of all custom appliances begins with a setup, and fixed custom systems are no exception. Any software that could be used to move teeth in the digital model of the dentition could be used to create the treatment setup. Once the treatment setup has been completed, it is imported into the CAD software of your choice; Rhino6 CAD software [10] was employed in this example. The first step in the design process is to establish the "wire plane". The choice of the wire plane is important in terms of design and logistical requirements of the lingual fixed appliance system [11,12]. With regard to the design consequences, there are significant changes in the required first and third order compensations as the wire plane migrates apically or occlusally [11]. The lingual anatomical variability is one of the primary factors that make lingual biomechanics difficult.

In addition to the anatomical problems with first and third order compensations, there are biomechanical issues with lingual bracket placement related to the point of force application and the center of resistance of the teeth (Figure 3). These biomechanical consequences of bracket position are well established in the literature [12,13,14,15, 22]. The logistical advantages are more obvious. In the maxillary arch, cervical positioning of the brackets results in fewer issues of occlusal interference with the mandibular dentition. There is a tradeoff between the biomechanical advantage of minimizing the first order offset with cervical bracket placement with the disadvantage of decreasing the inter-bracket distance in the lower arch. The precision of the bracket slot-wire interface is critical to the performance of lingual systems and factors such as decreased interbracket distance in lingual orthodontics and well documented lingual biomechanical issues are antithetical [18,19,20,21,23,24,25]. This is because there is an increased tendency for torque loss and extrusion of anterior tooth segments under Cl II mechanics and space closure [21]. The decrease in lingual interbracket distance results in a three fold inrease in wire stiffness for first and second order displacements and a one and a half fold increase for torsional displacements [22]. These factors result in significant clinical difficulties when treating patients using lingual brackets with traditional buccal orthodontic technique.

After the wire plane has been established, a wire conformation must be chosen [16,17]. While the choice of wire form is infinite, there are three main types of wire form: straight, mushroom, and individual (Figure 6).

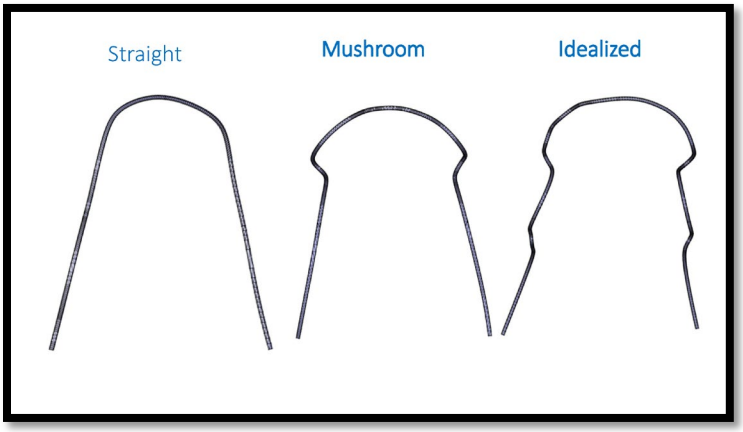

Figure 6: The three main types of wire forms are shown above: straight, mushroom, and individual. The straight wire form is convenient with respect to sliding mechanics; however, it will result in brackets with a larger profile to account for the first order compensations. The mushroom arch form reduces the required first order compensation in the area of the canines and still allows for some sliding mechanics

in the anterior and posterior. The individual wire conformation leads to bracket slots that are as close as possible to the lingual surface of the tooth, but is less convenient with respect to space appropriation and space closure.

The straight wire form is convenient with respect to sliding mechanics; however, it will result in brackets with a larger profile to account for the first order compensations. On the other hand, the mushroom arch form reduces the required first order compensation in the area of the canines and still allows for some sliding mechanics in the anterior and posterior. The mushroom arch form is an intermediate solution between the straight and individual wire conformation. The individual wire conformation leads to bracket slots that are as close as possible to the lingual surface of the tooth. This facilitates both the biomechanics and patient comfort [17].

Once the wire plane and wire conformation has been established, customization of the bracket can begin. The bracket is digitally suspended on the "wire", close to but not in contact with the lingual surfaces of the teeth (see Figure 7).

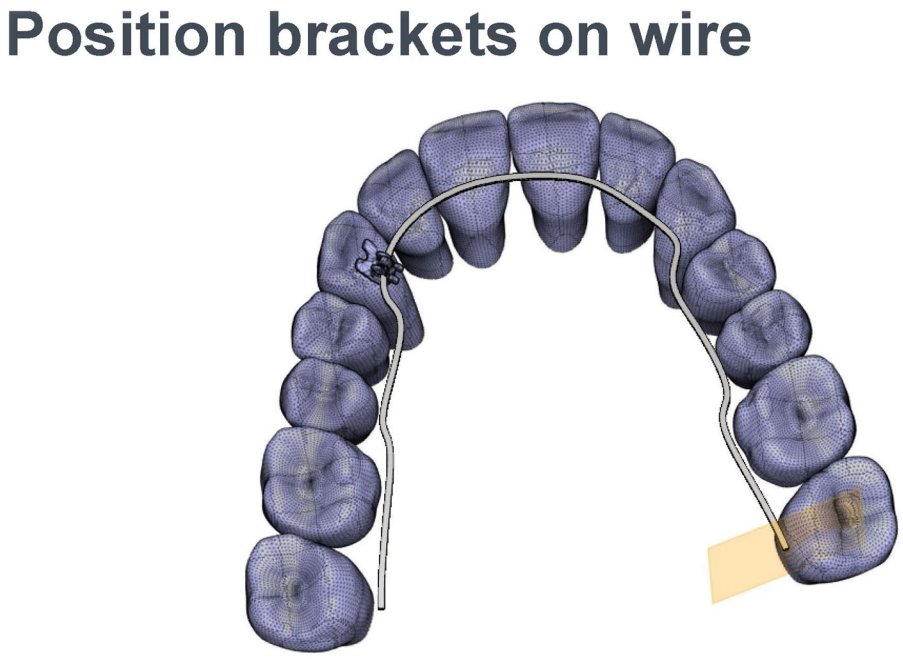

Figure 7: Figure 7 shows a digital bracket slot and wings are digitally suspended on the "wire". The wire, bracket slot, and wings are "tools" used to create the custom bracket bases and connector.

The closest distance from the bracket to the lingual surface of the tooth must be greater than or equal to the anticipated custom pad thickness. Empirically, we have found this minimum distance to be no less than 0.2 mm. There is tremendous flexibility in custom pad design (Figure 8).

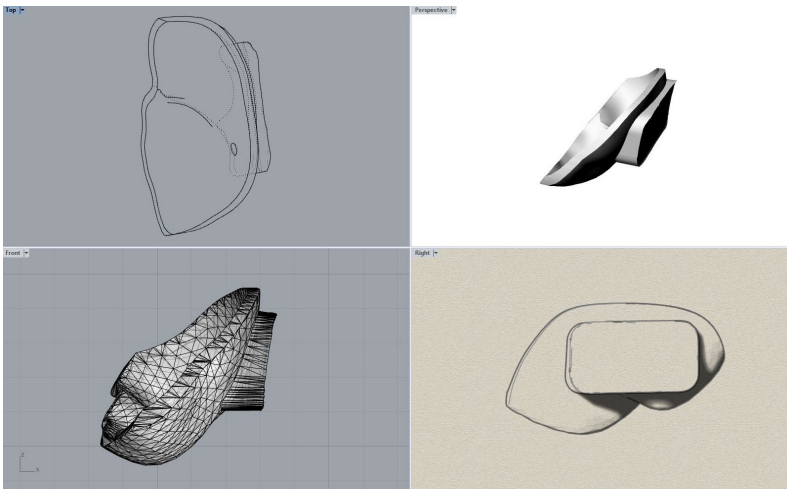

Figure 8: Figure 8 shows the custom base and connector; it is the custom connector that provides most of the prescription used to align the dentition.

The bracket slot and wings are positioned on the wire opposite each tooth. The bracket slot and wings are then connected to the custom base by the "connector". It is this "connector" that encodes the portion of the system prescription provided by the bracket. The wires provide the remaining portion of the prescription; the proportion of the information contained in the bracket and in the wire changes as wire complexity increases from "straight" to "mushroom" and to "individual". The custom bases with their connector can be seen in Figure 9.

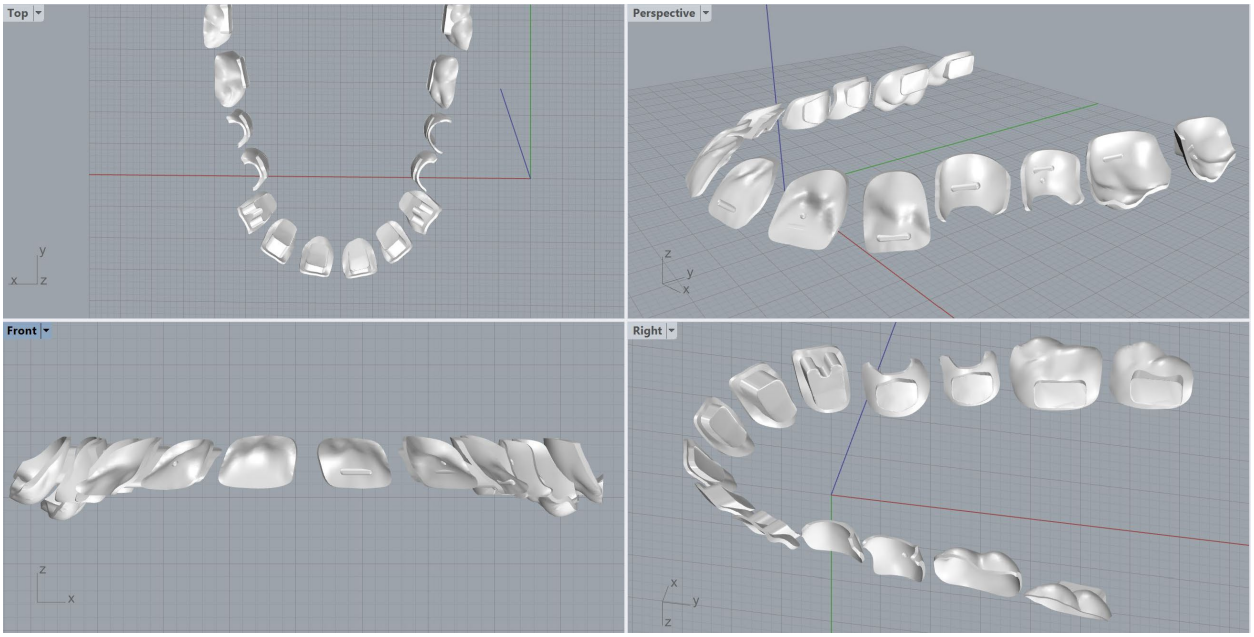

Figure 9: The complete set of custom bases and connectors are shown in this figure. Each of these custom bases have a connector with a unique shape that mimics the shape of the slot and wing component to facilitate accurate laser welding.

In the example shown here, the custom pad and connector are 3D printed (Chrome Cobalt) and, then, the bracket slot and wings are laser welded to the connector. Note that the shape of the connector mirrors the shape of the bracket base of the slot and wing portion in order to facilitate positioning for laser welding. The completed custom brackets after assembly are shown in Figure 10.

Figure 10: The complete set of Chrome Cobalt custom printed brackets are shown in this figure along with the custom wire hand bent from a 2D 1:1 printed wire card.

Once we have a set of custom brackets with the encoded prescription, we need to be able to accurately apply them to the patient. In order to accomplish this, we need to fabricate a bracket transfer system. This transfer system could entail jigs to transfer brackets directly or the fabrication of an indirect transfer tray. Jigs for direct transfer can be designed using the same CAD software used to design the brackets themselves. These jig STLs are then exported and the jigs can be printed using a resin printer. Digital design of individual jigs can be time consuming and accuracy of the use of jigs for bracket placement can be dependent on the type of jig designed and operator experience.

There are two methods for fabrication of an indirect transfer tray. In the first method, the tooth movement used to create the setup can be backed out of the setup model with the brackets in place. This results in the digital malocclusion model with digital custom brackets in place on the lingual surface. Brackets that have penetrations with tooth structure or another bracket can be digitally removed from the malocclusion model. Then, the transfer tray can be digitally designed, the tray STL exported, and printed by a resin printer. Afterwards, the physical brackets are inserted into the tray for transfer to the patient.

The second method of indirect transfer tray fabrication involves direct printing of the digital malocclusion model with the custom brackets and, then, indirect tray is fabricated on this printed malocclusion model. The physical custom brackets can afterwards again be inserted into the transfer

tray for delivery to the patient. An indirect tray fabricated using Polyvinylsiloxane (PVS) can be seen in Figure 11.

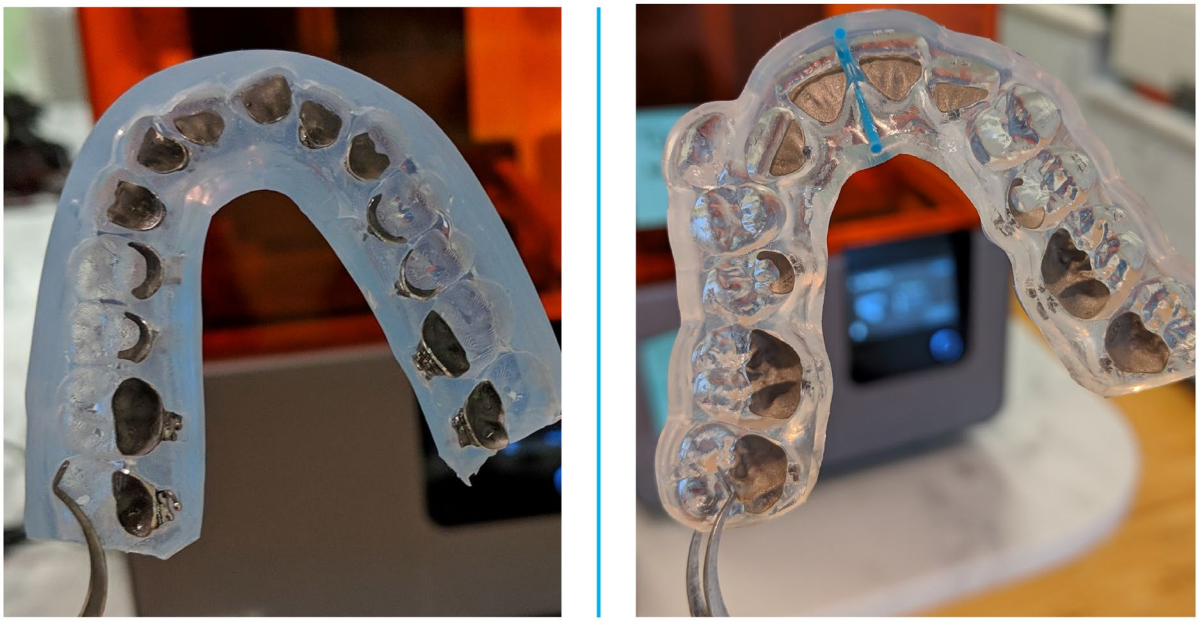

Figure 11: This figure shows the custom indirect transfer tray fabricated for our example custom lingual appliance system on the left and an indirect transfer tray used with the Incognito lingual appliance system offered by 3M Unitek on the right.

CONCLUSIONS

The advent of digital orthodontics and 3D printing has the potential to change the way orthodontists practice by moving the workflow associated with the design and fabrication of custom appliances in-house. In-house custom appliance design and fabrication allows orthodontists to truly customize appliance systems for their patients, coordinate the use of these appliances, and minimize cost making these appliances more accessible for our patients. Printer technology is improving at an incredible rate; the limiting factor in this transition is software. Commercial software for aligner staging defeats the goal of returning 100% control of the design and fabrication of orthodontic appliances to the orthodontist. As a profession, we should strive for control of both our data and workflow by working together as a community to develop software for staging aligners. One possibility is for the AAO to develop aligner staging software and offer it to AAO members at little or no charge.

An alternative model for the development of the software requires orthodontists as a community to develop the software for designing and printing custom fixed appliances with an open source license, only demanding that those who make improvements share those improvements with the community at no cost. The trend in clinical care over the last dozen years has been for corporations to market directly to our patients. More recently, some corporations have even begun to provide care directly to patients. Orthodontists have in many cases become tied to corporations as “providers” of these corporate appliance systems; these relationships vary from direct employees to loose affiliations

as unofficial sales people for their appliance systems. 3D printing has the potential to upend the power dynamic at play between orthodontists and corporate orthodontic entities. By working together, orthodontists can ensure the future of independent practice and full control over the care we offer our patients.

REFERENCES

1. Christensen C, Bohmer R, Kenagy J. Will Disruptive Innovations Cure Health Care. Harv Bus Rev 2000;78(5):102-112.

2. Hwang J, Christensen CM. Disruptive innovation in health care delivery: A framework for business-model innovation. Health Aff 2008;27(5):1329–1335.

3. Robertson L, Kaur H, Fagundes NCF, Romanyk D, Major P, Florers MC. Effectiveness of clear aligner therapy for orthodontic treatment: A systematic review. Orthod Craniofac Res 2019. doi:10.1111/ocr.12353.

4. Giancotti A, Greco M, Mampieri G. Extraction treatment using Invisalign®Technique. Prog Orthod 2006;7(1):32-43.

5. Eigenwillig P, Chhatwani S, Jungbauer R. Virtual planning and inhouse production of aligners with ArchForm Case based explanation of the digital workflow. Prakt Kieferorthop 2019;33(01/19):55-63.

6. Weir T. Clear aligners in orthodontic treatment. Aust Dent J 2017;62(1):58-62.

7. Yang L, Yin G, Liao X, Yin X, Ye N. A novel customized ceramic bracket for esthetic orthodontics: in vitro study. Prog Orthod 2019;20(1):39.

8. Krey KF, Darkazanly N, Kühnert R, Ruge S. 3D-printed orthodontic brackets - proof of concept. Int J Comput Dent 2016;19(4):351-362.

9. Jindal P, Juneja M, Siena FL, Bajaj D, Breedon P. Mechanical and geometric properties of thermoformed and 3D printed clear dental aligners. Am J Orthod Dentofacial Orthop 2019;156(5):694-701.

10. https://www.rhino3d.com/ Accessed January 2, 2020.

11. Stamm T, Wiechmann D, Heinecken A, Ehmer U. Relation between second and third order problems in lingual orthodontic treatment. J Lingual Orthod 2000;1(3): 5-11.

12. Geron, S., Romano, R., Brosh, T. Vertical forces in labial and lingual orthodontics applied on maxillary incisors – a theoretical approach. Angle Orthod 2004;74(2):195-201.

13. Scuzzo G, Takemoto K. Biomechanics and comparative biomechanics. In: Invisible Orthodontics: Current Concepts and Solutions in Lingual Orthodontics. Scuzzo G, Takemoto K, eds. Berlin: Quintessenz Verlags GmbH 2003;55-60.

14. Lombardo L, Scuzzo G, Arreghini A, Gorgun O, Ortan YO, Siciliani G. 3D FEM comparison of lingual and labial orthodontics in en masse retraction. Prog Orthod 2014;15(1):38.

15. Liang W, Rong Q, Lin J, Xu B. Torque control of the maxillary incisors in lingual and labial orthodontics: a 3-dimensional finite element analysis. Am J Orthod Dentofacial Orthop 2009;135(3): 316–322.

16. Fujita, K. New orthodontic treatment with lingual bracket mushroom arch wire appliance. Am J Orthod Dentofacial Orthop 1979;76(6):657-675.

17. Wiechmann D, Rummel V, Thalheim A, Simon JS, Wiechmann L. Customized brackets and archwires for lingual orthodontic treatment. Am J Orthod Dentofacial Orthop 2003;124(5):593-599.

18. Cash AC, Good SA, Curtis RV, McDonald F. An evaluation of slot size in orthodontic brackets—are standards as expected? Angle Orthod 2004;74(4):450-453.

19. Sifakakis I, Pandis N, Makou M, Eliades T, Katsaros C, Bourauel C. A comparative assessment of torque generated by lingual and conventional brackets. Eur J Orthod 2013;35(3);375-380.

20. Meling TR, Ødegaard J. The effect of cross-sectional dimensional variations of square and rectangular chrome-cobalt archwires on torsion. Angle Orthod 1998;68(3):239–248.

21. Siatkowski RE. Loss of anterior torque control due to variations in bracket slot and archwire dimensions. J Clin Orthod 1999;33(9):508–510.

22. Moran, KI. Relative wire stiffness due to lingual versus labial interbracket distance. Am J Orthod Dentofacial Orthop 1987;92(1):24-32.

23. Archambault A, Lacoursiere R, Badawi H, Major PW, Carey J, Flores-Mir C. Torque expression in stainless steel orthodontic brackets. A systematic review. Angle Orthod 2010;80(1):201-210.

24. Gioka C, Eliades T. Materials-induced variation in the torque expression of preadjusted appliances. Am J Orthod Dentofacial Orthop 2004;125(3):323–328.

25. Sebanc J, Brantley WA, Pincsak JJ, Conover JP. Variability of effective root torque as a function of edge bevel on orthodontic arch wires. Am J Orthod 1984;86(1):43-51.

DIGITAL DENTAL TECHNOLOGY: SYSTEMS EVOLUTION AND APPLICATION

Dennis J. Fasbinder, Stephen J. Sterlitz

ABSTRACT

The application of technology in dentistry has exponentially grown since it was first explored over three decades ago. What started as a vision to use rudimentary computer technology to restore a damaged single tooth with a ceramic material evolved into sophisticated and accurate digital imaging systems that are pervasive in every dental specialty. Early technology was not capable of accurately capturing the complex hard and soft-tissue anatomy of the entire oral environment without distortion. Consequently, initial dental applications of technology were limited. As technology developed, so did accuracy of the digital impression and the ability to leverage digital workflows for more than single-tooth restorations. The ability to combine accurate digital impressions with three-dimension digital radiographs in dental computer-aided-design (CAD) software support new treatment option workflows in orthodontics, periodontics, prosthodontics, endodontics, and oral surgery. This chapter will focus attention on current digital dental technology systems with the aims of understanding their capability and clinical applications for efficient implementation. Current scientific evidence on the clinical outcomes of these innovative workflows will be presented with the intent to provide guidance for practice integration.

KEY WORDS: CAD/CAM, Ceramics, Digital, Dental Technology

INTRODUCTION

One of the most common and critical procedures for dentistry is the ability to record the patient's intra-oral condition for evaluation, diagnosis, planning, and fabrication of devices outside of the patient's mouth. The ability to efficiently create an accurate replica of the dentition is conventionally dependent on the type of impression material utilized and the process of fabricating a stone model from the impression.

Computer Assisted Design/Computer Assisted Manufacture (CAD/CAM), Digital Technology and Computer-based Dentistry are terms more recently used to describe how improvements in technology have been applied to dental treatment. The ability to avoid the impression/model fabrication process by using a video recording of the dentition is a much more efficient process, equally if not more accurate than conventional impressions, and more comfortable to the patient. It is also proving to be the foundation for new practice workflows for patient treatment.

Due to the continued development and evolution of digital technology for dentistry, it can be difficult for practicing clinicians to understand differences in the systems and how they influence the treatment procedures. Computer technology continues to rapidly improve relative to graphics processing, data

processing speed, and ease of use, all of which significantly influence new dental technology for patient treatment. This chapter will provide a basis for understanding differences in digital systems and their applications in a dental practice.

Intra-oral System Development

What began in the 1980s as a vision to restore damaged teeth in a single appointment with a **ce**ramic **rec**onstruction (CEREC) has grown into a ubiquitous technology that affects all dental specialties. Dr. Werner Mormann, a Swiss dentist, and Marco Brandestini, an Italian electrical engineer, were the pioneers who collaborated to develop the first marketed application of a digital impression to support restorative dentistry. Siemens Dental marketed the concept in 1987 as the *CEREC system* [1,2]. This vision laid the foundation for the continued expansion of applications in computer aided design (CAD) and computer aided manufacturing (CAM) for dentistry.

Digital technology for dentistry is a function of computer assisted design, computer assisted manufacturing (CAD/CAM). The term "workflow" is commonly applied in digital dentistry to describe the steps required to reach the desired outcome. The three distinct steps in the digital restorative workflow are:

1) Digitize – capture the patient's intra-oral anatomy in a three-dimensional (3-D) digital format.
2) Design - application of CAD software to achieve a planned outcome.
3) Manufacture - transmit the digital design to a manufacturing device that will use CAM software to control production.

Early intra-oral scanners (IOS) relied on capturing multiple single images and utilized computer software to stitch together the overlapped single images to create a larger virtual model. With early technology, the model size rarely exceeded a quadrant. The number of images recorded, the speed of recording, and the size of the data files were limited by the graphics capability and processing speed of the computer. Due to the limits of computer technology available in the 1980s, the first clinical application for digital impression systems was limited to single tooth restorations. With the development of more capable technology, additional applications were added to the digital dental workflow. Modern IOS are video-based and are commonly used to record full-arch scans for diagnosis and treatment planning in under four minutes. Additional applications include orthodontic treatment planning and appliance fabrication, implant planning and restoration, and fabrication of removable prosthesis.

The CAD software programs have also followed a similar evolution as computer graphics and processing speed have improved. Early software was two-dimensional (2-D) based with significant time invested in learning how to interpret the various model presentations and edit functions. Modern software provides easy recognition of full color virtual models simulating the intra-oral environment. And editing tools and functions are more intuitive in design, allowing for a shorter learning curve for providers to become proficient.

Manufacturing devices in dentistry can either use subtractive manufacturing or additive manufacturing as the third step in the workflow. Although additive manufacturing, such as 3D printing, has advantages in material conservation and cost-effectiveness, definitive restorative materials like titanium, zirconia and glass ceramics are not possible to be printed at this time. Subtractive manufacturing in which the computer designed volume shape of the desired outcome is milled or cut from a premanufactured block or puck of material is the currently marketed system. It is important to appreciate these three distinct steps in the process in order to fully understand the capabilities and limitations of each unique digital impression system.

Due to the variety of digital systems in the dental marketplace that can be used in the CAD/CAM workflow, a convenient way to categorize the equipment is either as a digital impression system (see Table 1) or a chairside CAD/CAM system (see Table 2). Although both systems are capable of capturing a digital

impression with an IOS, the difference between the systems is how the data is managed after the oral anatomy is digitized. Digital impression systems focus on the first step of the CAD/CAM process – recording the intra-oral condition to a computer program. The primary focus of a digital impression system software program is to identify and manage the digital file because the intent is to electronically transfer the information out of the dental office and to the dental laboratory for fabrication of the desired restoration or appliance. Digital impression systems leverage the advantages inherent with the use of an IOS such as the comfort and efficiency of not using conventional impression materials as well as the convenience and accuracy of electronic transmission of the case to the dental laboratory. The chairside CAD/CAM systems apply all three steps of the CAD/CAM process in the dental office in a workflow designed to deliver a restoration in a single appointment.

Table 1: Digital Impression Systems.

System	True Definition	iTero	Trios 3	Apollo DI	DWOS
Manufacturer	3M (LAVA COS 2006)	Align Technology Inc 2007	3Shape 2010	Dentsply Sirona 2012	Dental Wings 2015
Camera	3D in motion; active wavefront sampling	Parallel confocal imaging	Principle of confocal microscopy	LED video	MultiScan Imaging Technology
Wireless camera	No	No	Yes	No	No
Portable option	Yes	No	Yes	No	Yes
Reflective powder	Yes	No	No	No	Yes
Monitor	Monochromatic	Color	RealColor	Color	Monochromatic
Touchscreen	Yes	No	Yes	Yes	Yes
Orthodontic applications	Yes	Yes	Requires add-on module	Yes	Yes
Implant applications	Yes	Yes	Yes	Yes	Yes

Table 2: Chairside CAD/CAM systems

System	CEREC OmniCam	CEREC PrimeScan	PlanScan Emerald	Carestream 3600	Glidewell i.o.
Manufacturer	Dentsply Sirona	Dentsply Sirona	PlanMeca E4D Technologies	Carestream Dental	Multiple manufacturers
Camera	LED video	SmartPixel Sensor	Multi-color laser	LED ActiveSpeed 3D video	Parallel confocal
Monitor	Color	Color	Color	Color	Color
Touchscreen	No	Yes	No	Yes	Yes
Orthodontic applications	Yes	Yes	Yes	Yes	Yes
Implant applications	Yes	Yes	Yes	Yes	Yes

One common concern of many dentists is the size of the camera used for scanning. Most manufacturers have trended towards cameras approaching the size of dental handpieces assuming that dentists are very comfortable using handpieces intra-orally. Consequently, a camera of similar size could be applied in a familiar and comfortable fashion. Although using a familiar design concept is a logical approach when introducing new technology, the size of the camera is also an ergonomic concern. Similar to curing lights, the entire camera does not need to fit in the mouth. Although a small sized camera head is an obvious advantage for intra-oral access, the ergonomics of the camera body may be a greater influence on the ease of intra-oral scanning since it has a direct impact on the maneuverability of the camera.

Accuracy

A critical step in achieving a successful outcome in dentistry is the ability to accurately record a patient's anatomy. Multiple studies have been conducted to demonstrate the accuracy of full arch digital impressions. A study conducted in 2017 by Renne et al evaluated the accuracy of seven digital scanners. The study evaluated both trueness, the ability to accurately record the actual dimension of an object, and precision, the ability to record repeated measurements regardless of the actual dimension of the object. Data analysis of their study led to the following conclusions: 1) Scanners differ regarding the speed, trueness, and precision of sextant scans, with the Planscan and the CEREC Omnicam providing the best combination of speed, trueness, and precision; 2) Scanners differ regarding the speed, trueness, and precision of complete-arch scans, with the 3Shape TRIOS providing the best combination of speed, trueness, and precision [3]. A separate study conducted in 2018 by Treesh et al evaluated 4 different intra-oral scanners: CEREC Bluecam, CEREC Omnicam, Trios Color, and Carestream 3500. They reported that all systems accurately captured full-arch scans within 100 µm of actual dimensions with the most distortion occurring at the terminal aspects of the arch [4].

There is great debate over the acceptable amount of error when it comes to dental procedures. A common standard to evaluate an indirect restoration is a gap of less than 100 µm between the prepared tooth and the margin of indirect restoration. Tolerances are even larger with removable prosthetic

dentistry due to the dynamic nature of soft tissue and the known complication of polymerization shrinkage of the polymethyl methacrylate material used in denture bases [5]. Orthodontic researchers have suggested that clinically acceptable models should be within 0.20-0.30 mm of actual values [6,7]. A 2018 study comparing the 3Shape TRIOS scanner with the iTero scanner found the average deviation between the scanners and an alginate diagnostic model was 0.057 mm in the maxilla and 0.069 mm in the mandible, well below the 0.2-0.3 mm values suggested by orthodontic researchers [8].

In comparison to conventional impressions, digital impressions have fewer variables that will affect both initial and long-term accuracy. The accuracy of a conventional impression can be affected by the consistency and placement of the impression material, proper disinfection and handling prior to model fabrication, proper measuring and handling of stone when pouring the model, and proper separation of the stone model from the impression. Each step in the conventional impression process has known problems and limitations; however, they have been managed by most dentists to provide accurate replicas of the intra-oral condition for decades. One significant limitation of the conventional method is the degradation of accuracy when multiple pours are made of the same impression. Digital impressions avoid many of the problems of conventional impressions such as volumetric changes during the setting reaction, the need to disinfect the physical impression, and packaging/shipping physical impressions to the dental laboratory. Digital impressions also have the added advantage that models can be fabricated with equal accuracy an unlimited number of times, because the digital file does not go through accuracy degradation as it is repeatedly processed.

MATERIALS

Restorations created using the chairside CAD/CAM workflow have the advantage of being monolithic. A monolithic restoration is able to maximize the material's physical properties because it is created from a dense, homogenous, lab-processed block. Final processing of the chairside CAD/CAM material in a controlled and repeatable workflow minimizes the effects of voids and porosity common with bi-layered restorations. Historically bi-layered restorations like porcelain-fused to metal (PFM) and, more recently, porcelain-fused to zirconia (PFZ) consisted of a strong, but unaesthetic, coping material that were covered with an esthetic veneering ceramic. As demonstrated by an *in vitro* study in 2011, the strength of the interface between the coping material and veneering ceramic is a significant weakness of the bi-layered restoration that could result in loss of the esthetic porcelain veneer or chipping of the veneering ceramic [9].

Monolithic restorative materials are delivered in a solid block ranging from 8 – 40 mm in size. The restorative material is mounted on a mandrel that allows precise placement in the chairside CAD/CAM manufacturing chamber to assure precision and accuracy during the manufacturing process (see Figure 1). Current chairside CAM dental restorations are created using subtractive manufacturing. Subtractive manufacturing is the process of removing material from the solid block based on the volumetric computer aided design of the restoration created by the software program (see Figure 2). There are two different types of burs used in subtractive manufacturing. The use of diamond burs is called "grinding" in the CAM process. The use of carbide burs is called "milling". Diamonds are primarily used with wet-grinding to minimize the risk of chipping. Carbide burs can be used wet or dry and are most effective milling materials less prone to chipping, such as acrylics or pre-sintered zirconia.

Figure 1. Examples of different milling block mandrels for various CAD/CAM milling units. Left-right: PlanMeca/E4D mill, CEREC MCX mill, ts150 mill, and Amann Girrbach mill.

Figure 2. Examples of full crowns subtractively milled from the mill block.

An effective chairside CAD/CAM restorative material must be capable of being efficiently manufactured and processed to support same-day or single appointment delivery of the restoration. Currently available chairside CAM units are capable of creating a single-unit restoration in less than 15 minutes, with many restorations taking less than 10 minutes to manufacture. Factors influencing manufacturing time are size of the restoration, complexity of the interior and exterior surface of the restoration, and the physical properties of the restorative material. Generally speaking, larger restorations made from higher strength, brittle materials take longer to manufacture.

The constant introduction of new restorative materials compatible with the chairside CAD/CAM workflow makes it challenging to decipher marketing trade names in order to understand the physical properties of the material. There are several categories of blocks used for chairside CAD/CAM restorations (see Table 3). There are nuances to the physical properties of each type of block that give them distinct advantages in certain clinical situations. Materials containing resin are inherently more resilient and less prone to fatigue fracture. Although ceramic blocks have a higher flexural fracture strength, they also are known to be brittle and experience catastrophic failure when overloaded. Consequently, a thorough understanding of CAD/CAM materials and their physical properties is essential to achieve a successful clinical outcome.

Table 3. Categories and brands of chairside CAD/CAM materials.

Category	**Material**	**Brand (Manufacturer)**
Adhesive Ceramic	Leucite-reinforced	IPS Empress CAD (Ivoclar) Initial LRF (GC)
	Feldspathic	Vita Mark II (Vita) CEREC Blocs (Dentsply Sirona)
High Strength Ceramics	Lithium disilicate	IPS e.max CAD (Ivoclar)
	Zirconia lithium silicate	Celtra Duo (Dentsply Sirona) Suprinity (Vita) Nice! (Straumann)
Resilient Ceramics	Nano-ceramics	Lava Ultimate (3M) CeraSmart (GC America) Block HC (Shofu) Tetric CAD (Ivoclar)
	Hybrid Ceramics	Vita Enamic (Vita)
Composites		Brilliant Crios (Coltene) Paradigm MZ100 (3M)
Zirconia	3mol%	CEREC Zirconia (Dentsply Sirona) IPS e.max ZirCAD (Ivoclar)
	4mol%+	Katana (Kuraray Noritake) 3M Chairside Zirconia (3M)

The topic of dental ceramics can be overwhelming, and the introduction of new materials is making it harder to place the material in a specific category in order to predict its physical properties. To better understand dental ceramics, it is easier to place them in three main composition categories: predominantly glass, particle-filled glass, and polycrystalline [10].

Predominantly glass dental ceramics have very good translucency that closely mimics the optical properties of enamel and dentin. *Vita Mark II* (Vita) and *CEREC Blocs* (Dentsply Sirona) are prominent examples of feldspathic glass dental ceramics. Both materials are fine-grained, homogenous feldspathic porcelain with an average particle size of 4 μm. The small particle size allows for a high-gloss finish and minimizes abrasive wear of the opposing dentition. *IPS Empress CAD* (Ivoclar) gains increased flexural strength with the addition of 35-45% leucite reinforced glass-ceramic and has a particle size that ranges from 1-5 μm. The presence of the glass component in these materials permits them to be etched with hydrofluoric acid, treated with a silane coupler, and adhesively bonded to the tooth using resin cement. Adhesive bonding of these materials is critical to their long-term success because the material is not sufficiently strong to support luting of the restoration with a conventional cement. A strong adhesive bond not only retains the restoration, but also contributes to the clinical strength of the restoration (see Figure 3).

Figure 3A-C. Pre-operative view, delivery and five-year recall of a feldspathic CAD/CAM onlay (Vita Mark II) for tooth #30.

Particle-filled glass dental ceramic blocks have a substantially greater flexural strength and fracture toughness compared to predominately glass dental ceramics. The particle-filled glass dental ceramic that has been part of the chairside CAD/CAM workflow the longest is *IPS e.max CAD* (Ivoclar). E.max blocks are referred to as "blue blocks" for their distinct blue/purple color that represent their pre-crystalized lithium metasilicate crystal orientation that must be heat treated in a porcelain furnace to transform into its full strength and color, lithium disilicate crystal. The "blue block" state of the material is easier to mill than the full-strength lithium disilicate material minimizing diamond bur wear and enables more accurate milling of the material without chipping. Crystallization of the *IPS e.max CAD* material results in a lithium disilicate crystal particle that fills 70% of the volume of the glass ceramic resulting in a restorative material with a flexural strength of 400Mpa. A recently introduced zirconia-reinforced, lithium silicate material, *Celtra Duo* (Dentsply Sirona), comes as a fully-crystallized block that purportedly allows the option to either polish the material after milling resulting in a flexural strength of 210 MPa, or glazing the material in a porcelain oven resulting in a flexural strength of 370MPa [11] (see Figure 4).

Figure 4A-C. Pre-operative view, crown preparation, and delivered zirconia reinforced lithium silicate crown (Celtra Duo) for tooth #19.

Until recently, polycrystalline dental ceramics such as full-contour zirconia restorations were not available as part of the chairside same-day restorative workflow. Although the physical properties of the material remain the same, innovation in the zirconia sintering furnace resulted in reduced time required to sinter zirconia after it is milled. Zirconia generally requires 6 to 8 hours of sintering heat treatment in a dental laboratory making it unacceptable for a same-appointment restorative material. The *SpeedFire Oven* (Dentsply Sirona) is an innovative induction porcelain oven capable of sintering zirconia in less than 30 minutes. It is integrated into the CEREC software program so a custom sintering-cycle specific to the

material thickness of each restoration is automatically sent during the CAM process, allowing a custom sintering profile for a single zirconia crown to be completed. The drastically reduced processing time enables zirconia to be treatment planned as a single appointment restorative material (see Figure 5).

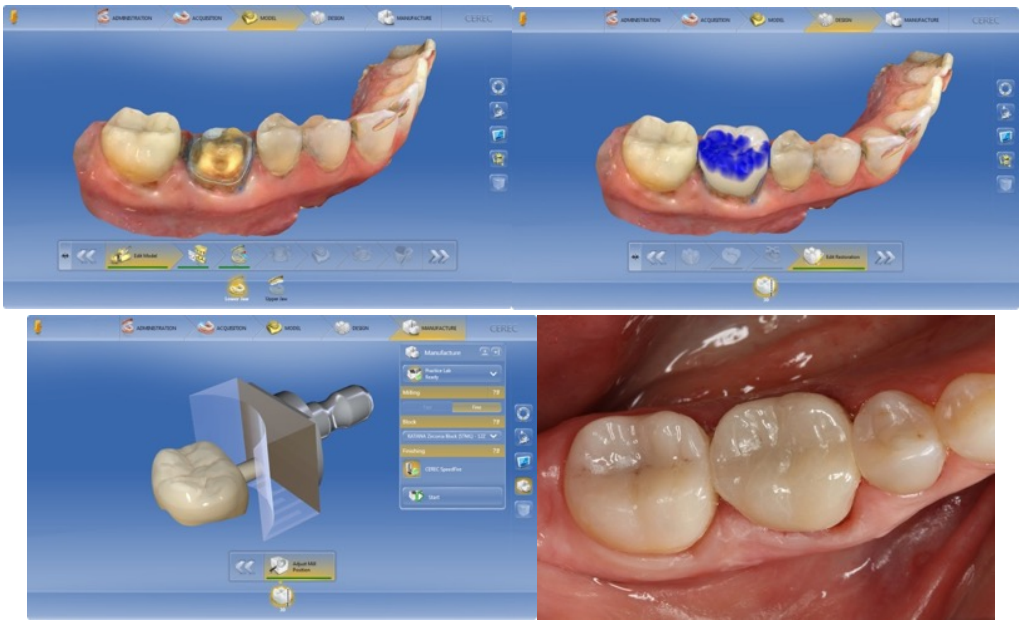

Figure 5A-D. CEREC CAD/CAM crown preparation virtual model, CEREC design of the crown, and crown proposal in the milling block for tooth #30. Delivered CEREC CAD/CAM full contour zirconia crown (Katana/Kuraray Noritake) for tooth #30. The crown on tooth #31 is a zirconia lithium silicate (Celtra Duo) crown.

Resilient CAD/CAM blocks can be further subdivided into a recently introduced "resilient ceramic" category and a composite resin category. The two resilient ceramics materials, *Lava Ultimate* (3M) and *Vita Enamic* (Vita) are designed to offer the benefits of easy handling similar to composite materials, but with the strength and surface finish of ceramics. *Lava Ultimate* is a nano-ceramic containing silica particles of 20 nm, zirconia particles of 4-11 nm, and agglomerated nano-size particles of silica and zirconia all embedded in a highly cross-linked polymer matrix. Vita Enamic is a hybrid-ceramic comprised of a dual-network structure where ceramic and polymer are merged together. The manufacturer claims this material incorporates the benefits of ceramic and composite resin material in one product, offering both strength and elasticity. *Cerasmart* (GC America) is a flexible nano-ceramic matrix with a homogenous distribution of nano-ceramic filler. The manufacturer claims it is a high-strength, 210 MPa, and force absorbing material for both natural teeth and dental implants (see Figure 6).

Figure 6A-C. Onlay preparation, 1-year recall, and five-year recall of a nano-ceramic onlay (Lava Ultimate) for tooth #30.

Composite CAD/CAM blocks can either be used for final restorations or as long-term provisional restorations. *Paradigm MZ100* (3M) is a lab-processed block based on Z100 direct composite restorative material chemistry. *Paradigm MZ100* has zirconia-silica filler particles that average 0.6 µm in size and is 85% filled by weight. The material is best applied in clinical situations where large composite restorations are possible, but the benefit of a monolithic highly polymerized material would result in a stronger, more durable restoration. *Brilliant Crios* (Coltene) are similar to the *Paradigm MZ100* blocks in that they have glass and ceramic fillers in an acrylate resin matrix. *Vita CAD-Temp* (Vident) and *Telio CAD* (Ivoclar) are lab-processed acrylic dental materials manufactured in 40 mm and 55 mm blocks to be long-term provisional restorative materials for single-unit crowns or fixed partial denture restorations. Subtractive-manufacturing of pre-processed acrylics avoids the complication of polymerization shrinkage experienced using the direct method of provisionalization.

WORKFLOWS & APPLICATIONS

Many dental offices have computers in each operatory and some clinicians have questioned if the IOS camera could be directly installed on their in-office computers rather than rolling a portable unit between operatories. The E4D Dentist™ system (D4D Technologies) was introduced in 2007. Their NEVO system features a portable camera connected to a laptop computer rather than encased in a rolling, portable unit. Planmeca invested in the company in 2013 and now markets PlanScan CAD/CAM Restoration System, driven by E4D Technologies. The CS 3500 Intraoral Scanner (Carestream Dental) also introduced a direct USB connection camera that can be used with a laptop computer rather than being housed in a portable cart unit. Although purported to be a more streamlined set-up, the laptop computer still must be located adjacent to the operating field for direct access to the imaging camera on either an adjacent counter or a cart.

The latest innovation in intra-oral scanners is the option of a wireless scanner that was introduced by 3Shape in 2017. The Trios 3 wireless scanner option operates on a rechargeable battery that can support up to 30 minutes of scanning time and sends data to the computer via a Wi-Fi dongle. The wireless option allows for a single camera to operate in multiple dental treatment rooms and send the digital impression to a single design center.

Another innovation for chairside CAD/CAM systems is the open architecture options offered for several digital impression systems. The E4D Design Center and E4D milling chamber became one of the first trusted connections with the True Definition Scanner (3M) in October 2012. This provided an opportunity for dentists using the True Definition digital impression system to also create restorations in-office. Data files recorded by the True Definition Scanner can be directly input into the E4D Design Center for in-office design of inlays, onlays, crowns, and veneers milled in the E4D milling unit. The iTero Intraoral Scanner (Align Technology) was similarly announced as being compatible with the E4D chairside design

software and milling chamber in October 2013. Another example is the IOS FastDesign system by IOS Technologies that was founded in 2007 and acquired by Glidewell Laboratories in 2012. It includes the FastDesign CAD software and the TS 150 in-office milling unit. It was announced in March 2013 that the TS 150 in-office milling machine became a trusted connection of the True Definition Scanner as well as integrated with the TRIOS digital impression solution (3Shape). In 2014, it was also integrated with the iTero IOS device. Digital files may be transmitted from all three IOS devices to the IOS FastDesign CAD software for fabrication of in-office inlays, onlays, and crowns with a TS 150 milling machine.

A more recent introduction by companies partnering to create an in-office solution is the PrograMill One mill by Ivoclar. It was introduced in 2017 and is a five-axis milling machine with an innovative milling process in which the workpiece rotates around the tool, ensuring that the tool never leaves the block, reportedly leading to shorter milling times. It is used in combination with the TRIOS scanner and design software by 3Shape for chairside CAD/CAM restorations.

Maintenance requirements for in-office milling chambers vary between systems based on the manufacturer's recommendations. All are water-lubricated milling systems with self-contained, closed water systems that recycle the water during milling. The water chamber needs to be cleaned periodically. Lubricant is usually added to the water to reduce friction and control heat during the milling process. The milling diamonds wear and will require changing, with the frequency of change based on the size and type of materials milled. High strength porcelain systems are more detrimental to milling diamonds than resin based restorative materials. Manufacturers also generally suggest a yearly preventive maintenance routine. Several CEREC milling units now allow for the use of carbide burs to mill zirconia blocks in a dry subtractive process. There is a vacuum connected to the milling chamber to minimize the milling dust from zirconia. The vacuum and milling chamber has periodic cleaning required to ensure consistent results.

Several of the chairside CAD/CAM systems also have the capability of functioning as a digital impression system providing flexibility to the provider to fabricate an appropriate restoration based on the specific clinical requirements of the case. The Sirona Connect system, the Planmeca Romexis Cloud Service, and the CS Connect system offer the opportunity to use chairside systems as purely digital impression techniques for cases the clinician desires to be fabricated in a dental laboratory. This offers a valuable tool for case fabrication by offering the full range of laboratory services in addition to the in-office options from the digital scanning.

Initial applications for chairside CAD/CAM systems were to produce single tooth restorations including inlays, onlays, veneers, and crowns. Some of the systems have evolved to have the ability to fabricate short-span fixed partial dentures (FPDs), custom abutments, adhesively bonded fixed partial dentures (Maryland Bridges), and temporary restorations in the dental office. In addition, by also connecting to dental laboratories as digital impression systems expanded services such as orthodontic clear aligners, bitesplints, surgical guides, and sleep apnea devices may be fabricated.

As .stl files have become available for export from both digital impression systems and chairside CAD/CAM systems, 3D printing has become an alternative to subtractive milling for manufacturing of the CAD design. Although there are no current restorative materials available for 3D printing, models for clear orthodontic aligners, bitesplints, and implant surgical guides are readily 3D printed by a number of in-office printers.

One rapidly growing application for in-office digital technology is for dental implant therapy. There are two primary applications. The first is during the planning phase of implant treatment. Cone Beam Computer Tomography (CBCT) has become a preferred preoperative 3D diagnostic tool for optimizing the surgical placement of the implant, and CAD/CAM designed surgical guides can be created to guide surgical implant placement. Several chairside CAD/CAM systems have the capability to export the .stl file from their software program and by using a second software program, merge it with the dicom file from the CBCT to provide a totally integrated prosthetic-influenced refinement for implant placement.

Surgical guides can also be ordered from the digital planning system, to be created either at a dental laboratory or in-office milling chamber. The CEREC OmniCam integrates seamlessly with the Galileos CBCT through proprietary Sirona Galaxis software. The PlanScan and Planmeca Romexis also allow integration of files with several CBCT systems. In addition, there are a number of third-party software programs, such as Blue Sky Plan (Blue Sky Bio), Invivo6 (Anatomage), and Simplant (Dentsply Sirona), that can import dicom and .stl files from chairside CAD/CAM system for implant planning and surgical guide fabrication (see Figure 7).

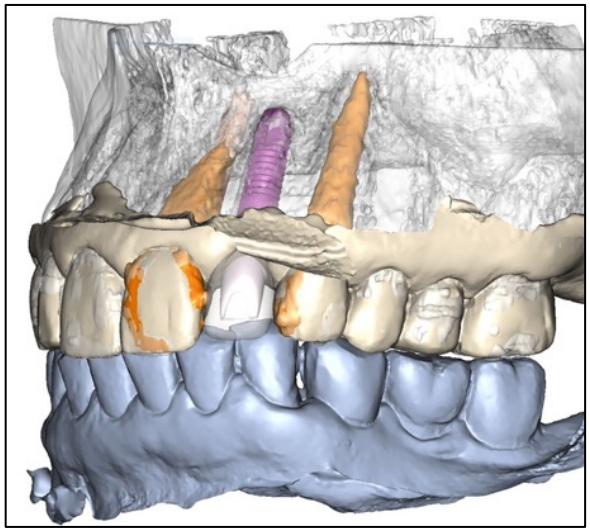

Figure 7. CBCT showing the planned implant location and restoration. Fabrication of the custom surgical guide will factor osseous anatomy, nerves, and root proximity.

A second implant-specific application for CAD/CAM is the in-office design and fabrication of custom abutments and restorations for implants. The introduction of Scan Posts and Scan Bodies by Sirona Dental provides intra-oral digital fixture level impressions that can be matched with overlaying soft tissue scans for the development and design of custom abutments for ten different implant systems using the CEREC OmniCam.

As the ease and efficiency of recording full arch scans has improved, orthodontic applications for digital impressions have significantly increased. Digital files are used for orthodontic diagnosis and treatment planning, case documentation, as well as appliance design and fabrication. Of particular interest to orthodontists is the ability to store case documentation electronically rather than committing significant storage areas to cataloging models and boxes.

Application of the digital workflow continues to grow in the orthodontic practice. Invisalign™ (Align Technologies) popularized the use of clear aligners for orthodontic treatment in 1997 [12]. Using a hybrid technique of digitizing a conventional impression, Align Technologies were the first to leverage the efficiency and predictability of CAD technology to progressively treat mild to moderate Angle's Class I malocclusion. As the accuracy of the digital scanners improved, the workflow progressed from an analog/digital hybrid to exclusively digital. As the technology improves, so does the ability to treat more complex cases.

CLINICAL LONGEVITY

A significant number of published studies report the long-term clinical performance of CEREC restorations, in contrast with a general lack of clinical evidence regarding other chairside systems. This is primarily due to the fact that the CEREC System has been available since the early 1990s and other systems have been more recently introduced. A systematic review of 29 clinical studies (2,862 CEREC ceramic inlays) reported a survival rate of 97.4% after a period of 4.2 years [13]. The primary mode of failure was fracture of the ceramic restoration. Less common failure modes included fracture of the tooth, wear of the cement, and postoperative sensitivity. Another systematic review focused on survival rates of longer-term clinical trials [14]. A total of 1,957 single-tooth restorations (98% anterior) fabricated with CAD/CAM technology were followed more for than 3 years of functional service. The calculated failure rate was 1.75% per year estimated per 100 restoration years, based on the survival rate of 91.6% after 5 years. The most common modes of failure reported were fractures of the restoration or the tooth. A number of longer-term studies of CEREC restorations have also been published. One study evaluated the longitudinal performance of 310 CEREC onlays [15]. One operator placed all restorations with an effort to create all preparation margins within enamel. After 8 years of follow up, 286 paired onlays were available for evaluation. The calculated survival probability was 99.3%. The only two failures observed in this study were fractures on maxillary premolars of one patient with occlusal parafunction. A study of 2,328 inlays and onlays for 794 patients in a private practice reported 35 failures over 9 years [16]. The Kaplan-Meier survival probability reported was 97.4% at 5 years and 95.5% at 9 years. Another study reported a Kaplan-Meier survival probability of 90.4% after 10 years for 200 Vitablocks Mark II restorations placed in 108 patients in private practice [17]. In a follow-up report of that study, the authors reported an 88.7% success rate at 17 years.[18]

A series of papers from 1991 to 2006 reported the clinical status of 1,011 CEREC restorations for up to 18 years [19-21]. The survival probability was 95% after 5 years, 91.6% after 7 years and 90% at 10 years. It declined to 84.9% at 16.7 years. There are a few studies of high strength chairside CAD/CAM restorations. One reported the performance of chairside CAD/CAM-generated IPS e.max CAD crowns [22]. A CEREC system was used to deliver 41 IPS e.max CAD full-contour crowns (34 patients). One crown exhibited secondary caries and two crowns received root canal treatment after two years. An ongoing longitudinal clinical study is evaluating the clinical performance of 100 IPS e.max CAD full-contour crowns [23-25]. The first 62 crowns were delivered with a self-etching bonding agent and resin cement (MultiLink Automix [Ivoclar]) or an experimental self-adhesive resin cement. A second group of 38 crowns was placed at a later time using a newer self-etching, self-curing, cement (SpeedCem [Ivoclar]). Each of the full-contour crowns was placed in a single treatment appointment with the CEREC system. There were no reported failures after two years and no chipping or cracking were clinically visible. The percent alpha score (the percentage of examined restorations with an evaluated characteristic not significantly different from the baseline evaluation) was above 95% for color match at all recall intervals and remained at 100% for margin adaptation and absence of caries for all crowns at five years. Four crowns debonded (3 cemented with the experimental cement [13, 20 and 36 months] and 1 with MultiLink Automix [36 months]). One crown cemented with SpeedCem presented evidence of crown fracture without loss of material at 48 months [26].

CONCLUSIONS

What began as a restorative vision to leverage digital technology in dentistry for single-tooth restorations now includes both diagnostic and therapeutic applications in orthodontic, implant, and removable prosthodontics. Advancements in technology resulted in more efficient and accurate additive and subtractive workflows resulting in better outcomes in less time. Modern materials and equipment

developed for the chairside manufacturing process enable treatment planning of high-strength ceramics for same appointment procedures. Decades of research demonstrated that the foundation of the digital dental vision, single tooth restorative dentistry, was successful and long lasting. Modern intra-oral scanners are accurate and capable of inclusion into all elements of the comprehensive general dentistry or specialty practice. The question in digital dentistry has changed from, "When will digital dental technology be evolved enough to include in my practice?" to, "How soon can I make digital dental technology a part of my everyday practice?"

REFERENCES

1. Duret F, Preston JD. CAD/CAM imaging in dentistry. Curr Opin Dent 1991;1(2):150-154.

2. Mormann WH, Brandestini M, Lutz F, Barbakow F. Chairside computer-aided direct ceramic inlay. Quintessence Int 1989;20(5:325-339.

3. Renne W, Ludlow M, Fryml J, Schurch Z, Mennito A, Kessler R, Lauer A. Evaluation of the accuracy of 7 digital scanners: An in vitro analysis based on 3-dimensional comparisons. J Prosthet Dent 2017;118:36-42.

4. Treesh JC, Liacouras PC, Taft R, Brooks D, Raiciulescu S, Ellert D, Grant G, Ye L. Complete-arch accuracy of intraoral scanners. J Prosthet Dent 2018;120:382-388.

5. Anderson GC, Schulte JK, Arnold TG. Dimensional stability of injection and conventional processing of denture base acrylic resin. J Prosthet Dent 1988;60:394-398.

6. Hirogaki Y, Sohmura T, Satoh H, Takahashi J, Takada K. Complete 3-D reconstruction of dental cast shape using perceptual grouping. IEEE Trans Med Imaging 2001;20:1093–1101.

7. Schirmer UR, Wiltshire WA. Manual and computer-aided space analysis: a comparative study. Am J Orthod Dentofac Orthop 1997;112:676–680.

8. Lee, KM. Comparison of two intraoral scanners based on three-dimensional surface analysis. Prog Orthod 2018;19:6.

9. Rekow ED, Silva NRFA, Coelho, PG, Zhang Y, Guess P, Thompson VP. Performance of Dental Ceramics: Challenges for Improvements. J Dent Res 2011;90(8):937-952.

10. Kelly JR. Dental Ceramics. JADA 2008;139 Supplement 4:S4-S7.

11. Charlton DG, Roberts HW, Tiba A. Measurement of select physical and mechanical properties of 3 machinable ceramic materials. Quintessence Int 2008;39:573-579.

12. Meier B, Wiemer KB, Miethke RR. Invisalign™ - Patient Profiling. J Orofac Orthop 2003;64(5): 352-358.

13. Belli R, Geinzer E, Muschweck A, Petschelt A, Lohbauer U. Mechanical fatigue degradation of ceramics versus resin composites for dental restorations. Dent Mat 2014;30(4):424-432.

14. Dentsply Celtra Duo Fact File. December 2013. Accessed at: http://www.scribd.com/doc/194110793/Celtra-Duo-Fact-File-Degudent#scribd.

15. Rusin RP. Properties and applications of a new composite block for CAD/CAM. Compend Contin Educ Dent 2001;22(6 Suppl):35-41.

16. Martin N, Jedynakiewicz NM. Clinical performance of CEREC ceramic inlays: a systematic review. Dent Mat 1999;15(1):54-61.
17. Wittneben JG, Wright RF, Weber HP, Gallucci GO. A Systematic Review of the Clinical Performance of CAD/CAM Single-Tooth Restorations.Int J Prosthodont 2009;22(5):466- 471.

18. Arneltz GV, Arneltz G. Reliability of non-retentive all-ceramic CAD/CAM overlays. Int J Computerized Dent 2012;15:185-197.

19. Posselt A, Kerschbaum T. Longevity of 2328 chairside CEREC inlays and onlays. Int J Comput Dent 2003;6(3):231-248.

20. Otto T, De Nisco S. Computer-aided direct ceramic restorations: A 10-year prospective clinical study of CEREC CAD/CAM inlays and onlays. Int J Prosthodont 2002;15(2):122-128.

21. Otto T, Schneider D. Long-term clinical results of chairside CEREC CAD/CAM inlays and onlays: a case series. Int J Prosthodont 2008;21(1):53-59.

22. Reiss B, Walther W. Survival analysis and clinical evaluation of CEREC restorations in a private practice. In: Morman WH, ed*. International Symposium on Computer Restorations* 1991: State of the Art of the CEREC-Method. Berlin, Germany: Quintessence Publishing 215.

23. Reiss B, Walther W. Clinical long-term results and 10-year Kaplan-Meier analysis of CEREC restorations. Int J Comput Dent 2000:3(1):9-23.

24. Reiss B. Clinical results of CEREC inlays in a dental practice over a period of 18 years. Int J Comput Dent 2006:9(1):11-22.

25. Reich S, Fischer S, Sobotta B, Klapper HU, Gozdowski S. A Preliminary Study on the Short-Term Efficacy of Chairside Computer-Aided Design/Computer-Assisted Manufacturing–Generated Posterior Lithium Disilicate Crowns. Int J Prosthodont 2010;23:214-216.

26. Fasbinder DJ, Dennison JB, Heys DR, Neiva GF. Clinical evaluation of lithium disilicate chairside CAD/CAM crowns at 4 years. J Dent Res 2012;91(Spec issue A): Abstract #645.

THREE-DIMENSIONAL ASSESSMENT OF TOOTH MOVEMENT: A NEW METHOD FOR SUPERIMPOSITION OF DIGITAL MODELS

Ahmed A Ghoneima, Sameh M Talaat

ABSTRACT

Superimposition of the patient's two-dimensional (2D) cephalograms is traditionally indicated whenever evaluation of orthodontic treatment and/or growth is required. Recently, superimposing the three-dimensional (3D) digital models or cone beam computed tomography (CBCT) images made it possible to assess these changes in a 3D manner. The current digital model software available in the orthodontic market rely on the surface-based best fit method for superimposing the digital models. This is because of the simplicity of the procedure for the end users; yet the systemic errors that may occur are totally neglected. The best fit superimposition method misses the remodeling that occurs in the anatomy of the treated patients. It was thus suggested that using stable anatomical landmarks as a reference plane for the superimposition process yields more accurate results. The aim of this project was to identify and evaluate a user-friendly, valid, and reliable technique to superimpose digital maxillary models on stable anatomical landmarks and perform subsequent 3D assessment of the orthodontic tooth movement to confirm reliability. We collected data from four different studies to investigate a newly introduced algorithm and software for superimposition of the digital dental models using stable anatomical landmarks. The technique offered an innovative method for 3D assessment of tooth movement. In addition, the new software algorithms studied in the current project were found to offer a valid and reliable technique for superimposition and were still simple to use.

KEY WORDS: Superimposition, Digital Dental Models, Tooth Movement, Cone Beam Computed Tomography, Anatomical Landmarks

INTRODUCTION

In the digital era, 3-dimensional (3D) imaging has become one of the most important tools used in the field of orthodontics. The idea of 3D digital imaging has proved to be an accurate method for patient diagnosis, and now 3D digital imaging has a major impact on clinical orthodontics. Interactive 3D images of hard and soft tissues of the dental patients provide quantitative evidence to aid the orthodontist in diagnosis, treatment planning, and outcome assessment [1-4]. Moreover, electronic storage of all patients' information, including study casts, eliminate the problems of storage, retrieval, maintenance of

models, and office management. Documentation of treatment progress and communication between professional colleagues also allows easier consultation [5-9].

In the final stage of orthodontic treatment, the orthodontist requires lateral cephalometric and panoramic radiographs prior to debonding of brackets to allow proper assessment of root positions with respect to the aimed tip, torque, and rotational values [10-12]. Also, superimposition between pre-treatment and post-treatment lateral cephalometric radiographs is performed to assess treatment outcome [13-15]. The innovation of 3D scanned models is an effective tool for the evaluation of the tooth angulations (measured as the angle between the long axis of the tooth and the occlusal plane when seen from the facial perspective, also known as mesio-distal tip), inclinations (measured as the angle between a tangent to the facial surface of the tooth and the occlusal plane when seen from the proximal perspective, also known as bucco-lingual torque) and rotational values needed to assess the treatment outcomes [16-18].

In the current project, four different studies were conducted to identify and assess the reliability and validity of a newly introduced algorithm for superimposition of digital dental models using stable anatomical landmarks. The first research study focused on the creation of a software program (Ortho Mechanics Sequential Analyzer, OMSA) that is capable of superimposing digital maxillary models in a user-friendly manner and performing 3D assessment of orthodontically treated teeth in six degrees of freedom. It was programmed to perform landmark based superimposition to avoid the inaccuracy of the best fit methods. The aim of the first study was to assess the validity of the OMSA software [19]. The second study was carried out to modify the algorithm to simplify the superimposition process. The amount of preparation needed by the end user to superimpose the digital maxillary models was reduced to only three mouse clicks. The study investigated the validity and reliability of the algorithm [20]. The rationale of the third study was to create an algorithm that can perform landmark based superimposition in a fully automatic manner without the need of the mouse clicks to define the stable anatomic landmarks. That was achieved by integrating a computer vision algorithm in OMSA. Maxillary digital models were scanned by intra-oral scanners that can scan color and surface texture as well as volume. The aim of this third study was to assess validity and reliability of this computer vision algorithm integrated in OMSA [21]. In the fourth study, the whole experience was performed on a new Augmented Reality platform, Microsoft HoloLens. The aim of this study was to test the validity and reliability of OMSA operated by using hand gestures to localize the stable anatomical landmarks on holograms of the digital maxillary models displayed by the Microsoft HoloLens [22].

The retrospective sample of the first study included the pre- and post-treatment CT images and the 3D digital maxillary dental models of 20 orthodontic patients with transverse maxillary deficiency. The study was approved by the Indiana University Purdue University Indianapolis Institutional Review Board Committee. The patients' ages ranged from 8 to 15 years (mean 12.3 ±1.9 years). They had been treated by rapid maxillary expansion with a hyrax appliance as part of their comprehensive orthodontic treatment. Models included in the study had no gross dental abnormalities or obvious distortions. Models of surgically assisted palatal expansion cases were excluded in order to be able to use the model's palatal rugae area and mid-palatal raphe as reference planes for superimposing the laser scanned pre-treatment and post-treatment models. The same sample was used for all four studies in this project [19].

Dental models were scanned using Ortho Insight 3D laser scanner (Motionview LLC**,** Hixson**,** TN) with scanning resolution set at 20 µm. The scan data of the pre-treatment and post-treatment models were exported from the laser scanner in STL format file extension. These STL files were imported into Ortho Mechanics Sequential Analyzer (OMSA, US Provisional Patent Application No. 61/771,328). After orienting the pre-treatment and post-treatment digital models, they were superimposed using the OMSA software by registering two points on the digital maxillary model. The first point was located at the distal end of the incisive papilla and the second point was located distal to the first point along the mid-palatal

raphe. The software is programmed to automatically draw a 3D reference plane on the palatal area for superimposing the pre-treatment and post-treatment digital models (Figure 1).

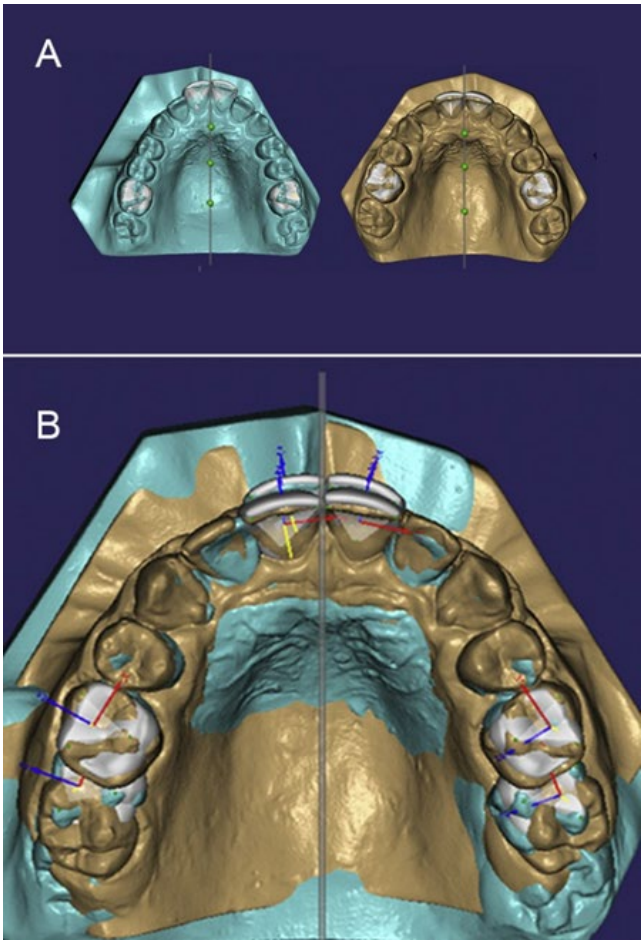

Figure 1. A) pre- and post-treatment digital models; B) Superimposition of the pre-treatment (blue) and post-treatment models based on registering 2 points along the midline of the maxillary dental models.

The CT DICOM files were imported into InvivoDental 3D (version 5.1, Anatomage, San Jose, CA). After landmark identification, 14 measurements (6 linear and 8 angular) were recorded from both the CT data and the digital models. All parameters were measured on both the digital models using the OMSA and the CT images using InvivoDental 3D. In order for the software to be able to simulate the root position, the outlines of the maxillary central incisors, canines, and first molar crowns were defined and outlined by positioning 3 dots on each tooth crown. Then an avatar (a simulated or virtual tooth and root) is automatically created for the tooth of interest showing the root positions according to the software algorithm (Figure 2).

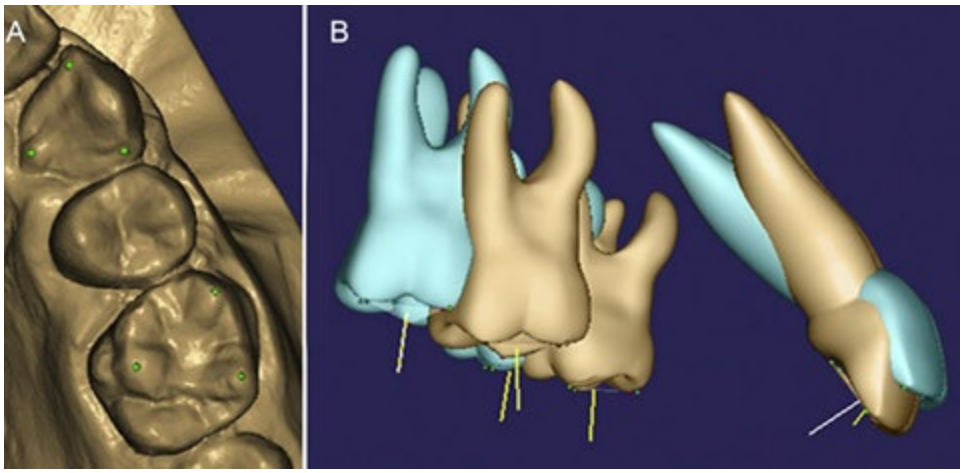

Figure 2A and B. The software simulates the root position by locating certain points (green dots) on the tooth crowns (Fig. 2A denotes occlusal view, Fig. 2B denotes sagittal view).

The software was programmed to define a coordinate system related to these teeth guided by the points placed by the operator as explained in the previous step. The software measures the relation between the teeth coordinates in its pre-treatment and post-treatment positions. The coordinate system is composed of the three axes of rotation around which a body can rotate in space (Figure 3).

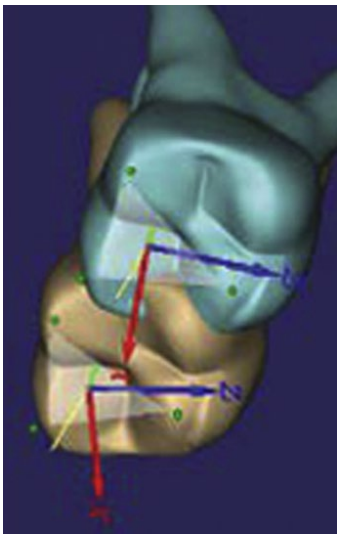

Figure 3. The coordinate system of the pretreatment and posttreatment teeth as generated by the software.

The angle difference between the labio-lingual/bucco-lingual axis of the pre-treatment and post-treatment avatars is used to describe the change in torque during treatment. The difference in tooth tipping can be described from the angle between the mesio-distal axes before and after treatment. The measured linear and angular changes were recorded in Microsoft Office Excel sheets for comparing with similar measurements taken from the CT images using the InvivoDental software. Measurements are described in Table 1.

Table 1. Definitions of linear and angular measurements used in the project.

Parameter	**Definition**
R1 Torque (°)	Change in right maxillary central incisor labio-lingual inclination
R1 Tip (°)	Change in right maxillary central incisor mesio-distal angulation
L1 Torque (°)	Change in left maxillary central incisor labio-lingual inclination
L1 Tip (°)	Change in left maxillary central incisor mesio-distal angulation
R6 Torque (°)	Change in right maxillary first permanent molar bucco-lingual inclination
R6 Tip (°)	Change in right maxillary first permanent molar mesio-distal angulation
L6 Torque (°)	Change in left maxillary first permanent molar bucco-lingual inclination
L6 Tip (°)	Change in left maxillary first permanent molar mesio-distal angulation
R6 Translation (mm)	Distance from the maxillary right first permanent molar furcation point to the mid-palatal raphe
L6 Translation (mm)	Distance from the maxillary left first permanent molar furcation point to the mid-palatal raphe
Intercanine width (mm)	Distance between right and left maxillary canine cusp tips
Intermolar width (mm)	Distance between tips of the mesio-buccal cusps of maxillary right and left first permanent molars

Measurements on digital models and on the CT images were repeated under the same conditions with a time interval of one week. All measurements were performed by the same examiner. Reliability was estimated as the extent to which the measurements on digital models and the CT images were repeatable under the same conditions. Validity was considered as the extent to which measurements made on the digital models and the CT images yielded equal results. In the second study, the superimposition algorithm was modified to reduce the amount of work needed to only three mouse clicks. This means that the digital model orientation steps were no longer needed because of this newly introduced simplified method (Figure 4). To test the validity and reliability of the 3 mouse clicks algorithm, the same sample was used. The digital models were superimposed using 3dMDvultus software (3dMD, Atlanta, GA) using the best fit surface-based method.

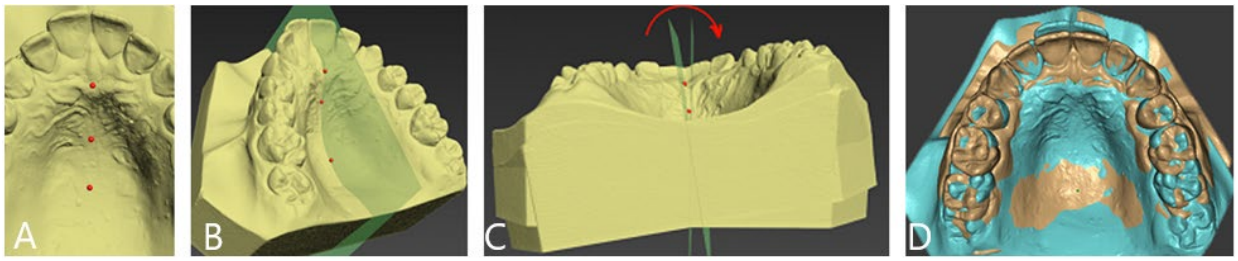

Figure 4. A) The three landmarks used for superimposition using OMSA software. B) Reference frame created by connecting the three selected landmarks along the mid-palatal raphe for model registration and superimposition. C) Model rotation to coincide the selected landmarks with the 3D coordinate. D) The final superimposition results after registration to the same reference frame.

Statistical analysis for the first two studies was carried out using SPSS 12.0.1 (SPSS, Chicago, IL) software. Intra-observer reliability was assessed by calculating intra-class correlation coefficients (ICC). Agreement between the digital models and the CT measurements was evaluated using intra-class correlation coefficients (ICCs), paired t-tests, and Bland-Altman plots. A p-value of ≤0.05 was considered statistically significant.

The aim of the third study was to evaluate the validity and reliability of 3D landmark-based palatal superimposition of digital dental models using computer vision algorithm added to the customized OMSA. For each case, the pre- and post-treatment digital models were superimposed using color detection capabilities of a computer vision algorithm added to OMSA as well as a conventional landmark based method (Figure 5). The same set of parameters was measured on the superimposed 3D data by the two software versions for comparison. In the fourth study, the aim was to assess validity and reliability of 3D palatal superimposition of holograms of 3D digital dental models using a customized OMSA installed on a Microsoft HoloLens device, compared to the conventional OMSA application running on a regular computer screen (Figure 6). Agreement in the superimposition outcomes among the two superimposition methods of both the third and fourth study were evaluated with Dahlberg error (DE), ICCs using two-way ANOVA mixed model for absolute agreement and Bland-Altman agreement limits (LOA).

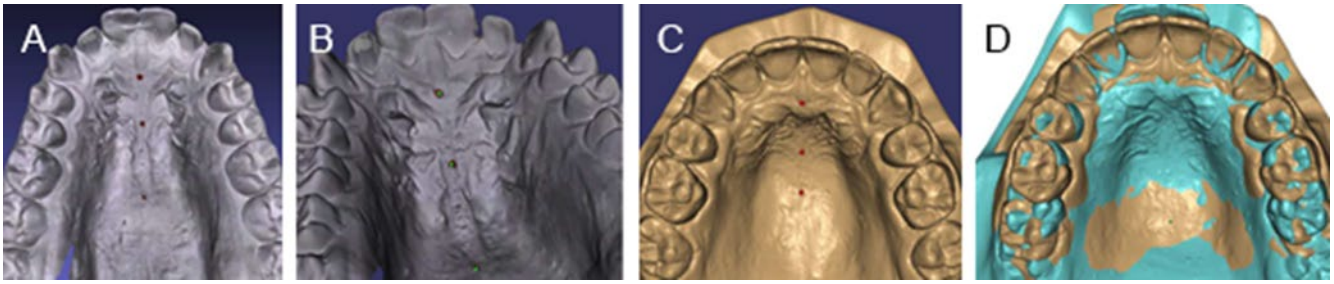

Figure 5. A) Digital model showing the marking with three red dots on the mid- palatal raphe. B) All the three points as green dots mapped to their relative landmarks, performed in the same way of the conventional OMSA superimposition algorithm. C) Selection of three landmarks along the mid- palatal raphe. D) Pre- and post-treatment digital models registered to the same frame of reference.

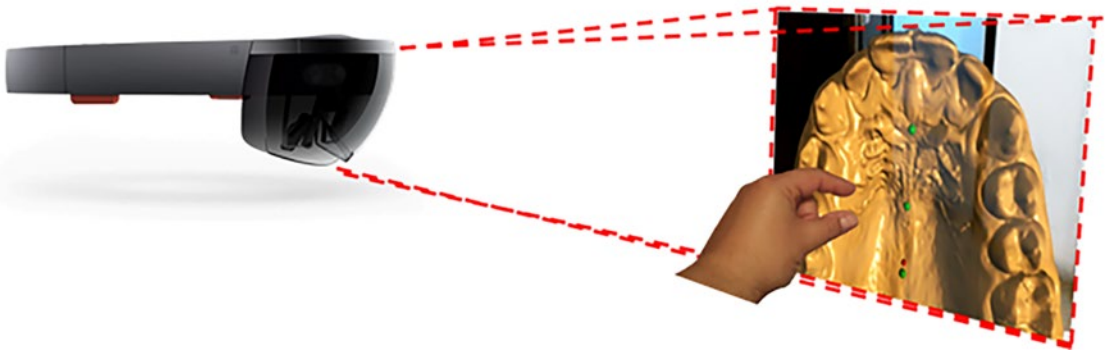

Figure 6. The three landmarks used for superimposition using stereovision to locate landmarks by HoloLens hand gestures.

RESULTS

In the first study, assessing the validity of the digital models using OMSA software by comparing it with the CT images using InvivoDental 3D, high agreement (ICC>0.9), a non-significant paired t-test, and no indication of agreement discrepancies were observed for R1 torque, L1 torque, L1 tip, R6 tip, L6 tip, L6 torque, L6 translation, intercanine Pre, intercanine Post, and intermolar Post. R1 torque had a high ICC and no significant mean difference but the Bland-Altman plot showed that the amount of disagreement between the methods was larger for higher measurements. R1 tip was consistently higher for the digital model than for CT, and the discrepancy was larger for higher measurements. R6 torque was consistently lower for the digital model than CT. R6 tip showed good agreement (ICC=0.89), with some indication of more disagreement for higher measurements. L6 tip showed moderate agreement (ICC=0.82) with a single outlier with large disagreement. R6 translation was generally higher for the digital model than CT. L6 translation had the lowest agreement between all measurements.

In the second study, modifying the algorithm to simplify the superimposition process, reliability of each method and agreement among the methods as measured by the ICCs was high. ICC≥0.90 was reported for all measurements except for R6 MB cusp tip with ICC of 0.88 using 3dMDvultus. Statistically significant differences were detected among the methods for R6 MB cusp tip, R6 DB cusp tip, L6 MB cusp tip, R1, and L1. The three mouse clicks algorithm had significantly lower R6 MB cusp tip than 3dMD ($p=0.0399$) and 3dMDvultus ($p=0.0272$).The 3 mouse clicks algorithm had significantly lower R6 DB cusp tip than 3dMD ($p=0.0128$) and Anatomage ($p<0.0001$) and 3dMD had significantly lower R6 DB cusp tip than Anatomage ($p=0.0003$). Anatomage had significantly higher L6 MB cusp tip than 3dMD ($p=0.0489$) and the three mouse clicks algorithm ($p=0.0117$). Anatomage had significantly higher R1 than 3dMD ($p=0.0054$) and the three mouse clicks algorithm ($p=0.0001$). Anatomage had significantly higher L1 than 3dMD ($p=0.0082$) and the three mouse clicks algorithm ($p=0.0003$).

In the third study, the Dahlberg error ranged from as low as 0.1 mm up to 0.4 mm. Hence, the absolute error did not exceed 0.5 mm for any variable. The relative Dahlberg error ranged from as low as 0.4% up to 15.3% with only two variables exceeding 10% (R1 and L1) due to the small value of their mean, which made Relative Dahlberg Error (RDE) high although their absolute DE were small with 0.2 mm and 0.3 mm, respectively. The mean difference between standard OMSA software and OMSA computer vision algorithm ranged from -0.2 mm up to 0.2 mm indicating small bias or shift from zero. For nine variables the mean differences were negative, meaning that OMSA computer vision algorithm tends to give larger values, while for the other three variables (L3 cusp tip, inter-canine width post-treatment, and inter-first molar width post-treatment) the mean differences were positive. Standard deviations of the differences ranged from 0.2 mm to 0.5 mm, again less than 0.5 mm for any variable. ICCs ranged from 0.98 to 1.00

with their lower 95% confidence limit ranging from 0.95 to 1.00. The following four variables, inter-canine width pre-treatment, inter-canine width post-treatment, inter-first molar width pre-treatment, and inter first molar width post-treatment, had in general the lowest RDE less than 1% and the highest ICC with all values above 0.99.

Finally, in the fourth study, reliability of each method and agreement among the two methods (computer based OMSA vs HoloLens based OMSA) as measured by the ICCs was high. ICC≥0.90 was reported for all measurements except for the distance between superimposed R6 MB cusp tips with ICC of 0.88 using the HoloLens. The computer based OMSA produced significantly higher distance between superimposed L6 MB cusp tip values than OMSA running on the HoloLens (P=0.0489) and OMSA (P=0.0117). The statistically significant differences between some of the measured parameters among the two superimposition methods were clinically acceptable from the orthodontic point of view.

CONCLUSIONS

Results obtained from all four studies indicated that the newly developed OMSA software offers a valid and reliable tool with regard to dental arch measurements obtained from 3D laser scanned models. It enables the operator to assess the tooth movement by determining the position of the crown and the root, where both linear and angular parameters can be measured. It could be considered a possible practical method that helps the orthodontist follow up the treatment progress in a non-invasive manner and without unnecessary radiation exposure. OMSA reduced the number of steps needed to perform landmark based superimposition of digital maxillary models to only three mouse clicks placed along the mid-palatal raphe.

With the evolution of color detecting intra-oral scanners, computer vision algorithms applied to the OMSA software offered valid and reliable superimposition of 3D digital maxillary models obtained by intra-oral color detecting 3D scanners. This helped to reduce the human errors required to locate registration points for landmark based palatal superimposition of 3D digital maxillary models. Finally, with the evolution of Augmented Reality (AR) technologies operating on smart glasses, and using the depth vision capabilities of the Microsoft HoloLens, OMSA was installed on Microsoft HoloLens. Hence, holograms of 3D digital maxillary dental models can be visualized, landmarks can be selected by stereovision and superimposed to interactively assess 3D orthodontic treatment outcomes in AR scenes. Advanced visualization using emerging technology such as AR warrants future study.

REFERENCES

1. Thiruvenkatachari B, Al-Abdallah M, Akram NC, Sandler J, O'Brien K. Measuring 3- dimensional tooth movement with a 3-dimensional surface laser scanner. *Am J Orthod Dentofacial Orthop* 2009;135:480-485.

2. Santoro M, Galkin S, Teredesai M, Nicolay OF, Cangialosi TJ. Comparison of measurements made on digital and plaster models. *Am J Orthod Dentofacial Orthop* 2003;124:101-105.

3. Schirmer UR, Wiltshire WA. Manual and computer-aided space analysis: a comparative study. *Am J Orthod Dentofacial Orthop* 1997;112:676-680.

4. Shah S, Sundaram G, Bartlett D, Sherriff M. The use of a 3D laser scanner using superimpositional software to assess the accuracy of impression techniques. *J Dent* 2004;32:653-658.

5. Rheude B, Sadowsky PL, Ferriera A, Jacobson A. An evaluation of the use of digital study models in orthodontic diagnosis and treatment planning. *Angle Orthod* 2005;75:300-304.

6. Whetten JL, Williamson PC, Heo G, Varnhagen C, Major PW. Variations in orthodontic treatment planning decisions of Class II patients between virtual 3-dimensional models and traditional plaster study models. *Am J Orthod Dentofacial Orthop* 2006;130:458-491.

7. Zilberman O, Huggare JA, Paikakis KA. Evaluation of the validity of tooth size and arch width measurements using conventional and three-dimensional virtual orthodontic models. *Angle Orthod* 2003;73:301-306.

8. Al-Dashti AA, Cook PA, Curzon ME. A comparative study on methods of measuring mesiodistal tooth diameters for interceptive orthodontic space analysis. *Eur J Pediatr Dent* 2005;6:97-104.

9. Asquith J, Gillgrass T, Mossey P. Three-dimensional imaging of orthodontic models: a pilot study. *Eur J Orthod* 2007;29:517-522.

10. Kuroda T, Motohashi N, Tominaga R, Iwata K. Three-dimensional dental cast analyzing system using laser scanning. *Am J Orthod Dentofacial Orthop* 1996;110:365- 369.

11. Macchi A, Carrafiello G, Cacciafesta V, Norcini A. Three-dimensional digital modeling and setup. *Am J Orthod Dentofacial Orthop* 2006;129:605-610.

12. Garino F, Garino GB. Comparison of dental arch measurements made on stone and digital casts. *World J Orthod* 2002;3:250-254.

13. Freshwater M. 3D digital dental models using laser technology. *J Clin Orthod* 2003;37:101-103.

14. Quimby ML, Vig KW, Rashid RG, Firestone AR. The accuracy and reliability of measurements made on computer-based digital models. *Angle Orthod* 2004;74:298-303.

15. Keating AP, Knox J, Bibb R, Zhurov A. A comparison of plaster, digital and reconstructed study model accuracy. *J Orthod* 2008;35:191-201.

16. Cha BK, Choi JI, Jost-Brinkmann PG, Jeong YM. Application of three-dimensionally scanned models in orthodontics. *Int J Comput Dent* 2007;10:41-52.

17. Chen H, Lowe AA, de Almeida FR, Wong M, Fleetham JA, Wang B. Three-dimensional computer-assisted study model analysis of long-term oral-appliance wear. Part 1: Methodology. *Am J Orthod Dentofacial Orthop* 2008;134:393-407.

18. Kusnoto B, Evans CA. Reliability of a 3D surface laser scanner for orthodontic applications. *Am J Orthod Dentofacial Orthop* 2002;122:342-348.

19. Talaat S, Kaboudan A, Breuning H, Ragy N, Elshebiny T, Kula K, et al. Reliability of linear and angular dental measurements with the OrthoMechanics Sequential Analyzer. *Am J Orthod Dentofacial Orthop* 2015 Feb;147(2):264-269.

20. Talaat S, Kaboudan A, Breuning H, Ragy N, Kula K, Ghoneima A. Validity and reliability of three-dimensional palatal superimposition of digital dental models. *Eur J Orthod*. 2017 Aug 1;39(4):365-370.

21. Talaat S, Kaboudan A, Abdelbary O, Kula K, Ghoneima A, Klien R, et al. 3D Superimposition of Dental Casts Based on Colored Landmark Detection Using Combined Computer Vision and 3D Computer Graphics Techniques. *Computer Methods in Biomechanics and Biomedical Engineering: Imaging & Visualization*. DOI: 10.1080/21681163.2019.1585295

22. Talaat S, Ghoneima A, Kaboudan A, Talaat W, Ragy N, Breuning H. Three-dimensional evaluation of the holographic projection in digital dental model superimposition using HoloLens device. *Orthod Craniofac Res*. 2019;22 (Suppl 1):62-68.

LONG-TERM DENTAL ARCH CHANGES IN EXTRACTION AND NON-EXTRACTION PATIENTS USING THREE-DIMENSIONAL (3D) DIGITAL MODELS

Preston Greer, Josh Knowles, Jeryl D. English, Wick G. Alexander, J. Moody Alexander, Sercan Akyalcin

ABSTRACT

Visualization and quantification of the dental arch form using 3D digital dental models enable a higher level of information for clinical and research purposes. In this manuscript, we investigated the long-term changes of the dental arches using digital dental models. The cohort included complete pretreatment (T1), posttreatment (T2), and postretention (T3) records of 63 orthodontic patients (n=32, extraction; n=31, non-extraction) with Angle Class I malocclusion, normal vertical and sagittal skeletal growth, and no apparent transverse discrepancy. The study groups were subdivided according to the initial mandibular dental arch form: ovoid, tapered, and square. Incisor irregularity and transverse linear widths at the level of canines, first premolars, and first molars were measured for all time periods. Additionally, average linear surface changes were evaluated from pretreatment to postretention. Significant group x time interactions were found for mandibular canine, maxillary and mandibular premolar as well as molar width measurements ($p<0.05$). There were also significant arch form x time interactions for mandibular premolar, maxillary and mandibular molar width measurements ($p<0.05$). However, group x time x arch form interaction was not significant for any of the arch width measurements studied. Frequency of arch form changes in the postretention period did not differ between the study groups. However, significant treatment and postretention differences occurred in the dental arch form for individuals with tapered and square arch forms when compared to individuals with ovoid arches ($p<0.05$). No evident difference was found between the extraction and non-extraction groups in the long-term evaluation of average surface changes.

KEY WORDS: 3D Models, Arch Form, Extraction, Non-extraction

INTRODUCTION

An abundance of treatment options became available recently due to the increased number of technological innovations including advancements in orthodontic wires, bracket designs, and access to three-dimensional (3D) applications [1-6]. One of the advantages these innovations provided was the ability to treat the majority of orthodontic cases without extractions utilizing better diagnostic approaches and incorporating better materials and techniques in the treatment [7-9]. However, there has been continuous discussion in orthodontics over the years debating if long-term retention of treatment

outcome is achievable, and if it can be credited to extraction, non-extraction, expansion, or arch form change [10,11]. Orthodontic cases most certainly benefit from virtual treatment planning platforms. The precision of measuring crowding, irregularity indices, Bolton discrepancy, and treatment projections are higher than ever [12]. The recent digital advances have been a huge asset in helping orthodontists make treatment decisions, specifically regarding premolar extractions [13,14]. Another advantage of using virtual digital technology is the ability to visualize and quantify the treatment changes using computer software.

The introduction part of this chapter is divided into four sections that includes a brief background on the topics that led to the origination of our investigation.

Three-dimensional (3D) Dental Models

Three-dimensional (3D) scanning technology has come a long way from the days of its inception in 1960s. The earliest digital 3D scanners of the 1980s used physical probes that contacted the surface of an object almost thousands of times until the device registered enough data points to acquire a 3D digital model [15]. By the end of 1985, computers made it possible to use white light, lasers, and shadowing to scan surfaces of objects [16]. The development of the animation industry enabled facial and body scanning in the 1990s. By 1996, 3D scanners were getting closer to the finish line - the only disadvantage they had was capturing reflections from shiny and transparent objects.

Considering the dental literature, one of the first papers that used laser scanning for analyzing casts was introduced in 1996. The cast analyzing system was based on collection of 90,000 sets of x, y, and z coordinates that were stored in the main memory of the microcomputer, and generation of 3D graphics took about 40 minutes [17]. The first prototype of a computer-based intraoral laser scanner appeared in 2000 [18]. From end of 1990s through the 2000s, the predominant type of 3D models used in orthodontics were based on commercial systems such as OrthoCad (Cadent, Carlstadt, NJ, USA), eModels (GeoDigm, Chanhassen, MN, USA), and Digimodel (Orthoproof, Albuquerque, NM, USA). These model systems relied on scanning a conventional impression or plaster model to produce the digital file. A systematic review concluded that digital models produced by these systems offered a high degree of validity when compared to direct measurement on plaster models and differences between the approaches were likely to be clinically acceptable [19].

One of the most exciting developments in orthodontics was the introduction of the iTero digital impression system (Cadent, Carlstadt, NJ, USA) in 2006. This intraoral scanning system was developed to scan full dental arches in 2008 and led to the development of the iOC powered by iTero (Cadent, NJ, USA) in late 2009 [20]. Following this date, many other intraoral scanning systems were introduced for orthodontic purposes. With current technology, intraoral scanners are offered with much more practicality in terms of scanning times, patient comfort, and portability [21,22].

A major advantage of using 3D models as opposed to physical models is the ability of registering the surface area to examine the changes from various time points. One of the earliest investigations of model superimposition relied heavily on the palatal surface anatomy [23]. The authors reported that when maxillary casts were superimposed on the identical palatal vault, 3D evaluation of tooth movement was achieved accurately. In the following years surface registration analysis was also used to evaluate the accuracy of newly developed 3D model systems for both the maxillary and mandibular dental arches [24,25]. In these investigations, best fit algorithm of the computer software allowed users to superimpose on all the surface points independent of the anatomy such as the palatal vault. Accordingly, surface areas that are not the same can visually and quantifiably be represented. It appears that same principle could be applied to investigation of long-term and/or relapse changes in the dental arches.

Dental Arch Form

The dental arch form has long been an area of interest in orthodontic study and research. Arch forms show variability in shape among the patient population; many clinicians and researchers have formulated treatment philosophies and principles pertaining to alteration or maintenance of the arch form. Chuck first defined the different arch forms in 1935 [26]. He classified them into three basic forms: tapered, ovoid, and square. The differences are observed mostly in intercanine and inter-first premolar distances, which determine the arc between the canine curvature and the angle of the arch going toward the molar region. Tapered arch form has the narrowest intercanine width, square has the widest, and ovoid arch form falls in between. These arch forms can vary up to 6 mm in intercanine widths.

The first longitudinal group study of the dental arches was performed by Sillman in 1964 [27]. He followed 65 Caucasian New Yorkers from varied economic levels, from birth to the age of 25 years and obtained 750 dental casts in total. His results showed the molar width in males increased from age 4 to 8 years and increased the same incrementally from age 8 to 12 years. Years 12 through 16 showed a width increase that was smaller than the previous time period. He also found that there was no significant change in maxillary molar width in males from age 16 to 20. Björk and Skieller's metallic implant study showed similar results [28]. They found that growth in the transverse dimension was complete around age 17 for most males. Another study showed the transverse dimensional growth was completed in the maxilla at age 17 for males and 16 for females [29].

The main arch forms used today are based on the catenary curve. This is the shape a chain would make if it were hung from both ends. It does fit most patients in the premolar, canine, and incisor regions. Normal dental arch form tapers inward posterior to the first molar. The Brader arch is a variation of the catenary curve and is based on a trifocal ellipse, which considers the 'tucked in' nature of second and third molars. Currier described the best fit of ellipsis and parabolic arch forms for three coordinate curves on mandibular and maxillary arches [30]. He found that maxillary and mandibular arches had different 'goodness of fit', but the ellipse arch had a better geometric correlation for the maxillary and mandibular arches.

The Alexander arch form (Alexander System, Ormco Corp., Orange, CA) was designed from hundreds of saved custom arch wires. These arch wires were then analyzed by superimposing them and finding the average custom arch form. The Vari-Simplex arch form (Alexander System, Ormco Corp., Orange, CA) is similar to what is commonly called the ovoid arch form. This arch form was found to best fit 44% of untreated cases, 53% of Class I malocclusions, and 60% of Class II malocclusions in their pretreatment arches [31]. However, a shape representing a combination of the "Par" and "Vari-Simplex" arch forms approximated to only 50% of the cases. It was also shown that cases that had changes in arch form during non-extraction treatment frequently were not stable and almost 70% showed significant long-term posttreatment changes [31]. Based on these results, it could be concluded that customizing arch form in the individual patient seems to be more than necessary.

Relapse

There are believed to be many causes of relapse: continued dentoalveolar growth and accommodations made by the teeth, supracrestal gingival fibers, modern diets, and modifying original arch form. At the crux of postretention stability lies the maintenance of intercanine width (ICW). Modifying mandibular ICW by expansion is believed to lead to increased relapse. ICW decreases slightly during the aging process and can cause lower incisor crowding. So, expanding the mandibular ICW can only increase the relapse potential of the lower arch [32]. A mandibular intercanine width increase can only be maintained with fixed retention. While relapse potential is stronger in the anterior region,

transverse expansion of the mandibular posterior teeth also shows some long-term instability, though in a lesser amount than the anterior. In one study, the mandibular intermolar expansion relapsed by 50% in patients with fixed lower retainers [33]. Among the other reasons for relapse are muscle function, gingival fibers, and lack of retention. The tongue has been shown to cause spacing when it is large or during swallowing parafunction. Gingival fibers between teeth and retention are related. Gingival fibers will rearrange after orthodontic treatment, but that can require up to eight months. So, a lack of proper retention can lead to teeth reverting back to their original positions [34].

There are many influences that affect the dental arch form in its development. Proffit described four primary factors: 1) intrinsic forces by tongue and lips, 2) extrinsic forces: habits/orthodontic appliances, 3) forces from dental occlusion, and 4) forces from the periodontal membrane [35]. He also described some secondary influences, including posture and eruption patterns. Lower intercanine width decreases on average 0.7 mm from 13-20 years of age. This trend continues throughout life and explains some lower incisor crowding often seen in the adult dentition. Statistically significant differences were not shown between Angle Class I and Class II malocclusions in adults as individuals get older. However, independent of the Angle classification, there were significant differences between age groups [36]. The dental arches continue to change and adapt throughout life and into the sixth decade, though the degree of change decreases with time. All changes reflect a decrease in arch width, depth, and perimeter, with a significant increase in the mandibular incisor irregularity index [37].

The process of arch constriction that accompanies anterior crowding appears to continue well after the cessation of active growth. The only way to ensure continued satisfactory alignment post-treatment is probably the use of fixed or removable retention for life. Mandibular incisor irregularity increases at 10 years after the retention, and it continues to increase by an average of about 1 millimeter from 10 to 20 years follow-up [38]. Some have proposed that expanding the dental arches early in life, during the mixed dentition, leads to greater stability. This anecdotal data is unfounded, though, and still results in relapse and crowding beyond acceptable limits [39]. Evidence also suggests that second molar distalization will not be effective and will not offer an acceptable solution to crowding [39]. Patients who initially present with mandibular anterior spacing are also not immune to progressive incisor irregularity over time. In a study of thirty cases with initial mandibular spacing, none of the patients developed spaces during retention, however, 46% of the patients developed incisor irregularity of 3.5 mm or more. Therefore, either fixed or consistent removable retention should also be utilized in patients who present with lower anterior spacing [40].

Myser *et al.* showed that in 74% of the patients, irregularity of incisors was typically less than 3.5 mm following the retention period with an average of 15.7 years follow-up [36]. Only 1.5% had severe irregularity at the long-term follow-up (>6.5 mm). This would indicate that orthodontic treatment is not inherently unstable. Tooth-size arch length discrepancies and irregularity were interrelated but could not be shown to explain all of the relapse that occurred after the retention period. However, mandibular malalignment could be attributed to a decrease in arch perimeter throughout treatment. Rotation of the canines was seen in broader arch forms in the long-term follow-up and indicated their importance in determining the arch form [36]. Relapse is an inevitable part of orthodontic treatment, but it is valuable to determine which portions may improve or worsen over time. In a group of postretention records taken at least ten years after treatment was completed, it was shown that occlusal contacts and marginal ridges improved over time, while alignment and rotations worsened [41].

Extraction vs. Non-extraction

It appears that alignment of anterior teeth as well as the arch form play an important role in the stability of orthodontic malocclusions. A study that compared extraction vs. non-extraction therapy showed that with both approaches mandibular irregularity increased more than the maxillary irregularity

even though no significant relapse occurred postretention [42]. However, the same study reported a statistically significant increase in mandibular intercanine width through treatment and a statistically significant decrease in mandibular intercanine width postretention. Intermolar widths decreased significantly during extraction treatment but remained stable in the long-term follow-up [42]. In the non-extraction group, intermolar width increased slightly during treatment and increased slightly during postretention, but not to a significant degree. This study correlated with Little's findings: irregularity at postretention was not correlated to the degree of crowding pre-treatment and hence, the decision to extract or not did not relate to long term stability [39]. Mandibular incisors were shown to become more crowded during the postretention phase (average 1 mm) in both groups [42]. Maxillary canine widths were shown to be more stable than mandibular intercanine widths after treatment. Second premolar widths in both groups decreased in the post retention phase [42].

A long-term stability study examined premolar extraction cases with Class I malocclusion [43]. Out of a sample of 32 patients, 80% of them had less than 3.5 mm of incisor irregularity, which was similar to the findings of Myser *et al* [36]. The remaining 20% exhibited between 3.5 to 6.5 mm of irregularity, and the strongest predictor of relapse was an increase in intercanine width [36]. Most patients (92%) who used removable retention experienced a decrease in intercanine width, thus the authors suggested lifetime retention when the intercanine width was expanded [43].

AIM

The objective of this study was to determine if long-term stability was affected by initial arch form, specifically when extraction and non-extraction patients were treated with a standardized arch form. The arch form changes were evaluated using linear measurements on digital dental models. Furthermore, a three-dimensional surface registration analysis was performed to investigate the post-retention changes in extraction and non-extraction groups.

METHODS

Institutional approval for this retrospective study was granted by the Committee for the Protection of Human Subjects under exempt status (UTH-DB-14-0015). All cases were selected from a private orthodontic office that had long-term records of thousands of patients. To be included in the study, individuals had to have normal vertical growth pattern (26°<SN-MP <38°), and acceptable mandibular incisor inclination (88° <IMPA <100°) at the pretreatment period. Individuals who had skeletal anomalies and overjet greater than 5 mm or smaller than 0 mm, craniofacial disorders, asymmetries, and missing teeth were not included. Individuals who were previously treated with functional appliances, maxillary expansion devices, and surgical procedures were also excluded from the study sample. Based on the defined criteria above, a study sample of 107 cases (n=53, extraction; n=54, non-extraction) was identified. Additionally, all cases had to have complete orthodontic records that included pretreatment (T1), posttreatment (T2), and postretention (T3) study models and cephalometric radiographs. The arch form subgroups were defined (Table 1) using the McLaughlin-Bennett dental arch template (Forestadent Bernhard Förster GmbH, Pforzheim, Germany). The final study sample included 31 non-extraction and 32 extraction patients (Table 1). The average age of the sample group was 12.9 ± 1.3 years.

Table 1. The study sample.

	Square	Tapered	Ovoid	Total N
Non-extraction	**N=7**	**N=9**	**N=15**	**31**
Extraction	**N=7**	**N=14**	**N=11**	**32**

The extraction decision was based on the need for space to resolve crowding and to ideally align the incisors in the extraction group. The mean values of mandibular incisor irregularity in the extraction and non-extraction groups were 8.4 ± 3 and 6.5 ± 2 mm, respectively. Orthodontic treatment of all cases had been completed by two investigators (W.G.A and J.M.A) with .018" x .025"-slot edgewise appliances using the Vari-Simplex arch form (Alexander System, Ormco Corp., Orange, CA). The extraction group had a treatment time of 27.5 ± 5 months, whereas the non-extraction group had a treatment time of 26.0 ± 6 months. The extraction and non-extraction groups were retained using an upper wrap-around Hawley retainer and lower 3-3 bonded retainer for a mean of 4.5 and 3.7 years, respectively. Post-retention (T3) records were taken at a mean of 17.0 ± 5 years in the extraction group and 13.0 ± 6.1 years in the non-extraction group.

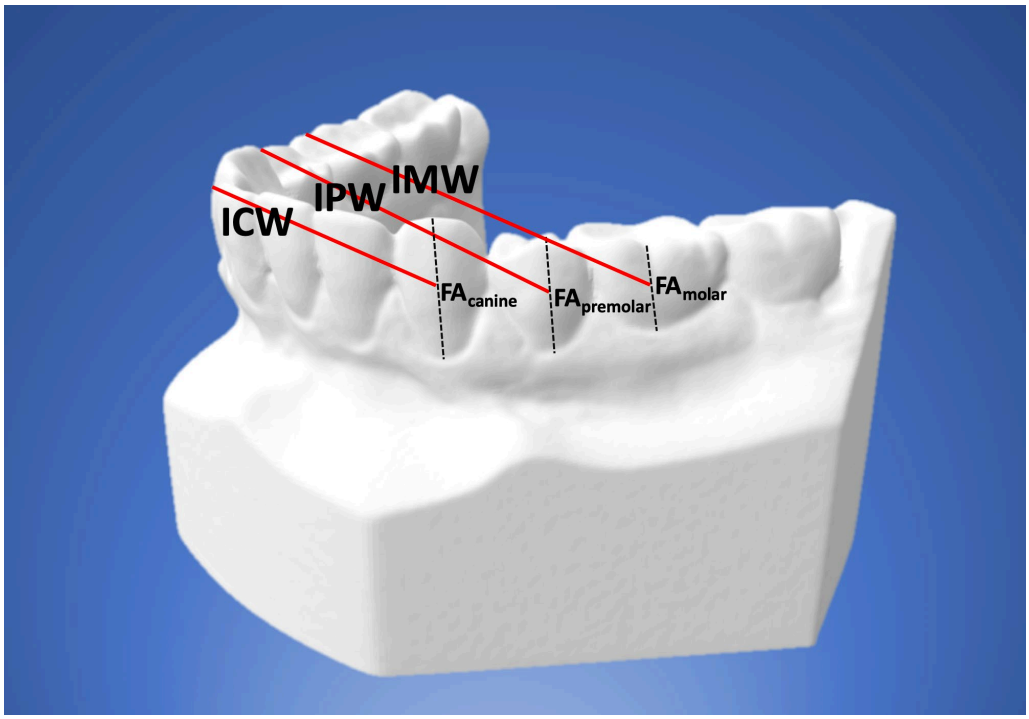

Figure 1. Intercanine width (ICW), interpremolar width (IPW), and intermolar width (IMW) measurements were collected from maxillary and mandibular model pairs from all three time points.

Maxillary and mandibular models of all three-time points (T1, T2, and T3) were scanned into digital stereolithographic (STL) files using Ortho Insight 3-D Laser Scanner (Ortho-Insight 3D, Hixson, TN, USA). Linear measurements were calculated for all time points on STL files using Motion View software (Ortho-Insight 3D, Hixson, TN, USA). Maxillary canine (ICW), first premolar (IPW), and first molar (IMW) widths were measured for all three time points using the facial axis (FA) points on the crowns (Figure 1). In our study, The FA points were defined as the midpoint of the longitudinal axis on the facial aspect of clinical crown corresponding to the most prominent part of the central lobe on each tooth except for the molars. For the first molars, the longitudinal axis of the crown was represented by the mesiobuccal groove. Second premolars were used for premolar width (IPW) measurements for T2 and T3 periods in the extraction sample. Percentage of patients that showed changes in the shape of arch form (+ change; or – / no change) and differences in incisor irregularity (mm) were recorded from T1-T2 and T2-T3. Additionally, an engineering software capable of surface registration of 3D STL files (RapidForm 2006; 3D Systems, Inc, Morrisville, NC) was used to evaluate the long-term relapse. Maxillary and mandibular arches from T2 and T3 were registered on their surfaces using a best fit algorithm to analyze the post-retention change. This analysis helped us to calculate the linear differences occurring on all points of the two digital file shells (Figure 2). Average linear differences for the maxillary (U average) and mandibular (L average) dental arches were computed.

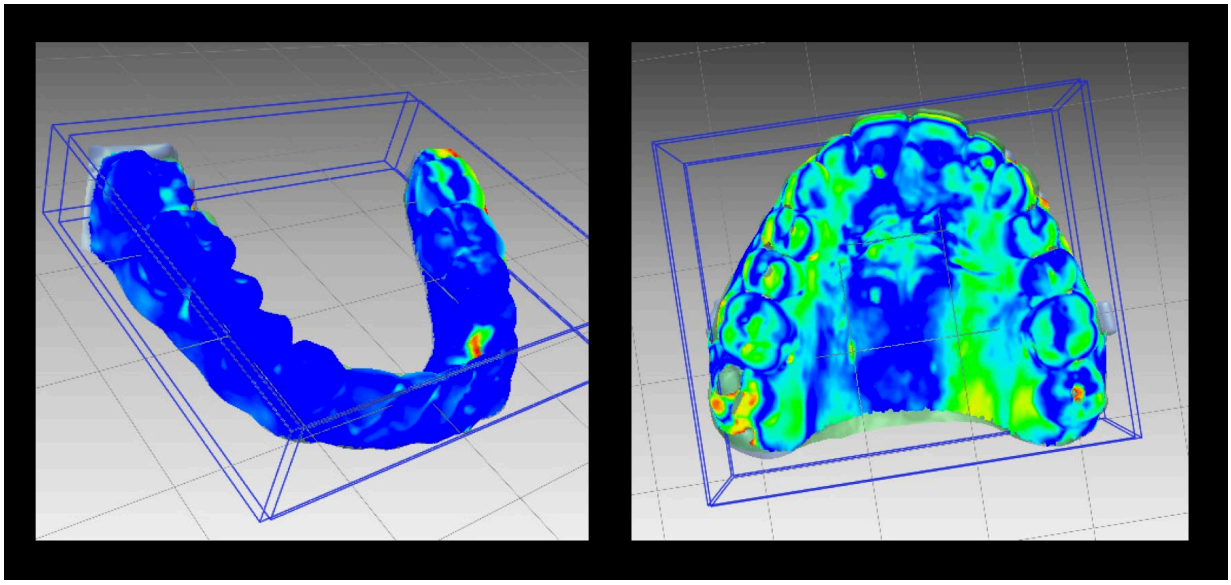

Figure 2. Registered T2 and T3 images of a mandibular (left) and maxillary (right) arch from a non-extraction patient. Varying colors depict the surface match between the two images: blue–green (excellent–good match), yellow–red (reduced–poor match). Computer algorithm was used to measure the maximum and average changes on the surfaces of the models.

SPSS (version 25; IBM, Armonk, NY, USA) was used for statistical analysis. According to the Shapiro-Wilk test, the data had a normal distribution ($p>0.05$). Levene's test verified that the group variances were equal ($p>0.05$). The data from ICW, IPW, and IMW measurements were analyzed using a three-way mixed analysis of variance (ANOVA) with the following main effects: treatment group, arch form, and time. Chi-square analysis was used to evaluate the shape of arch-form changes between extraction and non-extraction groups and between tapered, ovoid, and square arch form groups. Two-way analysis of variance (ANOVA) was used to analyze the difference in incisor irregularity for T1-T2 and

T2-T3 and the surface changes on the dental models between T2-T3 periods. Multiple comparisons were made with the Bonferroni post hoc test. Level of significance was set at $p<0.05$ for all tests.

RESULTS

Significant group x time interactions were found for mandibular ICW, maxillary and mandibular IPW and IMW measurements ($p<0.05$). There were also significant arch form x time interactions for mandibular IPW and maxillary and mandibular IMW measurements ($p<0.05$). However, group x time x arch form interaction was not significant for any of the arch width measurements studied. This finding indicated that the changes in ICW, IPW, and IMW were the same over time regardless of extractions and initial arch form. Frequency of arch form changes did not differ between the extraction and non-extraction groups between T1-T2 and T2-T3 comparisons. However, significant treatment (Figure 3; T1-T2) and long-term (Figure 4; T2-T3) differences occurred in the dental arch form for individuals with tapered and square arch forms when compared to individuals with ovoid arches ($p<0.05$).

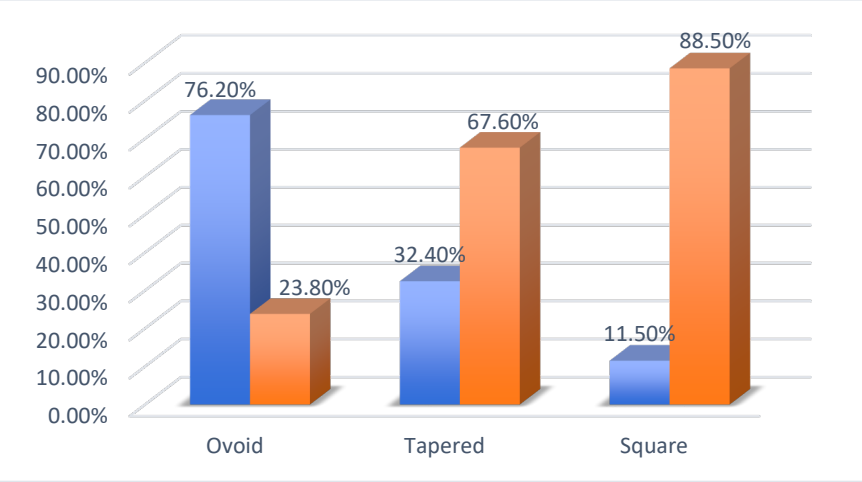

Figure 3. T1-T2 comparison of ovoid, tapered, and square arch form groups. Blue – no change; Red – change.

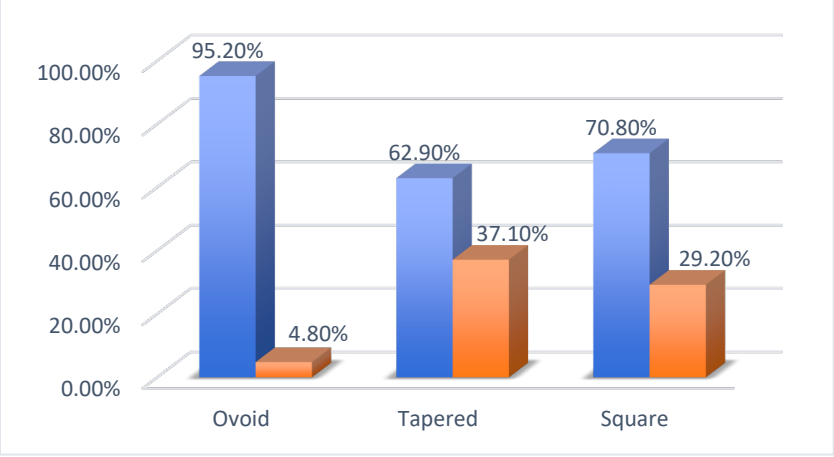

Figure 4. T2-T3 comparison of ovoid, tapered, and square arch form groups. Blue – no change; Red – change.

Changes in incisor irregularity after the treatment (T1-T2) and over the long-term (T2-T3) were comparable between the extraction and non-extraction patients when grouped according to the initial arch form type. Incisor irregularity displayed significant differences between the extraction and non-extraction groups for the T1-T2 period ($p<0.05$); however, no significant differences were found for the group x arch form interactions in any of the time periods investigated (Figure 5 and 6).

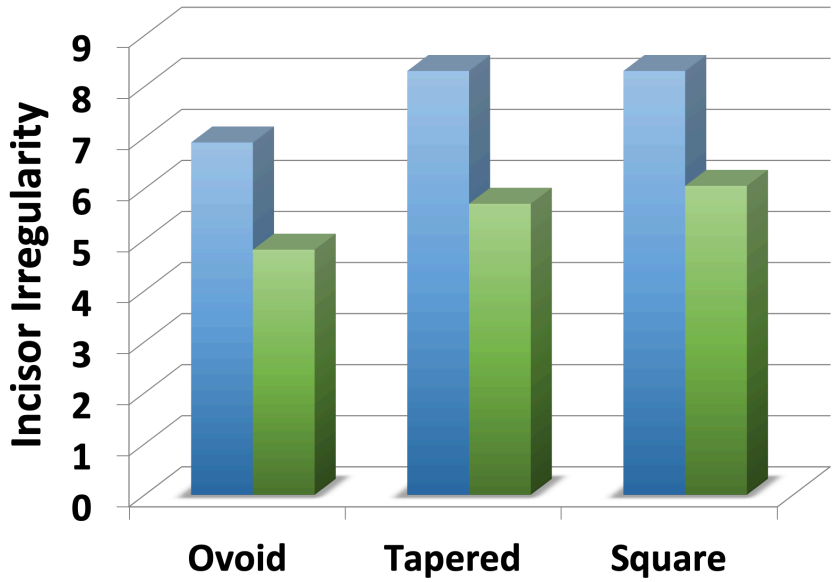

Figure 5. T1-T2 comparison of incisor irregularity score for extraction (blue) and non-extraction (green) groups.

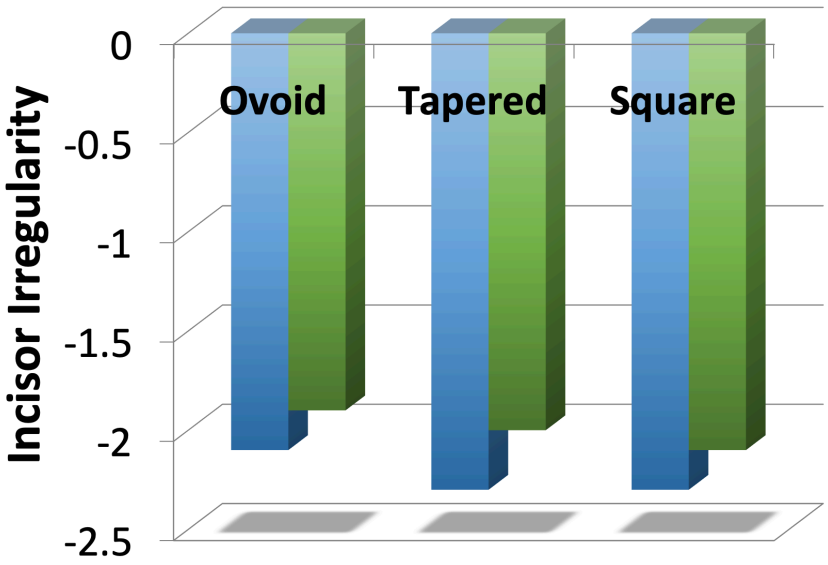

Figure 6. T2-T3 comparison of incisor irregularity score for extraction (blue) and non-extraction (green) groups.

Group type (extraction vs. non-extraction) and the arch form type (tapered, ovoid, square) did not have any significant impact on the long-term surface changes (T2-T3) of maxillary and mandibular dental models. No significant group x arch form interaction was found for U average and L average measurements.

DISCUSSION

It is widely accepted that after orthodontic treatment, teeth will relapse without meticulous retention protocols. The extent of this relapse has been studied ad nauseam, but not in relation to specific arch form types [10,11,36,39,44]. An often-debated issue is whether extraction or non-extraction treatment will lead to more instability. Intangibles, such as a clinician's expertise, are difficult to quantify, but evaluating results of specific treatment protocols can give invaluable insight into long-term prognosis. Orthodontists should know the relapse potential for their clinical diagnosis. There are typically three different arch forms described in the literature and all available orthodontic wires are a variation or combination of these.

Some studies suggested that in certain populations, the ovoid arch form is the most common type [45-46]. Similarly, the predominant arch form in our study population was also ovoid. We evaluated a sample group that was treated with a standardized arch form to evaluate the long-term changes to the dental arches. When looking at our results, the changes in ICW, IPW, and IMW were similar over time regardless of premolar extractions and the initial arch form. Visual inspection of shape changes in the dental arch form did not significantly differ between extraction and non-extraction groups for T1-T2 and T2-T3 time periods. However, significant differences occurred when the main effect was the initial arch form. That meant that individuals that initially had a tapered or square arch form experienced significant shape changes after treatment and in the long-term compared to individuals with an ovoid arch form. These findings were not surprising as the arch form used in the treatment of our sample group is a type of ovoid arch form. Customization of the arch form in the individual patient would be beneficial, by broadening or constricting the arch form to match the shape of mandibular basal arch [31].

A very interesting finding from this study was the absence of a significant difference in the relapse of incisor irregularity between extraction and non-extraction patients based on the initial arch form. This finding should be interpreted very carefully. Extraction patients certainly started with significantly more incisor irregularity. However, the decision of extraction or the initial arch shape had no significant effect over the long-term relapse. Our findings agreed with the conclusions of previously published papers [39,42]. The main difference in our study was the inclusion of the original arch form as a main effect. It appeared that using a standardized arch form would not affect the incisor irregularity post-retention. It is important to remember that extraction decision is influenced by many variables including the incisor irregularity. In Class I malocclusions, amount of crowding, the curve of Spee, midline discrepancy, overjet, and the incisor position could steer the case in favor of premolar extractions. Therefore, a larger sample with more elaborate diagnostic variables is needed to confirm our findings.

When contrasting our findings to the available literature, another important aspect of our study was the investigation of surface changes. Utilizing 3D models enabled us to perform a surface registration analysis that numerically assessed the average surface changes on the models. As shown in Figure 2, the surface registration analysis is also helpful for the visual inspection of matching areas on the model pairs. Based on our methodology, we calculated the average surface changes in maxillary and mandibular dental models between T2-T3 time periods. Our results indicated that the average surface change of Class I malocclusions when treated by a standard arch form would not be affected by the treatment group (extraction vs. non-extraction) or the initial arch form. Additional studies are needed to confirm our findings and also to elaborately investigate the nature of surface changes postretention. Since our findings averaged the positive and negative linear changes, it is important to quantify the changes from expansion

and constriction of the dental arch in a localized area as well as the amount of relapse that could be attributed to first, second, or third order movements.

CONCLUSIONS

1. When treated with a standardized ovoid-type arch form, individuals with tapered and square arch forms had a more frequently observed arch form shape change after treatment and post-retention compared to individuals with ovoid arch form.
2. Changes in incisor irregularity were not affected by the choice of premolar extractions or the initial arch form type.
3. When treated with a standardized arch form, average surface changes of maxillary and mandibular models of extraction and non-extraction patients classified according to their original arch form displayed similar results post-retention.
4. Relapse in arch form and dimensions predominantly occurred in individuals with tapered and square arch forms regardless of the premolar extractions.

REFERENCES

1. Kusy RP. Ongoing innovations in biomechanics and materials for the new millennium. *Angle Orthod* 2000;70(5):366-376.

2. Smith DC, Maijer R. Improvements in bracket base design. *Am J Orthod* 1983;83(4):277-281.

3. Sorel O, El Alam R, Changneau F, Cathelineau G. Comparison of bond strength between simple foil mesh and laser-structured base retention brackets. *Am J Orthod Dentofacial Orthop* 2002;122(3):260-266.

4. Sachdeva R. Sure-Smile: technology-driven solution for orthodontics. *Tex Dent J* 2002;119(7):608-615.

5. Garino F, Farino GB, Castroflorio T. The iTero intraoral scanner in Invisalign treatment: A two-year report. *J Clin Orthod* 2014;48(2):98-106.

6. Dalessandri D, Lazzaroni E, Migliorati M, Piancino MG, Tonni I, Bonetti S. Self-ligating fully customized lingual appliance and chair-time reduction: a typodont study followed by a randomized clinical trial. *Eur J Orthod* 2013;35(6):758-765.

7. Peck H, Peck S. A concept of facial esthetics. *Angle Orthod* 1970;40(4):284-317.

8. Verma SL, Sharma VP, Singh GP, Sachan K. Comparative assessment of soft-tissue changes in Class II Division 1 patients following extraction and non-extraction treatment. *Dent Res J* 2013;10(6):764-771.

9. Stroud JL, English J, Buschang PH. Enamel thickness of the posterior dentition: its implications for nonextraction treatment. *Angle Orthod* 1998;68(2):141-146.

10. Fleming PS, Dibiase AT, Lee RT. Arch form and dimensional changes in orthodontics. *Prog Orthod* 2008;9(2):66-73.

11. Heiser W, Richter M, Niederwanger A, Neunteufel N, Kulmer S. Association of the canine guidance angle with maxillary and mandibular intercanine widths and anterior alignment relapse: Extraction vs nonextraction treatment. *Am J Orthod Dentofacial Orthop* 2008;133(5):669-680.

12. Dowling AH, Burns A, Macauley D, Garvey TM, Fleming GJ. Can the intra-examiner variability of Little's Irregularity Index be improved using 3D digital models of study casts? *J Dent* 2013;41(12):1271-1280.

13. Grünheid T, Patel N, De Felippe NL, Wey A, Gaillard PR, Larson BE. Accuracy, reproducibility, and time efficiency of dental measurements using different technologies. *Am J Orthod Dentofacial Orthop* 2014;145(2):157-164.

14. Im J, Cha JY, Lee KJ, Yu HS, Hwang CJ. Comparison of virtual and manual tooth setups with digital and plaster models in extraction cases. *Am J Orthod Dentofacial Orthop* 2014;145(4):434-442.

15. Matter and Form – A brief history of 3D Scanning. 2014. https://matterandform.net/blog/a-brief-history-of-3d-scanning. Accessed August 24, 2019

16. Modena – History of 3D Scanners. 2018. https://www.modena.co.za/history-of-3d-scanners/. Accessed August 24, 2019

17. Kuroda T, Motohashi N, Tominaga R, Iwata K. Three-dimensional dental cast analyzing system using laser scanning. *Am J Orthod Dentofacial Orthop* 1996;110(4):365-369.

18. Commer P, Bourauel C, Maier K, Jäger A. Construction and testing of a computer-based intraoral laser scanner for determining tooth positions. *Med Eng Phys* 2000;22(9):625-635.

19. Fleming PS, Marinho V, Johal A. Orthodontic measurements on digital study models compared with plaster models: a systematic review. *Orthod Craniofac Res* 2011;14(1):1-16.

20. Kravitz ND, Groth CH, Jones PE, Graham JW, Redmond WR. Intraoral digital scanners. *J Clin Orthod* 2014;48(6):337-347.

21. Burzynski JA, Firestone AR, Beck FM, Fields Jr HW, Deguchi T. Comparison of digital intraoral scanners and alginate impressions: Time and patient satisfaction. *Am J Orthod Dentofacial Orthop* 2018;153(4):534-541.

22. Chalmers EV, McIntyre GT, Wang W, Gillgrass T, Martin CB, Mossey PA. Intraoral 3D Scanning or Dental Impressions for the Assessment of Dental Arch Relationships in Cleft Care: Which is Superior? *Cleft Palate Craniofac J* 2016;53(5):568-577.

23. Choi DS, Jeong YM, Jang I, Jost-Brinkmann PG, Cha BK. Accuracy and reliability of palatal superimposition of three-dimensional digital models. Angle Orthod. 2010 Jul;80(4):497-503.

24. Lightheart KG, English JD, Kau CH, Akyalcin S, Bussa Jr HI, McGrory KR, et al. Surface analysis of study models generated from OrthoCAD and cone-beam computed tomography imaging. *Am J Orthod Dentofacial Orthop* 2012;141(6):686-693.

25. Akyalcin S, Dyer DJ, English JD, Sar C. Comparison of 3-dimensional dental models from different sources: diagnostic accuracy and surface registration analysis. *Am J Orthod Dentofacial Orthop* 2013;144(6):831-837.

26. Chuck GC. Ideal arch form. *Angle Orthod* 1934;4:312-327.

27. Sillman JH. Dimensional changes of the dental arches: Longitudinal study from birth to 25 years. *Am J Orthod* 1964;50:824-42.

28. Björk A, Skieller V. Growth in the width of the maxilla studied by the implant method. *Scan J Plast Reconstr Surg* 1974;8:26-33.

29. Moyers RE, van der Linden FPGM, Riolo ML, McNamara, Jr. JA. Standards of human occlusal development. Monograph 5, Craniofacial Growth Series. Ann Arbor: Center for Human Growth and Development, University of Michigan Press, 1976: 83.

30. Currier JH. A computerized geometric analysis of human dental arch form. *Am J Orthod* 1969; 58:164-179.

31. Felton JM, Sinclair PM, Jones DL, Alexander RG. A computerized analysis of the shape and stability of mandibular arch form. *Am J Orthod Dentofacial Orthop* 1987;92:478-483.

32. Burke SP, Silveira AM, Goldsmith LJ, Yancey JM, Van Stewart A, Scarfe WC. A meta-analysis of mandibular intercanine width in treatment and postretention. *Angle Orthod* 1998;68(1):53-60.

33. Housley JA, Nanda RS, Currier GF, McCune DE. Stability of transverse expansion in the mandibular arch. *Am J Orthod Dentofacial Orthop* 2003;124(3):288-293.

34. Reitan K. Principles of retention and avoidance of posttreatment relapse. *Am J Orthod Dentofacial Orthop* 1969;55:776-790.

35. Proffit WR. Equilibrium theory revisited: factors influencing position of teeth. *Angle Orthod* 1978;48:175-186.

36. Myser SA, Campbell PM, Boley J, Buschang PH. Long-term stability: Postretention changes of the mandibular anterior teeth. *Am J Orthod Dentofacial Orthop* 2013;144: 420-429.

37. Dager MM, McNamara JA, Baccetti T, Frachi L. Aging in the Craniofacial Complex: Longitudinal Dental Arch Changes Through the Sixth Decade. *The Angle Orthod* 2008;78: 440-444.

38. Little RM, Riedel RA, Artun J. An evaluation of changes in mandibular anterior alignment from 10 to 20 years postretention. *Am J Orthod Dentofacial Orthop* 1988;93:423-428.

39. Little RM. Stability and relapse of dental arch alignment. *British Journal of Orthod* 1990; 17:235-241.

40. Little RM, Riedel RA. Postretention evaluation of stability and relapse-mandibular arches with generalized spacing. *Am J Orthod Dentofacial Orthop* 1989;95:37-41.

41. Aszkler RM, Preston CB, Saltaji H, Tabbaa S. Long-term occlusal changes assessed by the American Board of Orthodontics' model grading system. *Am J Orthod Dentofacial Orthop* 2014;145:173-178.

42. Erdinc AE, Nanda RS, Isiksal E. Relapse of anterior crowding in patients treated with extraction and nonextraction of premolars. *Am J Orthod Dentofacial Orthop* 2006; 129:775-784.

43. Boley JC, Mark JA, Sachdeva RC, Buschang PH. Long-term Stability of Class I premolar extraction treatment. *Am J Orthod Dentofacial Orthop* 2003;124:277-287.

44. Aksu M, Kocadereli I. Arch width changes in extraction and nonextraction treatment in class I patients. *Angle Orthod* 2005;75(6):948-952.

45. Paranhos LR, Lima CS, Alves da Silva RH, Júnior ED, Torres FC. Correlation between maxillary central incisor crown morphology and mandibular dental arch form in normal occlusion subjects. *Braz Dent J* 2012;23(2):149-153.

46. Gafni Y, Tzur-Gadassi L, Nojima K, McLaughlin RP, Abed Y, Redlich M. Comparison of arch forms between Israeli and North American white populations. *Am J Orthod Dentofacial Orthop* 2011;139(3):339-344.

HOW DOES NORMAL OCCLUSION AGE?

Daniela Garib, Felicia Miranda, Camila Massaro, Guilherme Janson, Lucia Cevidanes, Antonio Carlos Ruellas, Marilia Sayako Yatabe, Hera Kim-Berman, Rolf G. Behrents, James A. McNamara Jr.

ABSTRACT

With an increase in life expectancy, aging of the occlusion has become a subject of growing interest. This chapter aims to present the findings of a 47-year follow-up of normal occlusion subjects. Natural aging changes observed throughout the years are presented quantitatively, qualitatively, and by means of registration of digital dental models. Aging changes of the normal occlusion were discrete. Clinical crown height increased from adolescence to late adulthood. Mandibular inter-canine distance and arch perimeter decreased simultaneously to the increase of mandibular incisor crowding. Late mandibular incisor crowding has not led patients to seek orthodontic treatment. Despite slight dental changes, the occlusion seems to be the most stable feature of the face over the aging process.

KEY WORDS: Dental Occlusion, Aging, Dental Models, Orthodontics, Imaging, Three-Dimensional

INTRODUCTION

The continuous increase in life expectancy has changed the social and health scenario all over the world [1]. Back in Angle´s time, the average lifetime was no more than 50 years. In present days, people are living longer, and more individuals live beyond 80 years of age, with a great quality of life. In dentistry, the unpredictability of occlusal changes with aging is a challenge, since craniofacial growth and development never stop [2, 3]. A deeper understanding of the maturational changes of the normal occlusion is the key to achieving post-treatment stability and more consistent treatment plans for adult patients.

Considering the above-mentioned concerns, what do we know about aging of the normal occlusion? The study by Behrents [2, 3] showed that craniofacial growth is a continuous process, even into adulthood, with relevant changes in the soft tissues, mandibular rotations, and dental compensation [2, 3]. From early to late adulthood, constant uprighting of the incisors in both sexes, forward and downward mandibular displacement in men, and backward rotation in women were observed [2, 3]. Changes noticed by Behrents were mild, but consistent with existence of a continued remodeling throughout life [2, 3]. Many efforts have been made to learn more about how the untreated normal occlusion aging process takes place [4-12]. Decreases in inter-canine distance, arch length, and arch perimeter were previously reported until the fourth decade of life [5, 11-13]. Studies report high variability in overbite changes with aging in normal occlusion individuals [2, 5-8, 10, 12, 14]. Assessment of anterior teeth alignment is an important target of investigation, due to its clinical implications. An increase in incisor crowding with age

has been reported and the changes were greater in the mandibular arch [5, 10]. Tooth wear and changes in the gingival level were also observed as a consequence of aging [15-18].

In a longitudinal assessment of normal occlusion subjects up to the age of 20 years, arch length and inter-canine width decreased while incisor irregularity increased [10]. Changes in arch shape have included a tendency of a more rounded shape for the mandibular arch from 13 to 31 years of age [9]. Decrease in inter-canine distance, maxillary inter-molar width, overjet, and overbite were observed from 15 to 32 years of age [8]. A continuous decrease in inter-canine distance was also reported from 13 to 45 years of age [13]. From 25 to 46 years of age, increase in anterior crowding was observed, together with decreases in inter-canine distance and maxillary arch length [6]. However, no previous studies have extended the evaluation of normal occlusion maturation up to the sixth decade of life.

Dental model surfaces provide an accurate three-dimensional (3D) view of the dental arches and are reliable for clinical and research purposes [19, 20]. Most previous studies evaluating normal occlusal changes over time used stone casts or digital dental models, and some authors included radiographic and photographic assessments [2, 4-6, 11, 12, 14]. Investigation of maturational changes of the normal occlusion through superimposition of 3D models could add important information about the occlusal changes with aging. The craniofacial complex and the associated dental structures constantly grow, adapt, and age. Although changes in adolescence are greater, they also take place in adulthood, however, in an adaptive and decelerating pattern [2]. In this chapter, maturation of the normal occlusion over a 47-year follow-up period will be discussed.

Our initial sample was obtained in the sixties and seventies at Bauru Dental School, University of São Paulo, and comprised 82 White-Brazilians with a normal occlusion in the permanent dentition. In the ’60s, normal occlusion was characterized as a Class I molar relationship, tooth alignment or maximum 2mm incisor crowding, absence of crossbites, and normal overjet/overbite. Dental records were taken at 13 and 17 years of age at that time. From 2015 to 2016, the subjects were recalled at 60 years of age and a sample of 22 subjects was collected covering a 47-year follow-up period. Digital dental models were evaluated quantitatively, qualitatively, and by means of 3D image superimpositions [21-23]. The natural changes observed throughout aging are presented in the following pages.

QUANTITATIVE ANALYSIS

Clinical crown height strikingly increased from adolescence to late adulthood (Fig. 1).

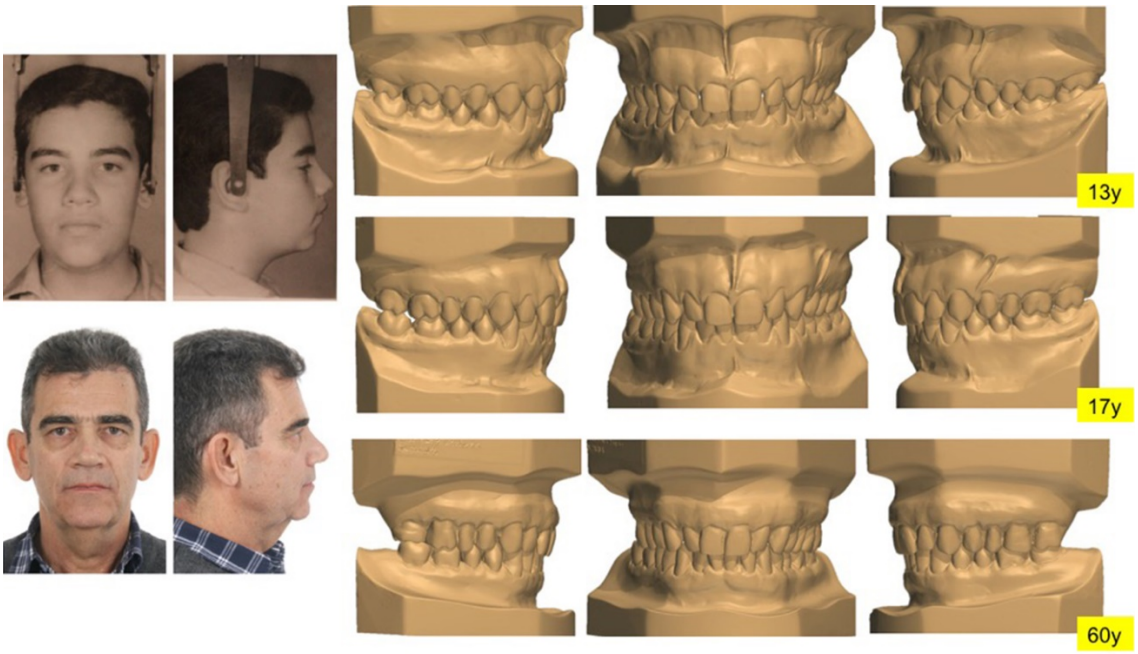

Figure 1. Extraoral photographs of subject at 13 and 60 years of age. Normal occlusion subject at 13, 17, and 62 years of age. Observe the clinical crown height increase with aging.

The increase of crown height varied from 0.5 to 3.2 mm from 13 to 60 years of age [21]. Crown height increase was due to apical migration of the gingival margin. The maxillary second molars displayed the greater increase probably because they were newly erupted at 13 years of age. The mandibular central incisors were the only teeth that maintained crown height stability during aging probably because apical migration of the gingival margin was compensated by incisal edge wear. From the early permanent dentition (13y) to early adulthood (17y), clinical crown height increase was already significant for all teeth except for the mandibular central incisors, varying from 0.5 (maxillary central incisors) to 1.1 mm (maxillary canines) [21]. Changes in clinical crown height within the first four years of the permanent dentition represent passive tooth eruption and gingival maturation. For this reason, in our adolescent orthodontic patients, decisions regarding surgical crown lengthening procedure should ideally be postponed to early adulthood.

Mesiodistal tooth size of all permanent teeth decreased a mean of 0.3 mm from the ages of 13 to 60 as a result of inter-proximal tooth wear [21]. From the second to the sixth decade of life, decrease of the mesiodistal tooth size accounted for 4 mm reduction of tooth width in each dental arch.

Mandibular incisor crowding index increased 2.5 mm from 13 to 60 years of age (Figs. 2 and 3). Late incisor crowding observed in normal occlusion subjects is probably associated with decreases in inter-canine distance and arch perimeter of 0.7 and 2.8 mm, respectively.

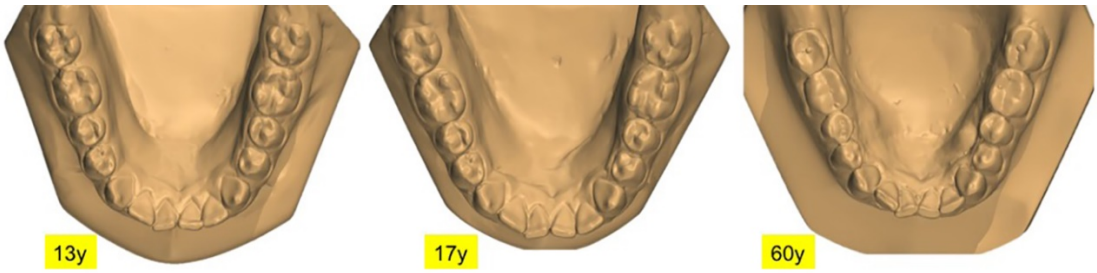

Figure 2. Mandibular occlusal view from the same patient shown in Figure 1. Observe the increase in mandibular incisor crowding over time.

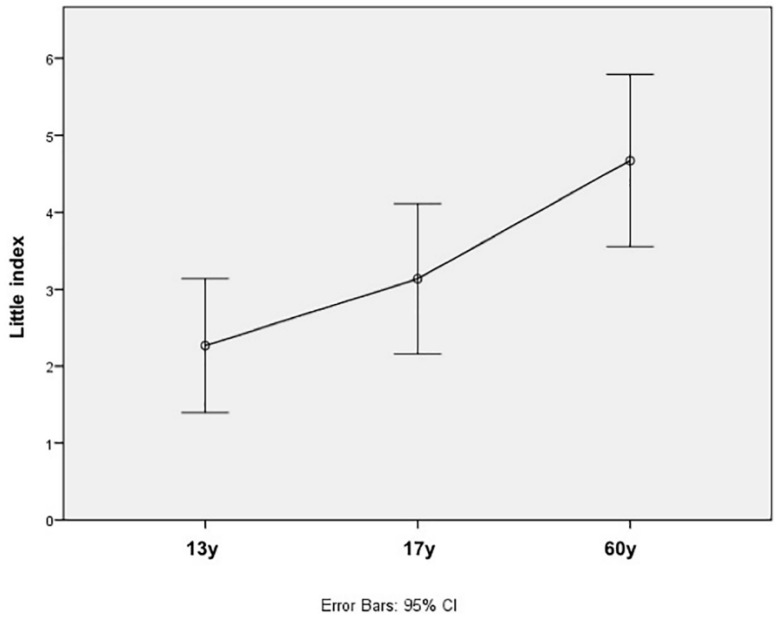

Figure 3. Increase of mandibular incisor irregularity with aging (N=22).

Maxillary late incisor crowding was small, around 1 mm in four decades, even though the maxillary arch perimeter decreased 3.5 mm in the same period. We speculate that maxillary incisors lose some mesiodistal angulation and become more upright over the years, minimizing the dental crowding in the maxillary arch.

Finally, slight decrease in overbite was observed during aging (Fig. 4). A mean overbite of 3.1, 2.3, and 1.7 mm was found at 13, 17, and 60 years of age. Overbite reduction is probably related to late mandibular growth, mainly in males, and to incisal edge wear. Overbite reduction was greater in men than in women. The overjet remained stable over time.

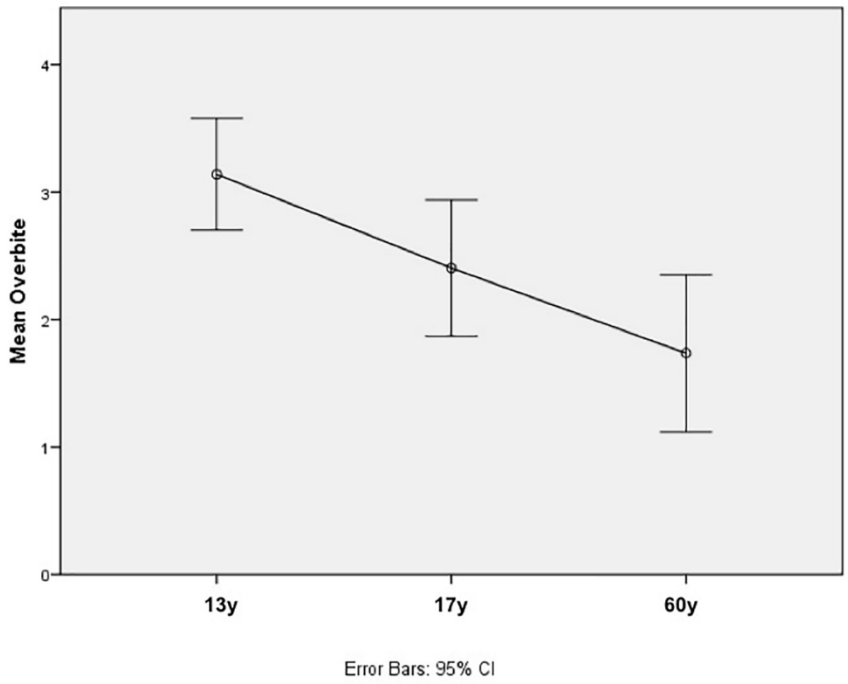

Figure 4. Decrease in overbite with time.

QUALITATIVE ANALYSIS

Normal occlusion was scored during aging according to the Six Keys of Normal Occlusion [24] (SKNO) and to the Objective Grading System (OGS) [22]. In early permanent dentition, normal occlusion subjects usually displayed distoangulation of the maxillary second molars. In late adulthood, more upright maxillary second molars were observed (Fig. 5A). In other words, angulation of maxillary second molars improved with aging, possibly in response to the decrease in maxillary arch perimeter. Additionally, some patients also demonstrated buccal tipping and displacement of the maxillary second molars from the ages of 13 to 60 years (Fig. 5B) [22]. A possible explanation for deterioration of the maxillary second molar alignment is the third molar development and eruption. Space restriction at the maxillary tuberosity might determine buccal movement of the maxillary second molars to accommodate the third molars during adulthood.

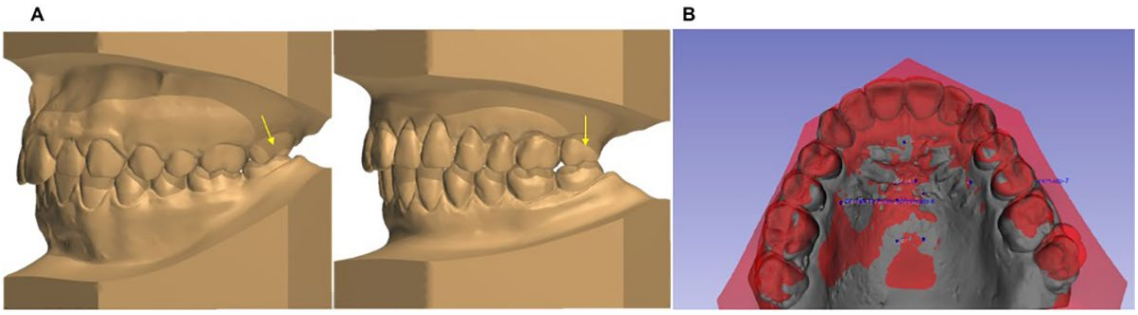

Figure 5. A- Maxillary second molar angulation improved from 13 to 60 years of age. B- Superimposition of digital dental models on the palatal rugae. Gray color is the 17-year old dental model. Red semitransparent color is the 60-year dental model. Observe that the maxillary second molars are buccally displaced during aging.

The OGS demonstrated improvement in marginal ridges leveling with time, probably due to occlusal tooth wear. Two male patients with severe occlusal tooth wear demonstrated deterioration of the anteroposterior inter-arch relationship to Class III molars and an edge-to-edge incisor overjet observed at the age of 60. These individuals still demonstrated a Class I facial pattern at late adulthood. We speculate that the severe tooth wear and flattening of the occlusal surface could be associated with the occlusal changes while the mandible displaced forward and downward during adulthood.

Permanent tooth loss was a relevant finding in our sample considering the subjects were not exposed to water fluoridation that began in 1974 in Brazil. The average number of tooth loss at the age of 60 years was 2.1 teeth per subject [22]. Tooth loss was observed in 70% of the normal occlusion sample and mandibular molars were the most frequently absent teeth [22]. Qualitative analyses also showed that late mandibular incisor crowding was more evident in patients without any tooth loss.

Self-perception During Aging

A patient centered analysis was conducted at late adulthood in individuals with normal occlusion. At 60 years of age, the subjects answered seven questions on esthetics and occlusal self-perception. Satisfaction with their smile esthetics was 100%. The median self-score for the smile was 8 and one third of the sample scored 10 for their smiles, on a 0 to 10 scale.

Only 40% of the sample had dental complaints and the most frequent was tooth discoloration in five out of 20 subjects. Dental or rehabilitation problems (three subjects), alignment (two subjects), tooth wear (two subjects), missing teeth (one subject), and inter-dental spaces (one subject) were also reported (Fig. 6A).

When subjects were asked if they had crowded teeth, 40% answered yes with a median of 0.5 on a scale of 0 (very unhappy) to 10 (no discomfort) (Fig. 6B). These answers reveal that late incisor crowding represented a slight discomfort for the subjects in late adulthood. No patient was willing to undergo orthodontic treatment.

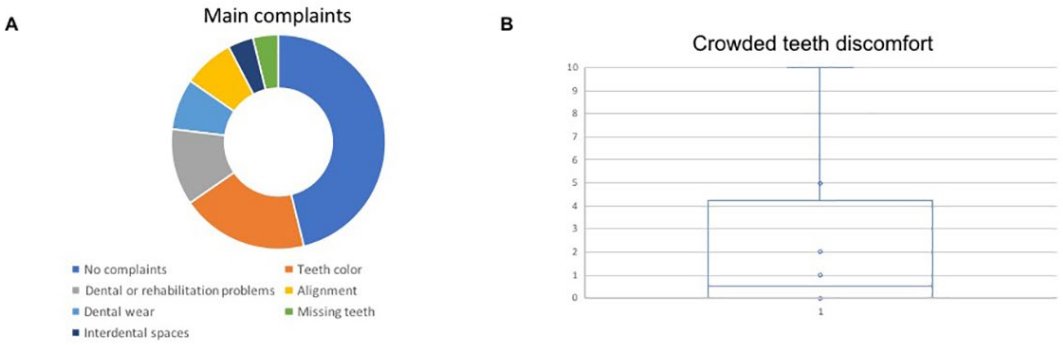

Figure 6. A- Main complaints of the normal occlusion subjects at 60 years of age. B- Level of discomfort regarding dental crowding in subjects with normal occlusion at late adulthood.

Digital Dental Model Superimposition

Three-dimensional tooth changes in the sagittal, frontal, and occlusal planes can be described by superimposing dental models. Using a reliable method of registration, individual tooth changes with aging can be better understood. For example, does decrease in mandibular inter-canine distance observed during maturation of the occlusion occur due to mesial or lingual mandibular canine displacement? No

previous study answered this question.

A subsample of normal occlusion without tooth loss at 60 years of age was used to evaluate changes in the mandibular arch. Mandibular models were registered using 13 landmarks on the mucogingival junction between each permanent tooth as described by Ioshida et al [25]. All the steps were performed in the Slicer software (https://www.slicer.org). Landmarks on the incisal tip of the anterior and buccal cusp tips of the posterior teeth were used to measure the 3-dimensional dental changes from early to late adulthood.

From 17 to 60 years of age, tooth eruption relative to the mucogingival junction for both anterior and posterior teeth ranging from 0.8 to 1.2 mm was observed in the mandibular arch. Transverse dental movements included very slight lingual displacements of canines and premolars. No mesial movement of canines was found as previously speculated. Actually, anteroposterior movements of the mandibular teeth were not expressive except for molars that drifted mesially (Fig. 7).

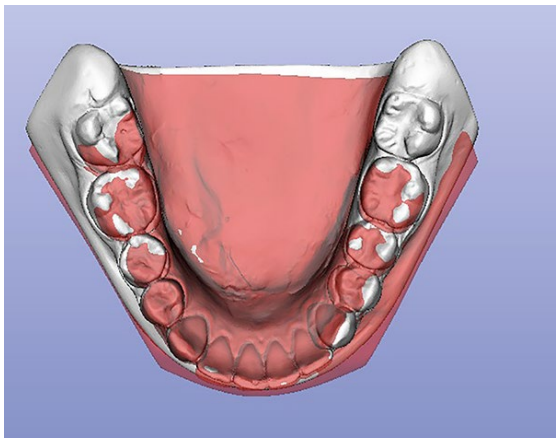

Figure 7. Superimposition of mandibular models. Gray color is the 17-year old dental model; red semitransparent color is the 60-year old dental model. Observe the mesial drift of molars with aging.

However, when we look at men and women separately, sagittal movement of the mandibular incisors during aging seems to be a discriminant factor. In all men, the mandibular incisors moved slightly lingually while in women, they moved labially, agreeing with Behrents' cephalometric findings [2, 3]. Mandibular incisor movements seem to compensate the mandibular anterior displacement in men and the backward rotation of the mandible in women occurring during aging [2, 3]. Figure 8 summarizes mandibular dental changes with aging in males and females.

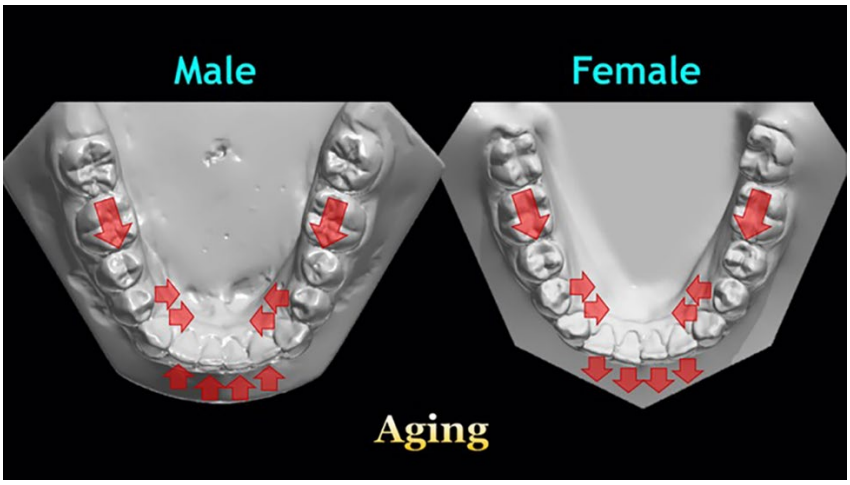

Figure 8. Male subjects seem to show a gradient of dental changes during aging where molars move forward, the incisors move slightly backward, and the canines and first premolars move medially. In female subjects, the dental arch ages similarly except for the incisors that move slightly labially.

In the maxillary arch, the challenge of superimposing maxillary models was the stability of the palatal rugae in the long-term. Spatiotemporal (4D) shape models that capture the dynamics of shape change over time are helpful for monitoring and measuring anatomical aging changes (as shown in the video linked to the QR code in Fig. 9) [26].

Figure 9. Spatiotemporal (4D) shape regression video showing changes of maxillary dental arch from 13 to 51 years of age. Registration of dental models at ages, 13, 17, 40, and 51 was used.

Maxillary dental models of the Michigan Craniofacial Growth Center taken from 13 to 51 years of age were superimposed on the palatal rugae using the software 3D Slicer. Our regression model shown in Figure 9 decouples the deformation parameters from the registered digital models at ages 13, 17, 40, and 51, allowing the complexity of the model to reflect the nature of the shape changes. The maxillary posterior teeth displaced occlusally and mesially. A remodeling in the anterior aspect of the alveolar ridge clearly took place.

Although many previous studies have demonstrated reliability of the palatal rugae as a reference region in the maxillary arch, no study had a longitudinal follow-up. Is the palatal rugae reliable for studying aging of the occlusion? Dental models of a sample of 15 normal occlusion subjects from the University of São Paulo and the University of Michigan were organized at the ages of 13, 17, and 60 [23]. T1 dental models were oriented using a 3D coordinate system in the Slicer software [23]. T2 models were registered on T1 models and T3 models were registered on T2 models [23]. Seven tooth landmarks were used to measure 3D dental changes. The conclusion was that superimposition methods using landmarks or regions of interest in the palatal rugae showed adequate reproducibility for a 5-year interval. In other words, from 13 to 17 years of age, palatal rugae are reliable for superimposing dental models and analyzing three-dimensional tooth changes. However, a lower than acceptable reproducibility was found

in the 40-year-interval. Registration of digital dental models from 17 and 60 years of age was difficult to reproduce, probably due to palatal rugae changes over the decades. Some loss of volume and definition of the palatal rugae was observed with aging (Fig. 10) [23]. Additionally, slight elongation of the lateral end of the third rugae was noticed.

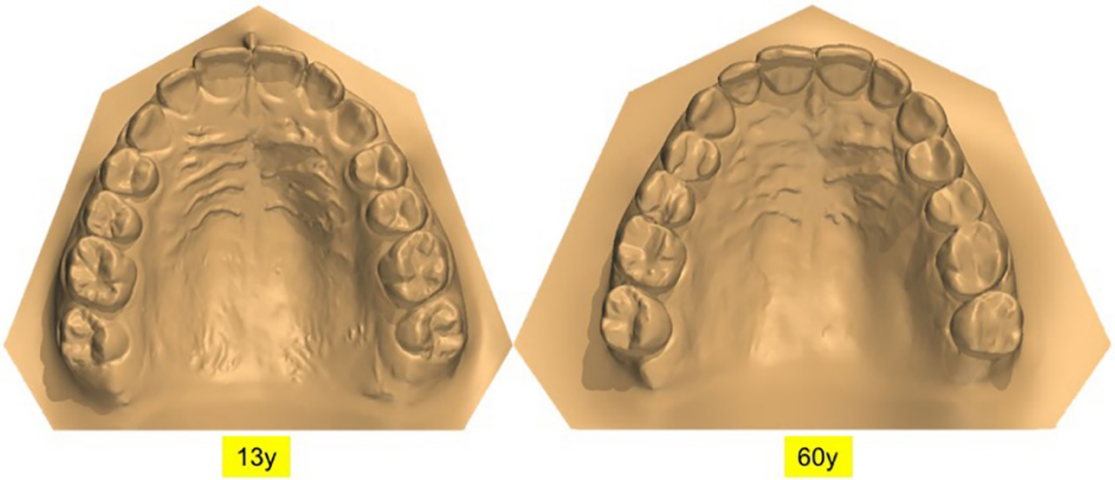

Figure 10. Observe the palatal rugae changes within a 40-year interval. A decrease of volume and definition was observed over the years.

CONCLUSIONS

Aging changes of the normal occlusion were small. Crown height increase was striking from 13 to 60 years in subjects with normal occlusion. From adolescence to early adulthood, clinical crown height increase was already important. The multidisciplinary dental team should consider the natural apical migration of the gingival margin occurring during aging before recommending surgical crown lengthening in patients with decreased height/width ratio of the maxillary incisors. Slight mandibular incisor crowding and tooth discoloration were some changes that were noticed by patients. However, late mandibular incisor crowding did not lead patients to seek orthodontic treatment.

Despite slight dental changes, the occlusion seems to be the most stable feature of the face throughout life. The smile represents the best memory of youth during the aging process.

ACKNOWLEDGMENTS

Authors thank the collectors of Bauru normal occlusion sample in the 60s and 70s decades: Dr. Renato Rodrigues de Almeida, Dr. Décio Rodrigues Martins, Dr. Sebastião Interlandi, Dr. Rui Fonseca, Dr. Paulo Fêo, Dr. Jairo Corrêa, Dr. Arnaldo Pinzan, Dr. José Fernando Castanha Henriques, and Dr. Marcos Roberto de Freitas.

REFERENCES

1. WHO. World Health Statistics.[Database on the Internet]. In: World Health Organization, Geneva, Switzerland 2018. www.who.int/gho. Acessed June 13, 2018.

2. Behrents RG. Growth in the aging craniofacial skeleton. Craniofacial Growth Series, Center for Human Growth and Development, The University of Michigan, Ann Arbor, MI 1985.

3. Behrents RG. An atlas of growth in the aging craniofacial skeleton. Craniofacial Growth Series, Center for Human Growth and Development, The University of Michigan, Ann Arbor, MI 1985.

4. Berg RE, Stenvik A, Espeland L. A 57-year follow-up study of occlusion. Part 2: oral health and attitudes to teeth among individuals with deep overbite at the age of 8 years. *J Orofac Orthop* 2008;69(4):309-324.

5. Bishara SE, Treder JE, Damon P, Olsen M. Changes in the dental arches and dentition between 25 and 45 years of age. *Angle Orthod* 1996;66(6):417-422.

6. Bishara SE, Treder JE, Jakobsen JR. Facial and dental changes in adulthood. *Am J Orthod Dentofacial Orthop* 1994;106(2):175-186.

7. Carter GA, McNamara Jr JA. Longitudinal dental arch changes in adults. *Am J Orthod Dentofacial Orthop* 1998;114(1):88-99.

8. Heikinheimo K, Nyström M, Heikinheimo T, Pirttiniemi P, Pirinen S. Dental arch width, overbite, and overjet in a Finnish population with normal occlusion between the ages of 7 and 32 years. *Eur J Orthod* 2012;34(4):418-426.

9. Henrikson J, Persson M, Thilander B. Long-term stability of dental arch form in normal occlusion from 13 to 31 years of age. *Eur J Orthod* 2001;23(1):51-61.

10. Sinclair PM, Little RM. Maturation of untreated normal occlusions. *Am J Orthod* 1983;83(2):114-123.

11. Thilander B. Dentoalveolar development in subjects with normal occlusion. A longitudinal study between the ages of 5 and 31 years. *Eur J Orthod* 2009;31:109–120.

12. Tibana RH, Meira Palagi LM, Miguel JA. Changes in dental arch measurements of young adults with normal occlusion--a longitudinal study. *Angle Orthod* 2004;74(5):618-623.

13. Bishara SE, Ortho D, Jakobsen JR, Treder J, Nowak A. Arch width changes from 6 weeks to 45 years of age. *Am J Orthod Dentofacial Orthop* 1997;111(4):401-409.

14. Tsiopas N, Nilner M, Bondemark L, Bjerklin K. A 40 years follow-up of dental arch dimensions and incisor irregularity in adults. *Eur J Orthod* 2011;35(2):230-235.

15. Löe H, Ånerud Å, Boysen H. The natural history of periodontal disease in man: prevalence, severity, and extent of gingival recession. *J Periodontol* 1992;63(6):489-495.

16. Morrow LA, Robbins JW, Jones DL, Wilson NH. Clinical crown length changes from age 12-19 years: a longitudinal study. *J Dent* 2000;28(7):469-473.

17. Paulino V, Paredes V, Cibrian R, Gandia JL. Tooth size changes with age in a Spanish population: percentile tables. *Med Oral Patol Oral Cir Bucal* 2011;16(6):e840-844.

18. Vieira EP, Barbosa MS, Quintão CC, Normando D. Relationship of tooth wear to chronological age among indigenous Amazon populations. PLoS One 2015;10(1):e0116138.

19. Dalstra M, Melsen B. From alginate impressions to digital virtual models: accuracy and reproducibility. *J Orthod* 2009;36(1):36-41.

20. Saleh WK, Ariffin E, Sherriff M, Bister D. Accuracy and reproducibility of linear measurements of resin, plaster, digital and printed study-models. *J Orthod* 2015;42(4):301-306.

21. Massaro C, Miranda F, Janson G, Rodrigues de Almeida RR, Pinzan A, Martins DR, et al. Maturational changes of the normal occlusion: A 40-year follow-up. *Am J Orthod Dentofacial Orthop* 2018;154(2):188-200.

22. Miranda F, Massaro C, Janson G, de Freitas MR, Henriques JFC, Lauris JRP, et al. Aging of the normal occlusion. *Eur J Orthod* 2019;41(2):196-203.

23. Garib D, Miranda F, Yatabe MS, Lauris JRP, Massaro C, McNamara Jr JA, et al. Superimposition of maxillary digital models using the palatal rugae: Does ageing affect the reliability? *Orthod Craniofac Res* 2019 [In press].

24. Andrews LF. The six keys to normal occlusion. *Am J Orthod* 1972;62(3):296-309.

25. Ioshida M, Muñoz BA, Rios H, Cevidanes L, Aristizabal JF, Rey D, et al. Accuracy and reliability of mandibular digital model registration with use of the mucogingival junction as the reference. *Oral Surg Oral Med Oral Pathol Oral Radiol* 2019;127(4):351-360.

26. Fishbaugh J, Paniagua B, Mostapha M, Styner M, Murphy V, Gilmore J, et al. Model selection for spatiotemporal modeling of early childhood sub-cortical development. *Proc SPIE Int Soc Opt Eng* 2019;10949:109490L.

UNDERSTANDING PERIODONTAL TISSUE RESPONSES TO MECHANICAL LOAD THROUGH THE USE OF THE PIG MODEL, *SUS SCROFA*

Priti Mulimani, Tracy E. Popowics

ABSTRACT

The delivery of optimum forces to the tooth-PDL-bone complex to achieve tooth movement depends on our understanding of the mechanically driven biological changes that occur during orthodontic treatment. This chapter provides a detailed discussion on the use of the *Sus scrofa* pig model to generate a better understanding of orthodontic load transmission through periodontal tissues. Through our tests on the Periodontal Ligament (PDL) of pigs' deciduous incisors and premolars, we found the incisor PDL to be stiffer than the premolar. We discuss the biological reasons underlying this finding and provide a molecular basis of explanation for PDL behavior and mechanotransduction. Additionally, we discuss the limitations of the rat model for testing biomechanical properties of PDL and share our experience in the use of the pig as an alternative model. We also use the data from our study to generate a better understanding of how the pig model may be applied to investigations of the mechanobiology of orthodontic tooth movement and the design of appliances.

KEY WORDS: *Sus Scrofa*, Periodontal Ligament, Biomechanical Properties, Orthodontic Tooth Movement, Animal Models

INTRODUCTION

A goal of orthodontic research is to generate an evidence-base of studies that may be used to direct clinical decisions with the best treatment outcomes [1]. Challenges abound in attaining this goal, however, since the biological and mechanical pre-requisites necessary to drive orthodontic tooth movement (OTM) in the most efficient and least noxious manner remain elusive. A critical factor seems to be, not the force applied to teeth per se, but the local stresses and strains these forces get translated into within the supporting tissues referred to as the Tooth-Bone-Periodontal Ligament (TBP) complex [2]. Exact determination of these local stresses and strains has proven challenging, in large part due to the unique behavior of the periodontal ligament (PDL) which is likened to a complex, fiber-reinforced substance that responds to force in a viscoelastic, non-linear, and time-dependent manner [3]. Consistent, non-destructive, *in vivo*, clinical monitoring and re-calibration of the constantly changing, complex, periodontal environment in human subjects is a near impossibility, at least with the technologies available today. Animal studies allow exploration of the mechanistic behavior of periodontal tissue and also serve as the basis for constructing biologically validated, finite element biomechanical models of the PDL for hypothesis testing [2]. Additionally, certain treatment modalities may require tests on animals to ensure safe translation of the approach to clinical trials; hence, characterizing the attributes of animal models precisely is crucial to determine the extent of applicability and extrapolation of findings to humans. This chapter will discuss the use of the pig, *Sus scrofa*, as a model for developing a better understanding of

orthodontic load transmission through periodontal tissue and the mandibular incisor and premolar will be evaluated for potential use in orthodontic research and the design of orthodontic treatment.

Periodontal Ligament Research in Orthodontics and Animal Models

The foundation for the scientific basis of OTM was laid down by the pioneering work of Swedish investigator Carl Sandstedt in 1904 on beagle dogs, through his systematic investigation of histological changes triggered in the periodontal ligament by orthodontic force application [4]. Classical studies by Oppenheim on monkeys in 1911 and on dogs by Gottlieb and Orban in 1931 and by Schwarz in 1932 paved the way for a greater understanding of the periodontal tissue response, which attracted much broader attention in orthodontics from 1950 onwards [4][5]. Subsequent research was classified by Ren et al. across two time periods. In the first, from the 1950s to 1980, studies mostly focused on optimal force by characterizing efficiency in orthodontic tooth movement (OTM) produced by light or differential force application as opposed to heavy forces. In the second period, from 1981-2001, orthodontic studies shifted more towards cellular changes, signaling pathways, root resorption, and effects of drugs on OTM [2]. Rapid advances in molecular biology techniques consequent to Human Genome sequencing in the late 90s and early 2000s ushered in the current Genomics era, and orthodontic researchers embraced advanced genetic engineering techniques ranging from knockout mouse models, "-omics" (genomic, transcriptomic, proteomic, metabolomic, microbiomic, salivaomic, etc.) analysis, single nucleotide polymorphism associations to microRNA regulation of OTM, exosome analysis, and gene therapy, to name a few [6].

Studies on biomechanical properties of the PDL include experimental and numerical approaches. Experiments in the PDL tissues of human or animal models typically measure strain changes, molecular signals, or tooth movement, whereas numerical analyses use mathematical equations and biomechanical models derived mostly from finite element methods. Experimental studies in the laboratory are usually carried out in animals such as mice, rats, cats, rabbits, monkeys, dogs, and pigs [7]. We carried out a rapid search of PubMed with the sole purpose of estimating the frequency of different animal models being used in orthodontic research pertaining to periodontal ligament (Table 1). (For a more rigorous and comprehensive search of multiple databases we refer readers to a 2011 systematic review on the topic [30]). As of 26th May 2019, the highest number of studies (995) was related to rats and least (37) to minipigs, concordant with the finding in a recent well-conducted systematic review [7].

Table 1. PubMed search results

No.	PubMed Query (Search date: 26th May 2019)	Items found
1	Search (orthodontic*) AND ((tooth movement) or (tooth displacement) or (periodontal ligament))	10131
2	Search ((rat OR rats)) AND #1	995
3	Search ((mice or mouse)) AND #1	251
4	Search (rabbit*) AND #1	66
5	Search ((cat OR cats)) AND #1	58
6	Search (((non-human primate*) OR (monkey*))) AND #1	49
7	(((sus scrofa) or (minipig*) or (porcine))) AND #1	37

At the University of Washington, the domestic pig - *Sus scrofa* - has been shown to be an important model for biomechanical studies of the craniofacial region including teeth, periodontium, midface, cranial sutures, midpalatal suture, temporomandibular joint, and muscles of mastication [8]. Dr. Susan W. Herring's extensive experimental studies on minipigs and the significant collaborative body of research it has produced, has made the pig one of the best understood animal models for craniofacial function. These studies range from *in vivo* studies of pigs during mastication to biomechanical and histological investigations of their tissues [9-17]. The most noteworthy point about *Sus scrofa* as an animal model is that its physiology and anatomy bear the closest resemblance to humans, outside of the non-human primate category such as monkeys [18]. The established infrastructure for animal care and ease of availability provide a stable foundation to further develop *Sus scrofa* as an animal model in orthodontic research.

Table 2 describes eleven studies evaluating PDL behavior in pigs screened and selected from the 37 PubMed search results by excluding studies analyzing PDL devoid of any context to dentistry and orthodontic tooth movement. These studies demonstrate that the non-linear PDL behavior gives rise to two different Young's modulus values and that loading velocity is inversely proportional to the strain generated within the PDL. Studies that combine experimental and numerical analyses reiterate the biological complexity of the PDL, due to its viscoelastic properties, individual variation in collagen fiber orientation, and root anatomy [23]. Thus, every tooth with its unique root shape, PDL surface area, collagen fiber orientation, intra- and inter-individual variation may have its own signature biomechanical behavior comparable to a fingerprint [30]. None of the studies, with the exception of one [26], have recorded these differences. To develop standardized, predictive and accurate PDL models, differences between tooth behavior within and between species need to be taken into account. The anterior mandibular teeth of pigs are easily accessible to *in vivo* experimentation, and thus are excellent candidates for *in vivo* orthodontic studies. With this in mind, we investigated the biomechanical properties of pig deciduous mandibular incisors and premolars and further evaluated their applicability to investigations of the mechanobiology of orthodontic tooth movement.

Table 2. Summary of studies on porcine PDL

No.	Study Reference	Pig specimen; technique used	Methodology	Result
1.	Knaup et al (2018) [19]*	5 mandibular deciduous premolars of pigs at 4-6 months; laser optical system for deflection measurement, micro-computed tomography (CT), finite element (FE) simulations.	Specimens were deflected buccal-lingually by a distance of 0.2 mm at loading times of 0.2, 0.5, 1, 2, 5, 10, and 60 seconds. Forces and torques were measured and iterative simulations were used to develop the FE model	Force increases during short periods of loading, i.e. 2.6 N (±1.5 N) and 1.0 N (±0.5 N) at 0.2 and 60 seconds respectively. FE simulations of material properties showed bilinear behavior -median value of the first Young's modulus between 0.06 MPa (2 seconds) and 0.04 MPa (60 seconds), and second Young's modulus between 0.30 MPa (10 seconds) and 0.20 MPa (60 seconds).
2.	Huang et al (2016) [20]*	Adult pig PDL specimen; Combined approach of theoretical modeling, nanoindentation measurement of material properties and FE simulation.	Used the FE model, to simulate the tooth movement under orthodontic loading in the transverse plane to predict the mechanical responses of the PDL.	Simulation results showed that local concentrations of stress and strain in the PDL are found. The V – W (Veronda & Westmann) exponential hyperelastic model and its implementation into FE code was validated.
3.	Chang et al (2014) [21]*	Premolar tooth with the mandible harvested for biomechanical testing; CT images, FE simulations.	Synchronized CT images obtained the displacement of the entire specimen during extrusion to aid 3-D reconstruction of FE model. Hyperelastic FE model used to simulate the biomechanical response of the PDL.	Volume variations of the tooth and the alveolar bone were less than 1%, implying that tooth displacement was caused mostly by displacement of the PDL. Nonlinear behavior of PDL observed in numerical model simulations.
4.	Papadopoulou et al (2014) [22]*	18 deciduous premolars of minipigs at 3 -12 months Micro CT and FE simulations.	Experimental data for tooth displacement of 0.2 mm in the lingual-buccal direction within predefined activation periods of 5, 10, 20, 30, 60, 120, 350, 450 and 600 seconds and micro-CT images were used to build a 3D FE model.	Non-linear force/displacement behavior occurred in a bilinear manner corresponding to two different Young's moduli, i.e. stress at 5 seconds was 2.2 MPa - E1= 0.10 MPa, E2 = 0.45 MPa – and stress at 600 secs was 0.65 MPa - E1= 0.02 MPa, E2 = 0.12 MPa, where E1 is lower limit and E2 is upper limit of Young's modulus.
5.	Papadopoulou et al (2011) [23] #	18 deciduous premolars of minipigs at 3 - 12 months.	Specimens were subjected to pre-defined linear displacements of 0.1 and 0.2 mm in the lingual-buccal direction within predefined activation times of 5, 10, 20, 30, 60, 120, 300, 450, and 600 seconds. Force at maximum displacement and 600 seconds after were measured using a 3D force torque sensor.	Forces at maximum displacement were 0.5 to 2.5 N for the 0.1 mm activation and showed extreme variation with the specimens, with comparable behavior at 0.2 mm activation. No significant correlation of forces with root volumes or root surfaces was found. Infer that force development at different displacement velocities is complex and dominated by the PDL biomechanical characteristics.
6.	Qian et al (2009) [24]*	16 samples of pig premolar tooth-bone-periodontal complex; digital images, FE analysis	Compression load applied to the occlusal tooth at 10 µm/s until a displacement of 200 µm was reached; load was held at this point for 5 mins. Load and displacement data were recorded to investigate the time-dependent behavior of PDL.	Load increased slowly at the beginning, followed by a rapid increase with progressively increasing displacement. A drop-in load at hold indicating load relaxation, interpreted as non-linear, viscoelastic PDL behavior. Root apices and furcation points were found to accumulate higher stress and strain.

7.	Natali et al (2007) [25]*	8 multi-rooted primary molars of minipigs at 3–12-months; Optical device to measure displacement, tissue-sections for 3D model fabrication and FE analysis	Tooth displacement data from experimental study and scans of stained tissue-sections at each level were used to construct the 3D model and conduct FE simulations.	The low strain rate characterizing the mechanical response, justified the assumption of a hyperelastic constitutive model, despite general time-dependent behavior of the PDL which seemingly require the use of visco-elastic or poro-elastic constitutive models.
8.	Tanaka et al (2007) [26] #	10 incisor and molar specimens of pigs aged 6–9 months; dynamic viscoelastometer to measure shear	20 cycles of dynamic shear in a supero-inferior direction along the long axis of the root were applied to specimens at each excitation frequency between 0.01 and 100 Hz. Complex dynamic shear modulus G*, the shear storage modulus G', the shear loss modulus G", and the loss tangent tan δ were determined as dynamic viscoelastic parameters	The dynamic elasticity was significantly larger in the coronal region than in the apical region although the dynamic viscosity was similar in both regions, leading authors to conclude that regional difference exists for the elasticity of the PDL rather than the viscous one. They attribute these observed differences in mechanical response, to collagen density, orientation and compression/shear coupling.
9.	Ziegler et al (2007) [27]*	8 multi-rooted primary molars of minipigs at 3–12-months; optoelectronic measurement of tooth displacement.	Forces of up to 6 N were applied to the tooth via the force/torque sensor and tooth displacement was 3-dimensionally recorded by the optoelectronic device; scans of stained tissue-sections at each level of the specimen were used to construct the 3D model and conduct FE simulations.	The material behavior of the PDL was non-linear and could be approximated with a bilinear parameter set consisting of two Young's moduli, E1= 0.05 MPa and E2=0.18 MPa and one ultimate strain, ε12=6.4 %, separating both elastic regimes. No significant differences in the material properties were determined for specimens with two, four, or six roots.
10.	Dorow et al (2003) [28]#	Pig mandibular anterior teeth	Stress-strain behavior of the periodontal ligament was examined until the tissue ruptured by using a clamping fixture in a uniaxial tensional experiment.	Initial phase of the stress-strain curve was particularly dependent on loading velocity and that the shape of the hysteresis curve was subject to a variation in loading velocity.
11.	Dorow et al (2002) [29] #	28 pig mandibular anterior teeth	The samples were loaded on a material testing machine with integrated force sensor and crosshead deflection measuring system. A special clamping fixture allowed the PDL part of the samples to be tested in a uniaxial tensional experiment.	Bilinear values of Young's modulus were obtained E1 = 0.15 N/mm2, E2 = 5.24 N/mm2, which depended on loading velocity. Reducing the loading velocity by a factor of 100 decreased E1 and E2 by approximately 37% and 7% on average, respectively.

* - Combined experimental-numeric approach; # – Experimental approach

MATERIALS AND METHODS

A convenience sample of six farm pigs of approximately two months of age, 50-60 lbs, including both males and females, was obtained. Pigs were sacrificed and specimens of the mandible, anterior to the deciduous fourth premolar were harvested. Soft tissues were removed from the mandibular body; however, the gingiva was maintained intact. Specimens were frozen in saline until further specimen preparation and testing. After a few weeks, specimens were thawed, and the mandibular segments were hemisectioned at the symphysis region. The right half mandibular segment was chosen for testing and was further cut at the diastema to divide it into incisor and premolar segments. These incisor and premolar

units were embedded in a base of dental acrylic using rectangular molds, such that the mandibular body was enclosed but alveolar bone with its surrounding intact soft tissues remained exposed (Figure 1). In each specimen preparation, the tooth identified for testing, i.e. central incisor (di1) or third premolar (dp3) was aligned with the axial direction of compressive loading. The occlusal surfaces of the incisor and premolar were minimally trimmed with a dental bur, to obtain a flat loading surface, for uniform contact with the testing machine. Adjacent teeth were ground down to the level of the alveolar crest, to ensure loading of the test tooth alone.

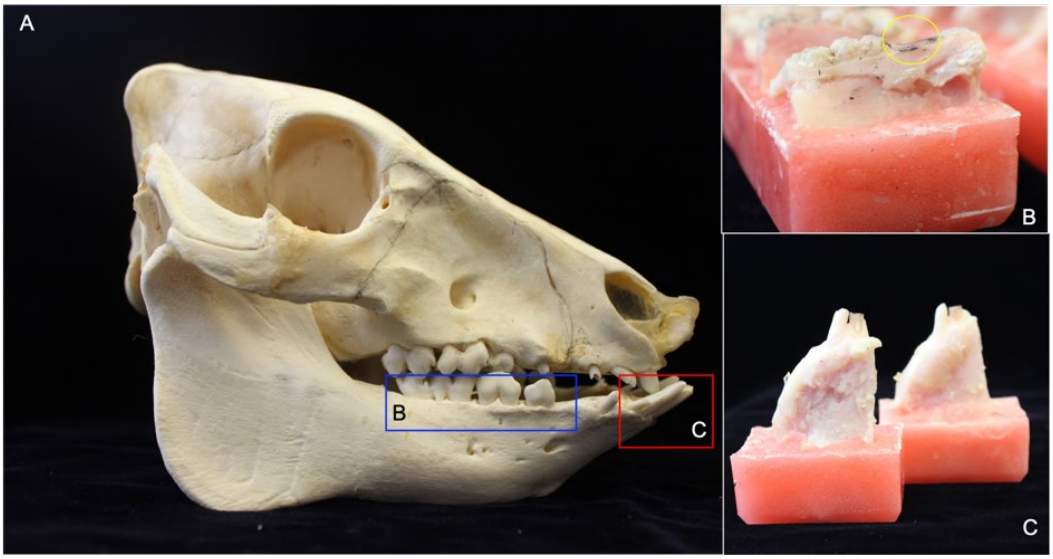

Figure 1. Specimen preparation for testing. A – Sus scrofa skull showing mandibular sections used for testing; B- Deciduous premolars 2, 3, and 4 with intact alveolar bone and surrounding soft tissues embedded in acrylic, yellow circle shows dp3 which was tested and then reduced to the alveolar bone level for cross-sectional area measurement; C- Incisors 1 and 2 with intact alveolar bone and surrounding soft tissues embedded in acrylic (labial view), di2 was later trimmed with dental bur to avoid interference with di1, which was used for testing, details of which are described in text.

Using a materials testing machine (MTS/Sintech), the occlusal surface of the test teeth was preloaded in compression at 0.3 mm/sec to 5 Newtons, and subsequently loaded until 2% strain was achieved (Figure 2). Articulating paper was used on the premolar and the ink transfer marks were checked between tests to ensure exclusive loading of dp3.

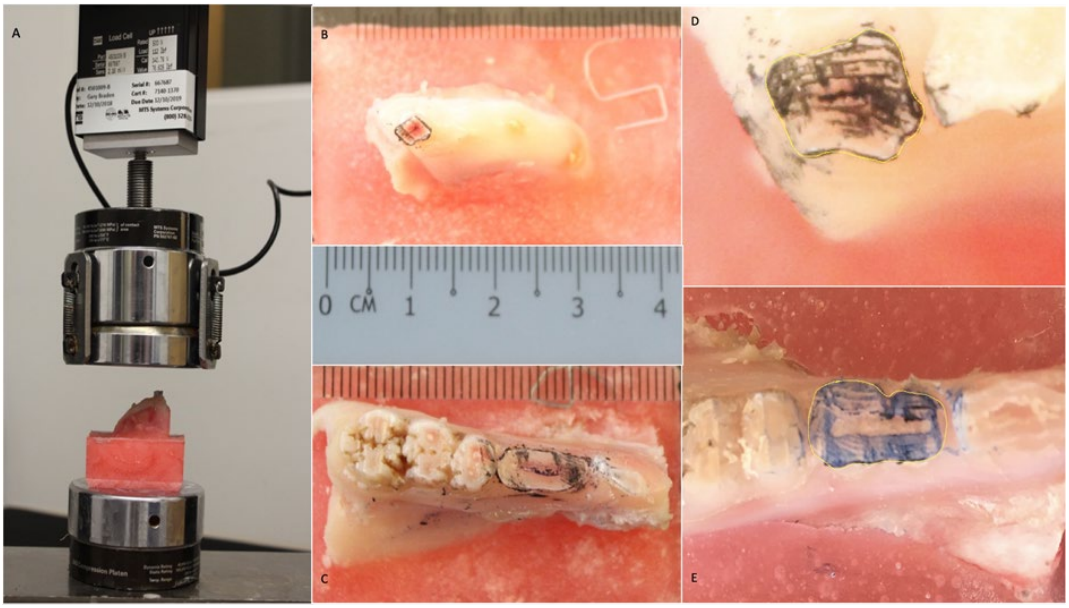

Figure 2. Specimen testing. A – Sample in position between the platens of materials testing machine; B, C – di1 (B) and dp3 (C) ground to maximum cross-sectional area, surface marked with articulating paper ink and photographed with scale; D, E – cross-sectional outline marked for di1 (D) and dp3 (E) and area measured using Image J software (NIH, Bethesda, MD, USA).

Six incisor specimens and five premolar specimens were tested. Pig number five had a partially erupting premolar, hence it had to be excluded from the test. A series of five tests was performed on each sample and data recorded in the Testworks software 4.0. Care was taken to keep the TBP complex of specimens moist by keeping them wrapped in saline soaked gauze pieces between tests. Following testing, each tooth was ground down with a dental bur to a point where the crown had maximum surface area and was photographed. Cross-sectional area was measured using Image J software (NIH, Bethesda, MD, USA) three times by one examiner, and an average of the three was taken as the final value (Figure 2). Applied compressive loads were divided by the cross-sectional area of each tooth and stress values were obtained. Stress-strain curves were plotted, and Young's modulus was calculated as slope for the area of the curve between 5 to 7 N/mm^2 (Figure 3). Mean and standard deviations for both groups were calculated. Wilcoxon Signed Rank test was used to compare the difference in Young's modulus between the incisor and premolar values.

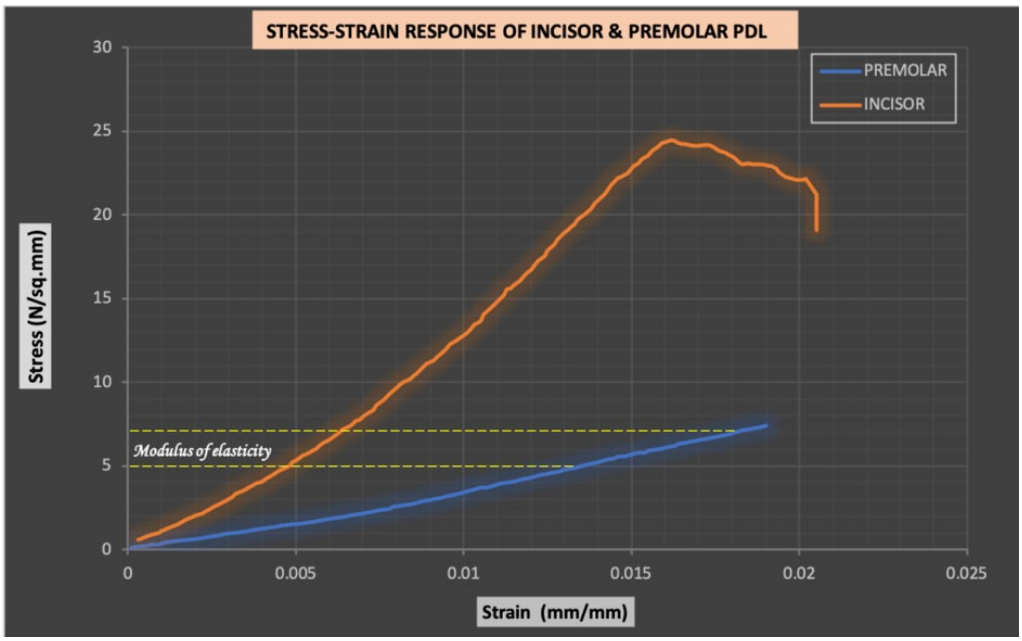

Figure 3. Representative stress-strain curve for the pig incisor and premolar under initial tissue loading conditions from specimen number 4; Young's modulus for both tooth types and in all specimens were measured between the 5 to 7 N/mm2 segment to ensure standardization.

RESULTS

For each of the specimen pairs, the incisor showed a higher stiffness (Young's modulus) than the premolars (Table 3; Figure 4). Mean Young's modulus for six mandibular incisors was 1455.32 (± 640.91) MPa and for five mandibular premolars was 638.29 (± 133.38) MPa (Figure 5). Although the Wilcoxon Signed Rank test did not show statistically significant differences between the Young's modulus for incisors and premolars ($p=0.06$), the incisor specimens showed a clear trend toward greater stiffness.

Table 3. Incisor (di1) and premolar (dp3) stiffness

Specimen no.	Young's Modulus (MPa)	
	Incisors	**Premolars**
1	1113.76	728.00
2	2660.00	601.78
3	931.29	663.88
4	1282.23	428.57
5	1082.87	-
6	1661.79	769.24
Mean (Standard deviation)	1455.32 (± 640.91)	638.29 (± 133.38)

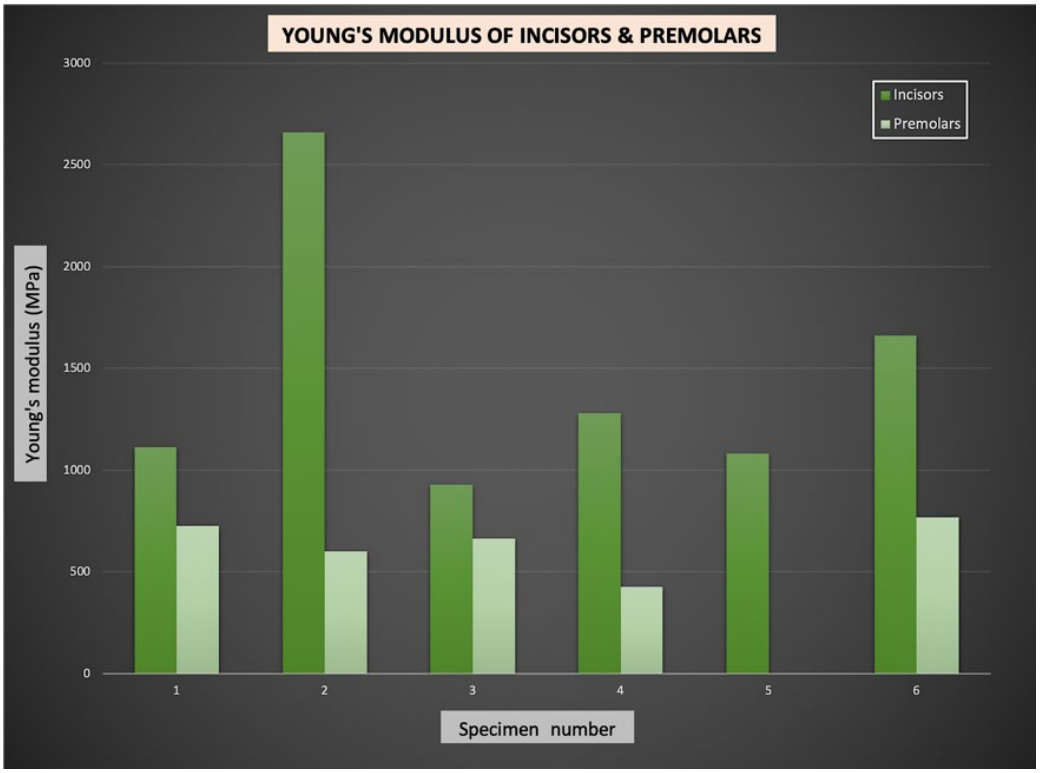

Figure 4. Comparison of PDL stiffness between pig incisors and premolars.

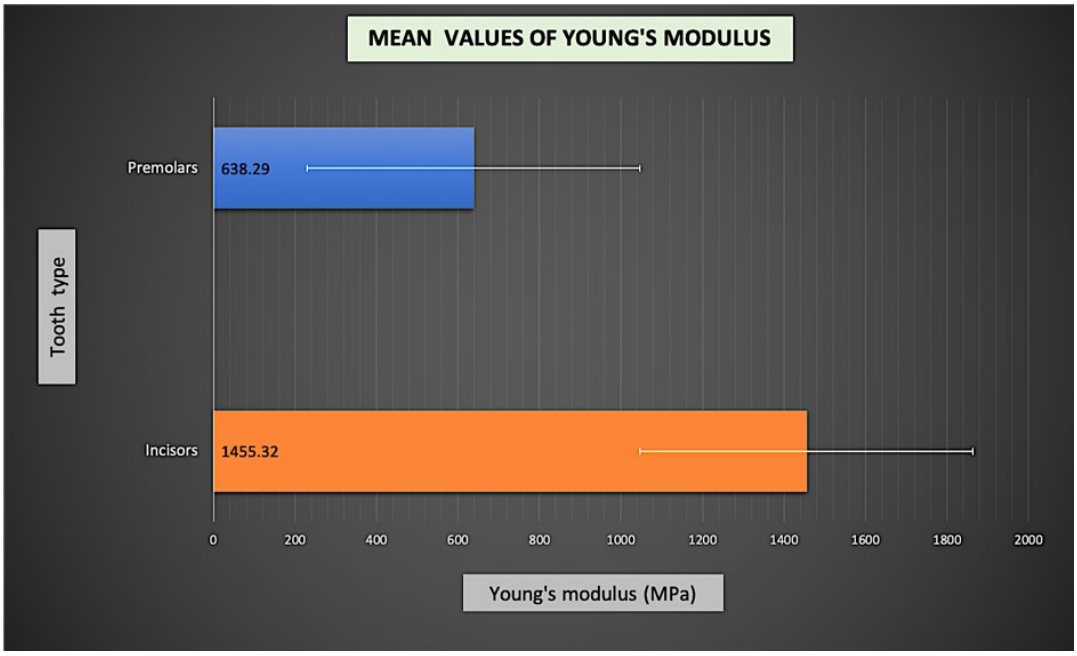

Figure 5. Mean values and standard deviations for pig incisor and premolar PDL stiffness.

DISCUSSION

The biomechanical properties of the PDL are important determinants of the success of applied orthodontic techniques and treatment strategies. The chain of signaling cascades, which trigger bone remodeling and OTM by longer-term application of force, are in continuum with and consequent to the biomechanical changes in viscoelastic components that occur within the PDL during the first few seconds of force application. Unlike pharmacological treatment of medical conditions, which is guided by a specific dose-response relationship between a drug and its effects, no such indicators are available for orthodontists to precisely link force levels and PDL tissue response. However, reference values of PDL behavior at different time points during force application, generated from well-conducted, standardized studies, can be used to eventually engineer a comprehensive, predictive model of the PDL to aid clinical decisions. With technology for real time, in vivo monitoring of PDL in a non-destructive manner currently still being unavailable, animal studies provide a valuable alternative. A critical factor that makes findings from animal studies applicable to humans is choosing the best representative animal model for condition under investigation based on an in-depth understanding of the comparative anatomy and biology of the animal model and identifying the differences in scale between animal and human systems.

We conducted our study with the intention of providing a foundation, to develop a standardized pig model for orthodontic tooth movement in the future. To do so, we had to first understand the PDL load transmission in the context of disparate shapes and sizes of the pig's teeth and quantify the differences if any existed. Hence, with this study we assessed the biomechanical behavior of the pig deciduous mandibular incisor and premolar PDL under initial tissue loading conditions, limited to a non-destructive strain of 2%. We obtained Young's modulus values of 1455.32 ($\pm$ 640.91) MPa and 638.29 ($\pm$ 133.38) MPa for incisors and premolars respectively, indicating a trend toward higher stiffness of the incisor PDL as compared to the premolar during initial loading, contrary to the default expectation that

the premolar being the larger tooth would have a corresponding stiffer PDL. Although the P value of 0.06 with the Wilcoxon Signed Rank test indicated no statistically significant differences, this could be attributed to the high intra-sample variation, the small sample size, and missing one sample from a pair.

These modulus of elasticity values can be interpreted to mean that the premolar shows larger strains with relatively low stresses, whereas greater stresses in the incisor were required to produce equivalent PDL strain (Figure 3). This means that for the same level of applied force, the subsequent extent and timing of bone remodeling triggered will be different for different teeth, which highlights the need for force calibration specific to the tooth being tested. The differential stiffness of PDL, particularly higher structural robustness and stiffness of incisor PDL compared to the premolar, should be kept in mind while designing orthodontic appliances for testing in the pig. This unexpected finding in the pig may be due to the exceptionally long root of its mandibular incisors compared to humans, which could be almost twice the size of its premolar roots [31]. Pigs exhibit typical rooting behaviors where they use their teeth to bite objects, dig, or burrow into the soil or chew grass [32]. The usage of teeth for these accessory functions could have a role to play in the severe proclination of lower incisors and their root length. Additionally, the pig enamel is structurally thinner overall and has less mineral density than human enamel, often resulting in wearing out of the of the enamel surfaces over its lifetime [33]. This could also be a factor contributing to development of long roots during its evolution, to counter occlusal instability arising from the progressive shortening of its crowns. With respect to the premolars, their shorter roots could be related to the larger and more superficially located inferior alveolar nerve canal imposing an anatomic limitation [34].

A review of Young's modulus in different PDL samples by Fill et al, found the values to be dispersed over an extremely broad range between 0.01 to 1379 MPa [30]. These values were derived from studies using both experimental and finite element (FE) analysis of PDL in humans and animals. This variation within and between samples may point to the unique behavior of each tooth PDL or differences in testing methods. Our samples similarly showed a wide range from a low of 931.29 MPa to a high of 2660 MPa within incisor specimens. Overall, our values were comparatively much higher, explained by two main differences – firstly, many of the other studies tested stiffness on buccolingual or mesiodistal force application [19,22], whereas we used intrusive forces. Secondly, since we set the maximum loading parameter as 2% of strain, applied force levels went as high as 330 Newtons for premolars and around 240 for incisors. Our values were comparable to those found in a similarly designed study, where the modulus of elasticity of molars ranged between 668 and 1117 MPa [35]. The high levels of forces generated in the pig PDL within the 2% strain limit is a testament to its load bearing capacity. Hence, orthodontic appliances should be designed to deliver forces sufficient enough to generate OTM in pigs, which may be much higher than humans. To scale the appliance design to a size that applies appropriate force levels in pig, root surface area calculations via CT investigations can provide more information.

Looking into the molecular changes provides a deeper understanding of these initial tissue-responses to force. The PDL is composed essentially of the cells (osteoblasts, osteoclasts, fibroblasts, epithelial cell rests of Malassez, monocytes and macrophages, undifferentiated mesenchymal cells, cementoblasts, and odontoclasts) embedded in an extra-cellular matrix (ECM) where well-defined collagen fiber bundles blend in an amorphous ground substance (proteoglycans, glycosamino-glycans, and glycoproteins) [36]. The configuration of the fibers and viscoelastic behavior of the ground substance determine the deformation characteristics of PDL to applied force. Ground substance components dissipate energy under persistent load by shifting their molecules gradually, thus producing characteristic non-linear, time-dependent behavior, i.e. lag between applied stress and generated strain [37-39]. ECM components like fibronectin link the outside of the cell to the actin cytoskeleton inside the cell. By thus triggering downstream signaling events to initiate long-term bone remodeling changes, they are critical for mechanotransduction of applied physical force to biological response [40]. However, heterogeneity in terms of PDL shape, thickness, root morphology, surface area, and tooth type, compounded by inter-

subject variations, make it highly challenging to develop a uniform, predictive PDL model [21]. This highlights the need for carefully conducted experiments in the appropriate animal model.

Each animal model has its utility and the choice of the appropriate animal model for PDL studies is critical, in obtaining data meaningful and relevant for clinical application to humans [23]. The rat model is most commonly used in orthodontic research. However, researchers have to make a careful assessment while choosing the animal model best suited for their studies, since morphologically, physiologically, and histologically the rat model is quite different from humans. Ease and availability are the two main reasons behind the huge popularity of rats as the animal of choice for orthodontic experiments. By virtue of their small size, it is relatively easy and inexpensive to house a large number of samples for any length of time and, also, it is easier to prepare rat histological slides compared to other animals [41]. Transgenic models are exclusively developed in small rodents, thus propelling their sustained usage and many antibodies required for molecular biology techniques are only available for rats and mice [41].

There are several shortcomings of the rat model, including the distal drift of molars and the continuous eruption of incisors. Continuous incisor eruption would interfere with anchorage considerations, appliance placement, and poor control of force direction while unaccounted distal molar drift could lead to under-estimation of experimental mesial molar movement [41]. The rat molar is approximately 50 times smaller than a human molar, necessitating re-calibration of experimental orthodontic appliance design such that it delivers force proportional to the root surface area of the human root. This also makes moving teeth over distances greater than 1 mm or in a bodily manner in rats a biologically and technically challenging feat [42]. The alveolar bone of rats is generally denser than humans, its cortical plates are thinner, and it has no osteons or marrow spaces. Rats also seem to have less abundant osteoid tissue along the alveolar bone surfaces than humans and that is a critical factor since removal of osteoid tissue determines the rate and efficiency of tooth movement [32,34]. Histological studies also indicate structural dissimilarities in the arrangement of periodontal fibers and a faster rate of turnover both physiologically and in response to orthodontic loading. Both researchers and those who peruse the research need to be cognizant of these facts and carefully consider how exactly the findings from rat studies would apply to a human system in order to avoid erroneous inferences based on misunderstanding. Rat studies are mostly recommended in scenarios where transgenic models can be deployed to check the mechanistic feasibility of signaling pathways and molecular events; these mechanisms are expected to be shared with larger animal models and may provide a more accurate picture closely reflecting the human condition [33].

In contrast, the larger animal models like non-human primates, cats, dogs, and pigs are deemed closer to human physiobiology. However, the 21st century has seen a significant decline in number of non-human primates, dogs, and cats in research [14]. This is attributable to a combination of factors including dogs and cats receiving special attention and protection, pressure from animal welfare activists and the almost human-like behaviors exhibited by non-human primates such as greater sentience to environment than previously assumed, self-awareness, affective emotional states, and intelligence [14,43]. Consequently, an eightfold increase in the number of peer-reviewed papers describing the use of pigs as biomedical models was observed over the past 30 years [44]. The domestic pigs are descendants of the wild ancestral species *Sus scrofa* (Eurasian wild boar) belonging to the order Artiodactyla, the even-toed ungulates. As demand for pigs in biomedical research spiked in the 1940s, miniature crossbreeds were developed across the world, to generate smaller sized hybrids for ease of handling and managing space, food, and medication requirements [8].

The domestic pig's jaw form, function, and biology, including its two sets of dentition - deciduous (I 3/3, C l/l, PM 4/4) and permanent (I 3/3, C l/l, PM 4/4, M 3/3), are remarkably convergent with humans. Their full set of complete deciduous dentition and prolonged period of mixed dentition afford feasible extrapolation of study findings to humans [8]. Primary dentition is either present at birth or erupts within a few weeks post-natally. The first permanent molar appears around the fifth month and all permanent

teeth complete eruption by 18 to 20 months of age. Tooth size of the pig is the same or somewhat larger than in humans, their post-canine tooth roots, especially premolars, bear striking anatomic similarity with humans. The jaw is much larger, providing excellent access to fabricate and deliver orthodontic appliances [37]. Pigs have an optimal growth rate, balanced such that experimental studies can be conducted fast enough to obtain results within reasonable periods of time and slow enough to allow tissue changes and implementation of treatment procedures which closely resemble humans [18]. The model is not without flaws and it diverges from humans in its extremely long and narrow arch form, severely proclined incisors, much larger molars and occasional obstinate behavior [8,18]. A systematic investigation of the dental and PDL characteristics of pig model seems promising. Data from our study could be used in the following ways:

1. The experimental data from our study can be taken as reference values to select the appropriate tooth model while designing studies on the *Sus scrofa* TBP complex.
2. To help in the design of an experimental orthodontic appliance for future biological studies in the pig model, which would apply forces scalable and applicable to human studies.
3. As a dataset that contributes towards building a more comprehensive database of experimental data for each time point or load application phase in the pig model.

Thus, by executing well-designed experiments, based on evidence-based information available on the *Sus scrofa* model as outlined in this chapter, more can be learned about the complexities of periodontal ligament changes during OTM, which is invaluable, since as of now such data cannot be directly obtained from human studies.

REFERENCES

1. Mulimani PS. Evidence-based practice and the evidence pyramid: A 21st century orthodontic odyssey. *Am J Orthod Dentofac Orthop* 2017;152.

2. Ren Y, Maltha JC, Kuijpers-Jagtman AM. Optimum Force Magnitude for Orthodontic Tooth Movement: A Systematic Literature Review. *Angle Orthod* 2003 Feb;73(1):86-92.

3. Jónsdóttir SH, Giesen EBW, Maltha JC. (2006). Biomechanical behaviour of the periodontal ligament of the beagle dog during the first 5 hours of orthodontic force application. *Eur J Orthod* 2006;28:547–552. doi:10.1093/ejo/cjl050.

4. Schwarz AM. Tissue changes incidental to orthodontic tooth movement. *Int J Orthod Oral Surg Radiogr* 1932;18:331–352. doi:10.1016/S0099-6963(32)80074-8.

5. Meikle MC. The tissue, cellular, and molecular regulation of orthodontic tooth movement: 100 years after Carl Sandstedt. *Eur J Orthod* 2005;28:221–240. doi:10.1093/ejo/cjl001.

6. Carlson DS. Evolving concepts of heredity and genetics in orthodontics. *Am J Orthod Dentofac Orthop* 2015;148:922–938. doi:10.1016/j.ajodo.2015.09.012.

7. Vansant L, Cadenas De Llano-Pérula M, Verdonck A, Willems G. Expression of biological mediators during orthodontic tooth movement: A systematic review. *Arch Oral Biol*

2018;95:170–86. doi:10.1016/j.archoralbio.2018.08.003.

8. Li Y, Liu Y, Liu ZJ, Popowics TE, Rafferty KL, Wang S HS. Oral biology and dental models. In: McAnulty PA, Dayan AD, Ganderup N-C HK, editor. *The Minipig in Biomedical Research.* Boca Raton, FL: Taylor & Francis 2012;487–511.

9. Herring SW. Morphological correlates of masticatory Patterns in Peccaries and Pigs. *J Mammal* 1985;66:603–617. doi:10.2307/1380787.

10. Xiaofeng H, Guixin Z, Herring SW. Age changes in mastication in the pig. *Comp Biochem Physiol Part A Physiol* 1994;107:647–654. doi:10.1016/0300-9629(94)90364-6.

11. Rafferty KL, Herring SW. Craniofacial sutures: Morphology, growth, and in vivo masticatory strains. *J Morphol* 1999;242:167–179. doi:10.1002/(SICI)1097-4687(199911)242:2<167::AID-JMOR8>3.0.CO;2-1.

12. Zhang F, Langenbach GEJ, Hannam AG, Herring SW. Mass properties of the pig mandible. *J Dent Res* 2001;80(l):327-335.

13. Herring SW, Rafferty KL, Liu ZJ, Marshall CD. Jaw muscles and the skull in mammals: the biomechanics of mastication. *Comp Biochem Physiol Part A Mol Integr Physiol* 2001;131:207–219. doi:10.1016/S1095-6433(01)00472-X.

14. Herring SW. TMJ anatomy and animal models. *J Musculoskelet Neuronal Interact* 2003;3(4):391–394; discussion 406-407. http://www.ncbi.nlm.nih.gov/pubmed/15758330. Accessed 26 May 2019.

15. Liu ZJ, Green JR, Moore CA, Herring SW. Time series analysis of jaw muscle contraction and tissue deformation during mastication in miniature pigs. *J Oral Rehabil* 2004;31:7–17. doi:10.1111/j.1365-2842.2004.01156.x.

16. Al Dayeh AA, Rafferty KL, Egbert M, Herring SW. Real-time monitoring of the growth of the nasal septal cartilage and the nasofrontal suture. *Am J Orthod Dentofac Orthop* 2013;143:773–783. doi:10.1016/j.ajodo.2013.01.012.

17. Soh SH, Rafferty K, Herring S. Cyclic loading effects on craniofacial strain and sutural growth in pigs. *Am J Orthod Dentofacial Orthop* 2018;154:270–282. doi:10.1016/j.ajodo.2017.11.036.

18. Weaver ME, Sorenson FM, Jump EB. The miniature pig as an experimental animal in dental research. *Arch Oral Biol* 1962;7:17-23. doi:10.1016/0003-9969(62)90044-4.

19. Johannes Knaup T, Dirk C, Reimann S, Keilig L, Eschbach M, Korbmacher-Steiner H, et al. Time-dependent behavior of porcine periodontal ligament: A combined experimental, numeric in-vitro study. *Am J Orthod Dentofacial Orthop* 2018;153:97-107. doi:10.1016/j.ajodo.2017.05.034.

20. Huang H, Tang W, Yan B, Wu B, Cao D. Mechanical responses of the periodontal ligament based on an exponential hyperelastic model: a combined experimental and finite element method. *Comput Methods Biomech Biomed Engin* 2016;19:188–198.

doi:10.1080/10255842.2015.1006207.

21. Chang C-H, Lei Y-N, Ho Y-H, Sung Y-H, Lin T-S. Predicting the holistic force-displacement relation of the periodontal ligament: in-vitro experiments and finite element analysis. *Biomed Eng Online* 2014;13:107. doi:10.1186/1475-925X-13-107.

22. Papadopoulou K, Hasan I, Keilig L, Reimann S, Eliades T, Jager A, et al. Biomechanical time dependency of the periodontal ligament: a combined experimental and numerical approach. *Eur J Orthod* 2013;35:811–818. doi:10.1093/ejo/cjs103.

23. Papadopoulou K, Keilig L, Eliades T, Krause R, Jager A, Bourauel C. The time-dependent biomechanical behaviour of the periodontal ligament--an in vitro experimental study in minipig mandibular two-rooted premolars. *Eur J Orthod* 2014;36:9–15. doi:10.1093/ejo/cjr134.

24. Qian L, Todo M, Morita Y, Matsushita Y, Koyano K. Deformation analysis of the periodontium considering the viscoelasticity of the periodontal ligament. *Dent Mater* 2009;25:1285–1292. doi:10.1016/J.DENTAL.2009.03.014.

25. Natali AN, Carniel EL, Pavan PG, Bourauel C, Ziegler A, Keilig L. Experimental-numerical analysis of minipig's multi-rooted teeth. *J Biomech* 2007;40:1701–1708. doi:10.1016/j.jbiomech.2006.08.011.

26. Tanaka E, Inubushi T, Takahashi K, Shirakura M, Sano R, Dalla-Bona DA, et al. Dynamic shear properties of the porcine molar periodontal ligament. *J Biomech* 2007;40:1477–1483. doi:10.1016/J.JBIOMECH.2006.06.022.

27. Ziegler A, Keilig L, Kawarizadeh A, Jäger A, Bourauel C. Numerical simulation of the biomechanical behaviour of multi-rooted teeth. *Eur J Orthod* 2005;27:333–9. doi:10.1093/ejo/cji020.

28. Dorow C, Krstin N, Sander F-G. Determination of the Mechanical Properties of the Periodontal Ligament in a Uniaxial Tensional Experiment. *J Orofac Orthop/Fortschritte der Kieferorthopädie* 2003;64:100–7. doi:10.1007/s00056-003-0225-7.

29. Dorow C, Krstin N, Sander F-G. Experiments to Determine the Material Properties of the Periodontal Ligament. *J Orofac Orthop/Fortschritte der Kieferorthopädie* 2002;63:94–104. doi:10.1007/s00056-002-0107-4.

30. Fill TS, Carey JP, Toogood RW, Major PW. Experimentally determined mechanical properties of, and models for, the periodontal ligament: critical review of current literature. *J Dent Biomech* 2011;2011:312980. doi:10.4061/2011/312980.

31. Patterson A, Popowics T. Experimental ex vivo traumatic intrusion in the mandibular incisors of the farm pig, Sus scrofa. *Dent Traumatol* 2014;30:423–428.

32. Ball RS. Husbandry and Management. In: McAnulty H, Dayan A, Ganderup N-C, eds. *The Minipig in Biomedical Research*. Boca Raton, FL: Taylor & Francis 2012;17–36.

33. Popowics TE, Rensberger JM, Herring SW. Enamel microstructure and microstrain in the fracture of human and pig molar cusps. *Arch Oral Biol* 2004;49:595–605. doi:10.1016/J.ARCHORALBIO.2004.01.016.

34. Štembírek J, Kyllar M, Putnová I, Stehlík L, Buchtová M. The pig as an experimental model for clinical craniofacial research. *Lab Anim* 2012;46:269–279. doi:10.1258/la.2012.012062.

35. Yeh K, Popowics T, Rafferty K, Herring S, Egbert M. The effects of tooth extraction on alveolar bone biomechanics in the miniature pig, Sus scrofa. *Arch Oral Biol* 2010;55:663–669. doi:10.1016/j.archoralbio.2010.05.014.

36. Nanci A, Bosshardt DD. Structure of periodontal tissues in health and disease. *Periodontol 2000* 2006;40:11–28. doi:10.1111/j.1600-0757.2005.00141.x.

37. Bien SM. Fluid dynamic mechanisms which regulate tooth movement. In: Staple PH, editor. *Advances in Oral Biology*. New York: Academic Press Inc 1966;173–201.

38. Uhlir R. Biomechanical characterization of the periodontal ligament: Orthodontic tooth movement. University of North Carolina at Chapel Hill; 2014. https://cdr.lib.unc.edu/concern/dissertations/f4752h288. Accessed 3 November 2019.

39. Embery G, Picton DCA, Stanbury JB. Biochemical changes in periodontal ligament ground substance associated with short-term intrusive loadings in adult monkeys (Macaca fascicularis). *Arch Oral Biol* 1987;32:545–549.

40. Alberts B, Johnson A, Julian L, Morgan D, Raff M, Roberts K, et al., editors. Cell junctions and the extracellular matrix. In: *Molecular Biology of the Cell*. Sixth. New York and Abingdon: Garland Science 2008;1035–1090.

41. Ren Y, Maltha JC, Kuijpers-Jagtman AM. The rat as a model for orthodontic tooth movement--a critical review and a proposed solution. *Eur J Orthod* 2004;26:483–490. http://www.ncbi.nlm.nih.gov/pubmed/15536836.

42. Ibrahim AY, Gudhimella S, Pandruvada SN, Huja SS. Resolving differences between animal models for expedited orthodontic tooth movement. *Orthod Craniofacial Res* 2017;20:72–76.

43. Ferdowsian HR, Beck N. Ethical and Scientific Considerations Regarding Animal Testing and Research. *PLoS One* 2011;6:e24059. doi:10.1371/journal.pone.0024059.

44. Gutierrez K, Dicks N, Glanzner WG, Agellon LB, Bordignon V. Efficacy of the porcine species in biomedical research. *Front Genet* 2015;6:293. doi:10.3389/fgene.2015.00293.

VIRTUAL AND AUGMENTED REALITY IN DENTISTRY

Hera Kim-Berman, Esther Suh

ABSTRACT

Dental education is based on 3 domains; (1) cognitive domain – knowledge and critical thinking, (2) affective domain – empathy and behavior management, and (3) psychomotor skills domain – technical procedures and treatments. Preclinical courses are introduced to the novice dental student to facilitate development of fine motor skills and control of new tools, knowledge of therapeutics, biomaterials, and techniques prior to patient care where integration of the acquired dental skills and patient management occurs. Technology has been used to improve support for preclinical and clinical teaching, including development of virtual reality (VR) educational tools for human anatomy, dental anatomy, and maxillofacial surgery planning. However, although VR hardware and software have advanced in recent years, the available tools are few in number and the use of VR technology in dentistry is still at its infancy. In this chapter, we introduce the concepts of augmented and virtual reality with associated hardware and software development. Additionally, we review the published literature and preliminary results related to virtual reality in medical and dental education and its clinical application.

Key Words: Augmented Reality, Virtual Reality, Orthognathic Surgery, Virtual Dental Library, Dental Anatomy

INTRODUCTION

Although computing was conceptualized hundreds of years prior to the 1940's arrival of the modern electronic computer, the evolution and growth of modern technology since then has led to the universal utilization and dependence on it. Raised around society's social-technological development and digital media, matriculating dental students are altering the way they think, interact, produce, and consume information. Rather than integrating technology into dental school based on the simple application of and fascination with information technology (IT), educators have questioned how to maximize IT utilization to improve clinical care, education, and research; measure those improvements, and most effectively integrate these technologies into the dental curriculum.

For the dentist, demonstrating proficiency in the following domains relates to success in the dental profession: (1) cognitive (knowledge and critical thinking), (2) affective (empathy and behavior management), and (3) psychomotor skills (technical procedures and treatments). In dental education, technology has been used to support preclinical and clinical teaching, share effective educational content and methods, leverage technology-mediated changes in the balance of power between faculty and students and build a learner-centered information infrastructure [1]. A major component of dental

preclinical courses is developing psychomotor skills and the control of new tools and techniques prior to patient care [1]. Although most dental schools train students using traditional methods, such as mounted typodonts to practice on plastic teeth, some schools use computer-aided simulations of preparations, restorations, and wax-ups in preclinical courses [2]. Technology, such as the simulations, began to support the development of psychomotor skills required of dental students. Amidst the growing popularity of technology-based learning, it is important to identify the educational goals and evidence-based integration when choosing the type of technology to incorporate into a curriculum [2].

Emerging technology, including augmented reality (AR) and virtual reality (VR), is starting to be integrated into dental education. VR educational tools for human anatomy, dental anatomy, and maxillofacial surgery planning have been developed; however, the available tools are few in quantity and the use of virtual reality technology in dentistry is still in its infancy.

DEFINITIONS: VIRTUAL REALITY AND AUGMENTED REALITY

Virtual reality (VR), a relatively new technology platform that immerses a user in a curated environment and situation, has caught the attention of researchers as a viable way to enhance educational resources. Research shows VR can be used in medical and dental preclinical environments to simulate experiences, enhance critical thinking abilities, and increase confidence prior to working in a clinical setting [2].

Designed in the 1950s and prototyped in the early 1960s, Morton Heilig's Sensorama Simulator was the first classical VR device created in history. This machine simulated a motorcycle ride through New York using haptic motion from the seat, scents and winds to mimic the road and 3-dimensional motion picture that filled up most of the user's peripheral vision. Following this innovation, engineers have been pursuing VR for decades. In 1965, Ivan Sutherland designed the first VR head-mounted display system (HMD) [3]. Although advancements have been made, the technology is far from its goal of achieving complete user immersion, where users are unable to differentiate computer-generated data from reality [4]. In addition to these advancements through VR evolution, researchers have applied this technology to any area where computers are involved. VR is broadly applicable and currently VR has been applied for military, entertainment, and educational purposes [5].

VR can be fully immersive using a head mounted device (HMD) or it can be non-immersive by using stereoscopic glasses or 2D monitors. In both cases, the users interact in an entirely computer-generated virtual world [6]. Augmented reality (AR), which evolved as an extension of VR, supplements the real world with virtual content to enhance user perception [7]. The earliest AR experiments involved Sutherland's (1968) HMD, which was a transparent HMD and position sensing system, enabling the virtual image to appear at a fixed position in space [8]. Researchers define AR as a technology which (1) combines real and virtual imagery, (2) is interactive in real time, and (3) registers the virtual imagery with the real world [9]. AR technology allows computer-generated virtual images to overlay physical objects and calibrate to the user's real-world environment for user interaction. These virtual models are stored in virtual libraries, retrieved from the libraries during runtime, registered, and rendered onto the real-time scene [7]

AR and VR, though similar in terms of utilizing computer-generated information to modify, augment, replace, or interface with user perception, differ by the user's frame of reference or environment. VR utilizes virtual environments where all perceived information is computer-generated (e.g. flight simulation for pilots), while AR applications inserts virtual content centered within the real world through smart glasses or a camera and screen (e.g. PokemonGo game using smartphones). Past and present research investigates the feasibility and integration of AR/VR technology platforms. Researchers

continue to present the potential of various AR/VR applications in education, especially in the area of medical and dental training where rapid information transfer is critical [10].

REVIEW OF LITERATURE

Literature presents VR as a valid tool for science education, providing students with mentally-immersive learning [11]. VR systems present advanced user interfaces with synthetic computer-generated 3-dimensional (3D) environments, allowing user immersion, interaction, and navigation [12]. Software programs, along with the hardware (headset and controller), have been designed for various medical and dental applications to study VR as a teaching approach and learning model.

Many medical applications of VR involve the study of human anatomy. Cardiac anatomy is one of the most challenging topics to teach due to its complex 3D form [13]. Educators have integrated cadaveric dissections in the cardiac anatomy curriculum as a teaching approach to expand spatial intelligence, defined as "a capacity for mentally generating, rotating, and transforming visual image," beyond rote memorization [14]. Using a cardiac virtual environment, Maresky et al. analyzed the spatial intelligence of 42 first-year medical students who were separated into a VR and non-VR group [15]. As a result, the researchers validated the use of a VR simulation as a part of the course curriculum by studying the effect of VR as an adjunct to the traditional cardiac dissection experience [15]. Moro et al. agree that anatomic cadaver dissections provide the most effective method of learning human anatomy [16]. However, the structure of these learning experiences is very limited. On average, 10 to 12 medical students are limited to one cadaver for approximately three hours per week, which then requires them to self-direct their studying using supplemental resources [17]. Since AR/VR allows hands-on immersive learning, Moro et al. aimed to understand whether learning skeletal anatomy using AR/VR software was as effective as tablet-based applications [16]. As a result, there was no significant difference in student test scores between the different learning modes, and both AR and VR were as effective as tablet-based learning about anatomy. However, they found that AR/VR, as a supplement, promotes intrinsic benefits such as increased learner immersion and engagement [16].

Simulations train students to be proficient in medical procedures. Of the various training models, VR simulators are advantageous in that performance metrics are embedded into the software, enabling continuous performance feedback and allowing feasible implementation of proficiency-based training [18]. Gutiérrez et al. investigated the effect of the degree of VR immersion (fully-immersed HMD or partially-immersed screen-based display) on the learning performance of first-year medical students [19]. Software engineers designed the VR simulation for these novice students to learn without consequences as they experienced a life-like medical situation. The study demonstrated a positive effect of VR simulation on learning as seen by improved knowledge structure and an enhanced effect with full immersion compared to partial immersion [19]. Some medical situations occur in the operating room where expert surgeons demonstrate lower complication rates dependent on extensive surgical experience and skill [18,20]. Inexperienced cataract surgeons have trained on VR simulators such as Eyesi (VRmagic, Mannheim, Germany) to reduce complication rates and develop proficiency for live cataract surgery. By combining medical information and data within VR systems, surgeons can visualize the incorporated data, improve patient safety and lower complication risk [20]. Literature validates the use of Eyesi ophthalmic surgical simulators to improve the learning curve to acquire microsurgical skills [18,21,22].

VR simulations, without limitation to cataract surgery, are used in a multitude of surgical trainings such as basic suturing and knot tying, dissections and virtual anatomy laboratory, arthroscopy, interventional radiography and cardiology, maxillofacial surgery, laparoscopy, peritoneal lavage, epidural injection, neurosurgery, trauma training, and others [23]. VR models for operational training simulate real time surgery in a VR environment customized with mock-up instruments and tissues. Simulation designers

can associate real time surgical equipment to electromagnetic tracking systems to augment user perception and increase fidelity of simulations [18]. Simulations are one of many methodologies in the medical applications of VR. When evaluating the effects of different methodologies of learning (text, video, and VR) on motivation and competency of medical students, immersive VR technology significantly increased both outcomes, suggesting VR technology integrated into medical curricula is a beneficial learning methodology [23].

Although VR applications are common and much more developed in medical than dental fields, the literature presents VR applications in dentistry and their utilization to improve dental education and clinical skills [20]. VR is favored over screen-based technology due to the increased perception of user immersion in the virtual environment. An important feature of VR, when applied to a teaching environment, is its ability to provide users with a sense of immersion and presence [11]. A dental training system using VR technology simulates a patient and heightens visualization capabilities necessary when novice dental students learn new techniques. Chen et al. describe the components of a VR dental training system and how the components interact with the user to increase user immersion. For example, a force touch feedback system (haptic device), Phantom Desktop (Sensable Technologies, Inc., Woburn, MA), limited to a certain sensitivity, was implemented into the VR space in which direct dental operations using dental instruments can be performed in real time [24]. A separate study utilized Phantom Desktop as a virtual software system to aid in learning and practicing psychomotor skills for cavity preparations in endodontics [25]. This study did not use fully-immersive VR technology. Instead, it demonstrated that the partially-immersive VR with an input/output device that senses the body's movements when used in conjunction with a desktop computer software application, can decrease the learning curve of dental anatomy, handling drilling instruments, and approaching challenges associated with endodontic procedures [25].

Another dental application of VR-based technology uses an advanced simulation unit called DentSim (Image Navigation Ltd., New York, NY) to aid first-year dental students' preparative operative training. The study data are supportive of VR-based technology as an educational tool [26]. For example, VR technology that is used to learn and visualize dental anatomy stimulates student learning [12]. An application achieving this purpose is Tooth Atlas 3D (eHuman, Milpitas, CA), which uses stereoscopic 3-dimensional (3D) models displayed on a 2D screen to teach dental anatomy. Kim-Berman et al. utilized emerging technologies in AR and VR to develop a Virtual Dental Library and a smartphone-compatible AR virtual tooth identification test [27]. Although users had some difficulty in visualization, manipulation, and technical difficulties related to smartphones, this study successfully demonstrated criterion validity of an AR virtual assessment tool for tooth identification [27]. Additionally, the VR Patient (Virtual Reality Patient), a fully immersive simulated patient module in a virtual reality environment allowing manipulation of the upper and lower jaws and chin in three planes of space, was developed to help students understand diagnosis and treatment planning of orthognathic surgical procedures (Fig. 1) [28].

Figure 1. Jaw simulation using Virtual Reality Patient with Oculus Rift head mounted device and touch controllers.

Although Sakowitz et al. showed that third year dental students were able to improve their understanding of diagnosis and treatment planning of orthognathic cases using both 2D prediction tracing and the VR Patient method, the preliminary results failed to demonstrate a significant relationship between fidelity and improved outcomes in student learning with respect to VR [28]. However, the results of this study should be considered cautiously given the nature of the study's small sample size and the variability of the data. Currently, VR and AR-based educational tools are not yet fully accepted and incorporated in dental education due to the lack of research and more evidence to support the fidelity of VR/AR dental educational tools is needed.

VR HARDWARE

Virtual reality (VR) is implemented by utilizing interactive devices such as gloves, headsets, or head mounted devices or helmets [29]. Most fully immersive VR hardware is engineered as a head mounted device (HMD). Although the number of companies offering VR HMDs is growing, for the purpose of this chapter, the Oculus Rift (Oculus VR Inc, Menlo Park, CA) and the Oculus Go (Oculus VR Inc, Menlo Park, CA) will be discussed in detail.

In 2012, backed by numerous supporters and investors, the first Oculus HMD prototype was introduced, followed by Developer Kit version 1 and Developer Kit version 2 [29, 30]. In 2016, Oculus VR Inc. was acquired by Facebook and Oculus VR released its first consumer version of the Oculus Rift HMD. This marked the first major commercial release of an affordable VR headset with sensor-based tracking [31]. The sensing in the Oculus Rift is performed using a single circuit board made up of a microcontroller, gyroscope, accelerometer, magnetometer, and infrared LED sensors. These major components provide three-axis measurements to track the orientation of the headset [32]. The Oculus Rift senses rotational movement using six degrees of freedom (6DOF) and positional movement with outside-in tracking. The

outside-in tracking system senses positional movement of the headset and two controllers relative to the sensors, or Oculus constellations, placed in the environment external to the headset. Two constellations are sufficient in providing limited positional movement, but a third constellation is required for 360 degrees of positional tracking. With built-in headphones and microphone, the Oculus Rift is a desktop VR headset, which means it does not require a power outlet, but must be plugged into a computer. In the effort to increase affordability, portability, and usability, the Oculus Go device was released in 2018 [33]. More recently, in 2019, Oculus Quest and Oculus Rift S, which do not require external sensors, were released.

The Oculus Go consists of a three degrees of freedom (3DOF) headset and one controller. While the 6DOF Oculus Rift and Quest track rotational and positional movement, the 3DOF Oculus Go has the ability to track only rotational movement, which was an effort to specialize these mobile headsets in 360-degree experience. The Go and the Quest devices are standalone VR headsets, running independently from a computer or outside-in trackers [34]. They use a mobile processor that wirelessly connects to mobile devices without requiring direct connection to a computer.

VR SOFTWARE FOR DENTAL APPLICATIONS

Virtual Reality (VR) headsets with software programs are designed by computer scientists and engineers in collaboration with researchers and clinicians to deliver the VR experience for medical and dental education [35]. Our research group at the University of Michigan, School of Dentistry have collaborated with the Duderstadt Center (University of Michigan, Ann Arbor, MI) using the in-house VR software engine, Jugular (University of Michigan, Ann Arbor, MI), for jaw surgery simulation. Additionally, in cooperation with a start-up company, Gwydion Inc. (Ann Arbor, MI), a private AR and VR software developing company, the Virtual Dental Library was developed using the Arthea software. Arthea, now owned by the University of Michigan, College of Engineering, is a VR engine software that supports multiple devices, including the Oculus Rift and Oculus Go, and enables users to directly upload content or 3-dimensional (3D) models using multiple file types (FBX, OBJ, STL, WRL, PDB, DAE, and DICOM) into a virtual library. The uploaded files are converted and shared so users can view models in VR and AR, remotely access the content, and interact with peers from customized libraries [27].

VR AND PRECLINICAL DENTAL EDUCATION

Leveraging VR hardware (Oculus HMD) and software (Jugular and Arthea) we have conducted studies to evaluate student learning in dental anatomy, student self-assessment in tooth preparations and restorations, orthognathic treatment planning, and user experience.

Dental anatomy is fundamental for operative dentistry since proficient knowledge allows appropriate carving of teeth preparations and reproduction of anatomical details for dental restorations to appear natural with proper functionality. Traditionally, tooth morphology is taught through lectures, textbooks, and with assessments testing the students' ability to sculpt teeth using wax blocks or identify morphology and prepare teeth using preserved and/or manufactured teeth [36]. Most studies that evaluate improvements of learning dental anatomy and carving by various teaching methods have shown heterogeneity in their results, providing insufficient evidence to support a standard methodology for teaching and assessing students' dental anatomy knowledge [36]. New methods involving technology are being introduced to preclinical and clinical courses to facilitate dental education [37]. An example is computer-based software systems that utilize text, photographs, illustrations, lectures, aural pronunciation, terminology, and assessments to aid in learning dental anatomy [38]. Another example is

AR and VR software as an adjunct to learning dental anatomy and the preparations of teeth for restoration.

At the University of Michigan, School of Dentistry, the Virtual Dental Library of the human dentition, which is accessible to students through a VR head-mounted device (HMD), computers or application on mobile devices, was developed (Fig. 2).

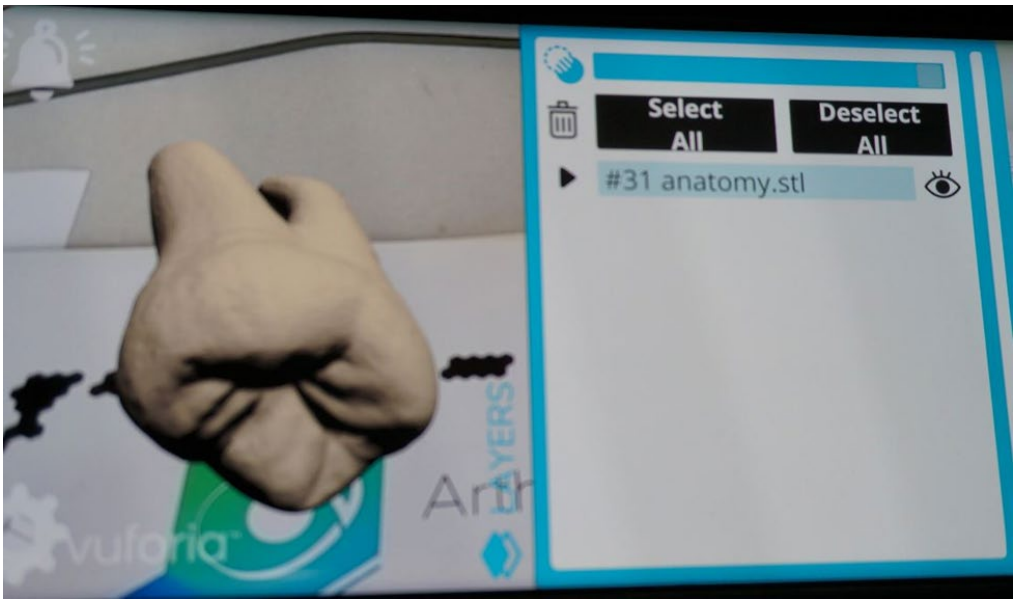

Figure 2. Screenshot of Virtual Dental Library in augmented reality using Arthea software and smartphone.

Supported by VR HMDs Oculus Rift and Oculus Go and software such as Arthea, students can spatially view ideal resin teeth, extracted human teeth, prepared resin teeth for operative and prosthodontics restorations, impressions of teeth, and provisional restorations. The Virtual Dental Library was developed using a conceptual model of the educational triangle involving student, teacher, and learning tool [27]. The interrelationship of the educational triangle influences academic (quantitative) and affective (qualitative) outcomes. This conceptual model can potentially influence education in curriculum reform, higher order of learning, lifelong learning, and lead to research and development of hardware/software updates and product design. Students and faculty members can upload content or 3D models to expand and customize the library, share with peers, and develop virtual assessment tools such as a virtual tooth identification test. The virtual tooth identification test has been demonstrated as a valid assessment tool that evaluates students' knowledge of dental anatomy [27, 39].

Student self-assessment is another area where VR technology can be incorporated in preclinical dental education. Students are expected to objectively and accurately evaluate their preclinical work against a standard. Without external feedback, students may become accustomed to repeating clinical error. Confusion regarding the quality of students' work may also stem from lack of consistent feedback from faculty members even after intense calibration [40]. The American Dental Association accreditation standard demands that "graduates must demonstrate the ability to self-assess, including the development of professional competencies and the demonstration of professional values and capacities associated with self-directed, lifelong learning [41]." Dental students experience several years of an educational system where their psychomotor preclinical skills are regulated by instructor feedback and performance assessments, suggesting that self-assessment may be a valid measure of clinical skills when other parameters are maintained. More accurate self-assessments occur when self-assessment data is

reconciled with other sources of evaluation, which is usually related to students' increased familiarity of the content [42]. VR systems can be used to improve the accuracy of self-assessment and consistent faculty feedback due to the advantages of measurement in a visualization space in VR rather than with the naked eye [43]. Studies show increased intra-rater reliability, consistency of assessments by the same grader at different times, and inter-rater reliability, consistency of assessments between graders, of technology-based compared to traditional tooth preparation assessments by students and graders [39,40,44]. However, there is a lack of studies demonstrating significant reliability testing for self-assessment when using VR in preclinical dental courses.

Usability is as important and necessary as validity and reliability testing when supporting changes in methodologies of learning, teaching, and testing in preclinical dental courses [37,45]. Usability refers to the user's perspective in how well a design enables functioning, performance, and well-being. In technology, it is the degree of ease and learnability with which a hardware and software can be used to achieve goals efficiently and effectively, which is recognized as an important aspect of successful product design [46]. Information technology (IT) companies are constantly revising designs to enhance usability for user satisfaction, efficiency, and effectiveness while others have studied the methodology in which usability is tested [47,48].

Efficiency can be measured by collecting task completion times. Researchers testing technology have evaluated the time taken to complete individual questions, the number of steps required to learn and complete a task, and percentage of questions completed correctly to assess which software is more efficient for the users [49]. Effectiveness can be measured by comparing user performance with a predefined level in terms of speed, errors, number of steps taken, and whether the task was completed within a time limit [48]. Recently, we published a study to evaluate validity and user experience of using an AR virtual tooth identification test with mobile devices in a preclinical dental anatomy course [27]. AR environments, involving the perception of virtual supplements placed in the real world, require marker implementation, calibration, type of user interface, and effective viewing and manipulation [50]. Although the AR tooth identification test was positively correlated ($p<.01$) with the real tooth identification test, comprehensive final examination scores and the overall grade the student earned for the course, user experience data showed that there was some difficulty in viewing and manipulating the AR application on smartphones and students also reported technical difficulties such as prolonged loading time of test items or loss of battery life [27]. There was also a concern by the users that the variety of phone models may advantage students using the newer and better models in a test situation [27]. Usability testing continues to be a developing area of study, especially in technology [48,49,51].

VR AND ORTHOGNATHIC SURGICAL PREDICTION

Orthognathic procedures involving syndrome and non-syndrome jaw deformities are inherently challenging to plan, teach, and execute due to the complex bone and muscle structure found in the craniofacial region. Successful orthognathic treatments can have a positive effect on an individual's quality of life. Misdiagnosis and improper treatment planning, however, can lead to complications and deficiencies in surgical correction, which may alter basic functions [28]. Most graduate orthodontic programs in the United States and worldwide currently teach diagnosis and treatment planning of surgical orthodontic cases using two-dimensional (2D) radiographs and methods using manually traced lateral cephalometric radiographs where upper and lower jaw and chin can be cut out from the tracing and, then, moved to help plan the surgery [52]. Digitized tracings are used to perform these predictions for diagnosis and treatment planning. However, these methods are limited to movement and visualization in a single

sagittal plane, making it difficult to analyze a patient with a complex three-dimensional (3D), upper and lower jaw asymmetry using 2D methods [28].

With the introduction of 3D data and advances in 3D imaging, orthognathic treatment planning is trending more toward using advanced visualization techniques and 3D technology to plan treatment for complicated cases in hopes of accurately predicting and achieving better treatment outcomes [53,54]. Advances in 3D Virtual Surgical Planning (VSP) software were developed to improve treatment planning prediction and surgical outcomes [53-56]. With the help of software engineers who perform the virtual simulations, VSP leverages patient data through cone beam computed tomography (CBCT) and dental casts to fabricate a 3D-printed surgical splint [57]. However, due to the limited access to the software from private companies and limited view using a 2D computer monitor, VSP is challenging to utilize as patients present for diagnosis and treatment options at the pre-surgical time point. From the traditional 2D prediction tracing technique to VSP, both methods presented limitations in orthognathic surgery diagnosis and treatment planning [52-54]. This led to the development of Virtual Reality Patient (VR Patient) (Ann Arbor, MI), which uses an entirely artificial, computer-generated environment for orthognathic surgical simulation where students can interact with the VR Patient and set the parameters for what occurs in the environment.

With the collaboration of the University of Michigan, Duderstadt Center, the VR Patient (Ann Arbor, MI) was developed using Jugular software. The VR Patient was developed to simulate a patient module from CBCT data in a VR environment where the upper and lower jaws and chin can be manipulated in three planes of space, helping students understand and visualize diagnosis and treatment planning of surgical procedures for orthognathic cases (Fig. 3) [28]. VR Patient is meant to be used as a teaching tool for students to experiment with multiple procedures and movements. The VR Patient allows model manipulation with six degrees of freedom, making it possible to perform multiple and unlimited trials to mimic several jaw surgery procedures in a virtual environment [28].

Comparing VR Patient and the 2D prediction tracing methods, we conducted a comparative preliminary study to evaluate the feasibility of the testing methods and to compare student understanding in diagnosis and treatment planning complex orthognathic cases. The study participants were third-year dental students who were inexperienced and had minimal knowledge in orthognathic surgery. The study demonstrated that dental students were able to improve their understanding of diagnosis and treatment planning of orthognathic cases using both 2D prediction tracing and the VR Patient method immediately after the educational intervention ($p<0.05$). Although VR Patient demonstrated increased feasibility to learning diagnosis and treatment planning of orthognathic cases, the study did not show a significant relationship between fidelity of the VR Patient model and improved outcomes in education when compared with the 2D method. Study limitations, such as small sample size, data variability, and decreased usability as well as accessibility of technology due to the VR Patient software version used were discussed. In the attempt to minimize these study limitations, the study provided suggestions for future full-scale studies, which are currently underway to investigate the effects of increasing fidelity (2D to 3D to VR) of the educational tools for evaluating complex orthognathic cases [28].

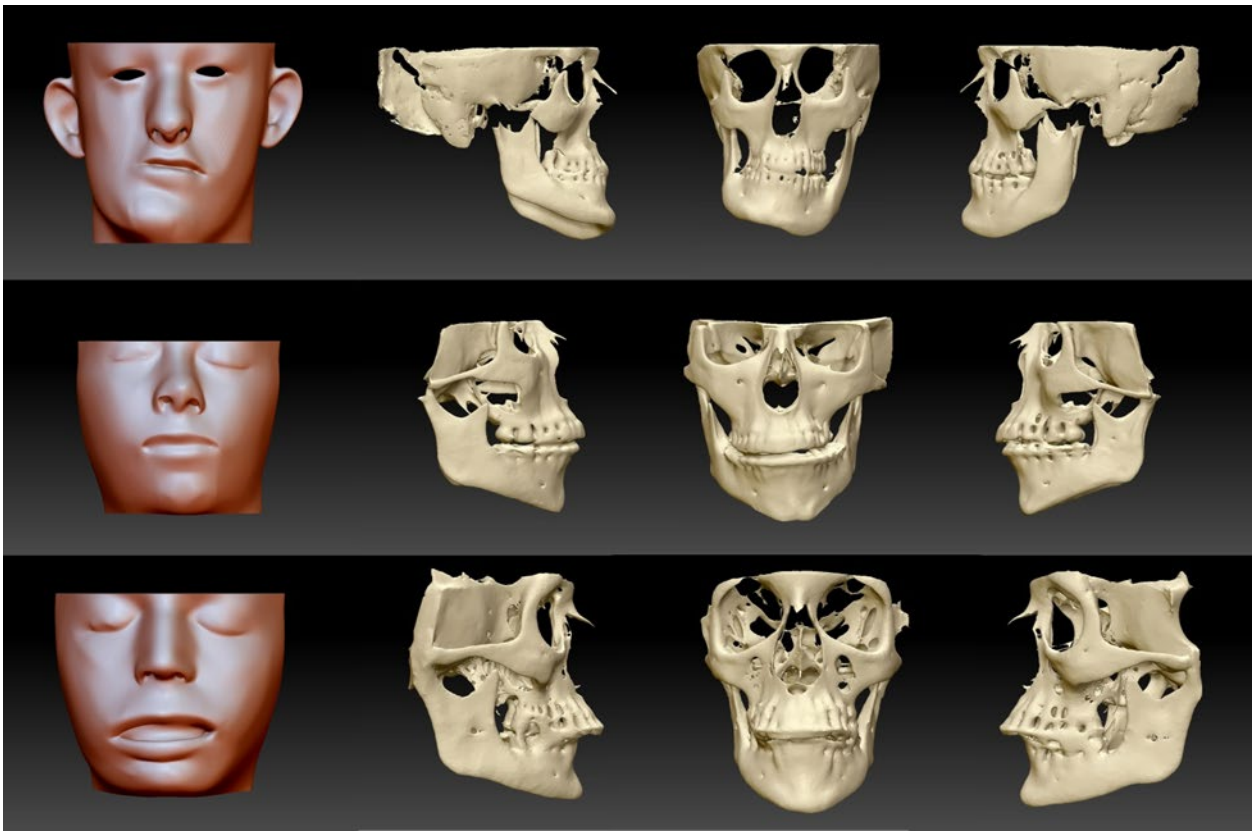

Figure 3. Examples of Virtual Reality Patient (VR Patient) modules demonstrating multiple cases with varying complexity in jaw deformity. VR patient can be viewed and manipulated with 6 degrees of freedom for maxillary LeFort I and mandibular bilateral sagittal split osteotomy, and genioplasty procedures using oculus Rift head mounted device and touch controllers.

FUTURE STUDIES AND VR IMPLEMENTATION

Based on the previously discussed study results, we were able to implement the use of VR HMDs and the Virtual Dental Library for the University of Michigan, Dental School Class of 2023 for preclinical laboratory courses during the first year (Fig. 4). Additionally, the VR Patient for orthognathic treatment has been incorporated into the orthognathic surgery course for the graduate orthodontic residency program. Future studies have been designed and are currently investigating the fidelity of educational tools and models in terms of virtual reality. With VR hardware and software improvements, ongoing and future research directions include validity, usability, and reliability testing of various VR educational tools; evaluating student and faculty assessment; and investigating effects of increasing fidelity (2D to 3D to VR) of the educational tools.

Figure 4. First year dental students using Oculus Go head mounted devices and the Virtual Dental Library in dental anatomy course.

CONCLUSION

Dental education is changing continuously with the introduction of new technological and advanced visualization innovations. Further research and development in augmented and virtual reality in association with hardware and software development for medical and dental applications also should continue along with technological innovations to improve student learning.

ACKNOWLEDGEMENTS

Funding for the studies described in this chapter was provided in part by the LeGro Fund (University of Michigan, Ann Arbor, MI) , Center for Research on Learning and Teaching (University of Michigan, Ann Arbor, MI) and Oculus Education Group (Oculus VR Inc, Menlo Park, CA).

REFERENCES

1. Segura C, Halabi D, Navarro N: Design and Validation of a Basic Dental Psychomotor Skills Test for Novice Dental Students. *J Dent Educ* 2018, 82(10):1098-1104.

2. Callan R, Haywood V, Cooper J, Furness A, Looney S: The validity of using e4d compare's "% comparison" to assess crown preparations in preclinical dental education. *J Dent Educ* 2015, 79(12):1445-1451.

3. Sutherland IE: The ultimate display. In: *Proceedings of the International Federation of Information Processing (IFIP) Congress 65: 24-29 May 1965; New York, NY*: Spartan Books; 1965: 506-509.

4. Boas YAGV: Overview of virtual reality technologies. In: *Interactive Multimedia Conference: 2013; Southampton, England*: University of Southampton; 2013.

5. Branda E: Review: Oculus rift. *J Soc Archit Hist* 2015, 74(4):526-528.

6. Orlosky J, Kiyokawa K, Takemura H: Virtual and augmented reality on the 5G highway. *J Inf Process* 2017, 25:133-141.

7. Bergig O, Hagbi N, El-Sana J, Kedem K, Billinghurst M: In-place augmented reality. *Virtual Real* 2011, 15:201-212.

8. Janin A, Myzel D, Caudell T: Calibration of head-mounted displays for augmented reality applications. In: *Proceedings of IEEE Virtual Reality Annual International Symposium: 1993*: IEEE; 1993: 246-255.

9. Zhou F, Duh HBL, Billinghurst M: Trends in augmented reality tracking, interaction and display: A review of ten years of ISMAR. In: *2008 7th IEEE/ACM International Symposium on Mixed and Augmented Reality: 15-18 September 2008; Cambridge, UK*: IEEE; 2008: 193-202.

10. Yuen SC, Yaoyuneyong G, Johnson E: Augmented reality: an overview and five directions for AR in education. *J Educ Technol Dev Exch* 2011, 4:119-140.

11. Shu Y, Huang YZ, Chang SH, Chen MY: Do virtual reality head-mounted displays make a difference? A comparison of presence and self-efficacy between head-mounted displays and desktop computer-facilitated virtual environments. *Virtual Real* 2018, 23(4):437-446.

12. Dias DRC, Neto MP, Brega JRF, Gnecco BB, Trevelin LC, Guimarães MdP: Design and evaluation of an advanced virtual reality system for visualization of dentistry structures. In: *2012 18th International Conference on Virtual Systems and Multimedia (VSMM): 2-5 September 2012; Milan, Italy*: IEEE; 2012: 429-435.

13. Stanford W, Erkonen WE, Cassell MD, Moran BD, Easley G, Carris RL, Albanese MA: Evaluation of a computer-based program for teaching cardiac anatomy. *Invest Radiol* 1994, 29(2):248-252.

14. Gardner HE: Multiple Intelligences: New Horizons in Theory and Practice. New York, NY: Basic Books; 2003.

15. Maresky HS, Oikonomou A, Ali I, Ditkofsky N, Pakkal M, Ballyk B: Virtual reality and cardiac anatomy: Exploring immersive three-dimensional cardiac imaging, a pilot study in undergraduate medical anatomy education. *Clin Anat* 2019, 32(2):238-243.

16. Moro C, Štromberga Z, Raikos A, Stirling A: The effectiveness of virtual and augmented reality in health sciences and medical anatomy. *Anat Sci Educ* 2017, 10(6):549-559.

17. Snelling J, Sahai A, Ellis H: Attitudes of medical and dental students to dissection. *Clin Anat* 2003, 16(2):165-172.

18. Thomsen ASS, Bach-Holm D, Kjærbo H, Højgaard-Olsen K, Subhi Y, Saleh GM, Park YS, la Cour M, Konge L: Operating room performance improves after proficiency-based virtual reality cataract surgery training. *Ophthalmology* 2017, 124(4):524-531.

19. Gutiérrez FPJ, Pierce J, Vergara VM, Coulter R, Saland L, Caudell TP, Goldsmith TE, Alverson DC: The effect of degree of immersion upon learning performance in virtual reality simulations for medical education. *Stud Health Technol Inform* 2007, 125:155-160.

20. Huang TK, Yang CH, Hsieh YH, Wang JC, Hung CC: Augmented reality (AR) and virtual reality (VR) applied in dentistry. *Kaohsiung J Med Sci* 2018, 34(4):243-248.

21. Oetting TA: Surgical competency in residents. *Curr Opin Ophthalmol* 2009, 20(1):56-60.

22. Mahr MA, Hodge DO: Construct validity of anterior segment anti-tremor and forceps surgical simulator training modules: attending versus resident surgeon performance. *J Cataract Refract Surg* 2008, 34(6):980-985.

23. Sattar MU, Palaniappan S, Lokman A, Hassan A, Shah N, Riaz Z: Effects of virtual reality training on medical students' learning motivation and competency. *Pak J Med Sci* 2019, 35(3):852-857.

24. Chen L, Fujimoto H, Miwa K, Abe T, Sumi A, Ito Y: A dental training system using virtual reality. In: *2003 IEEE International Symposium on Computational Intelligence in Robotics and Automation: 16-20 July 2003; Kobe, Japan*: IEEE; 2003: 430-434.

25. Marras I, Nikolaidis N, Mikrogeorgis G, Lyroudia K, Pitas I: A virtual system for cavity preparation in endodontics. *J Dent Educ* 2008, 72(4):494-502.

26. Buchanan JA: Experience with virtual reality-based technology into teaching restorative dental procedures. *J Dent Educ* 2004, 68:1258-1265.

27. Kim-Berman H, Karl E, Sherbel J, Sytek L, Ramaswamy V: Validity and user experience in an augmented reality virtual tooth identification test. *J Dent Educ* 2019, 83(11):1345-1352.

28. Sakowitz S, Inglehart MR, Ramaswamy V, Edwards S, Shoukri B, Sachs S, Kim-Berman H: A comparison of 2-dimensional prediction tracing and a virtual reality patient method for diagnosis

and treatment planning of orthognathic cases in dental students: A randomized preliminary study. *Master's Thesis.* Ann Arbor, Michigan: University of Michigan; 2017.

29. Desai PR, Desai PN, Ajmera KD, Mehta K: A review paper on oculus rift-a virtual reality headset. *International journal of engineering trends and technology (IJETT)* 2014, 13(4):175-179.

30. A brief history of oculus [https://techcrunch.com/2014/03/26/a-brief-history-of-oculus/]

31. Oculus Rift CV1 teardown [https://www.ifixit.com/Teardown/Oculus+Rift+CV1+Teardown/60612]

32. LaValle SM, Yershova A, Katsev M, Antonov M: Head tracking for Oculus Rift. In: *2014 IEEE International Conference on Robotics and Automation (ICRA): 31 May-7 June 2014; Hong Kong*: IEEE; 2014: 187-194.

33. Oculus Go review: Finally, cheap and easy VR for everyone [https://www.engadget.com/2018/05/01/oculus-go-review/]

34. Oculus Go overview [http://support.insitevr.com/en/articles/1857409-oculus-go-overview]

35. Information systems for business and beyond [https://resources.saylor.org/wwwresources/archived/site/textbooks/Information Systems for Business and Beyond/Textbook.html - _Chapter_3:_Software]

36. de Azevedo RdA, da Rosa WL, da Silva AF, Correa MB, Torriani MA, Lund RG: Comparative effectiveness of dental anatomy carving pedagogy: a systematic review. *J Dent Educ* 2015, 79(8):914-921.

37. Schleyer TK, Thyvalikakath TP, Spallek H, Dziabiak MP, Johnson LA: From information technology to informatics: the information revolution in dental education. *J Dent Educ* 2012, 76(1):142-153.

38. Wright EF, Hendricson WD: Evaluation of a 3-D interactive tooth atlas by dental students in dental anatomy and endodontics courses. *J Dent Educ* 2010, 74(2):110-122.

39. Jhangiani RS, Chiang IA, Price PC: Research Methods in Psychology, 2nd edn. Victoria, BC: BCcampus; 2015.

40. Germans D, Spoelder H, Renambot L, Bal H, van Daatselaar S, van der Stelt P: Measuring in Virtual Reality: A Case Study in Dentistry. *IEEE Transactions on Instrumentation and Measurement* 2008, 57(6):1177-1184.

41. McPherson KR, Mennito AS, Vuthiganon J, Kritzas YG, McKinney RA, Wolf BJ, Renne WG: Utilizing self-assessment software to evaluate student wax-ups in dental morphology. *J Dent Educ* 2018, 79(6):697-704.

42. Commission on dental accreditation [https://www.ada.org/~/media/CODA/Files/pde.pdf?la=en]

43. Lindemann RA, Jedrychowski J: Self-assessed clinical competence: a comparison between students in an advanced dental education elective and in the general clinic. *J Dent Educ* 2002, 6(1):16-21.

44. Hamil L, Mennito A, Renné W, Vuthiganon J: Dental students' opinions of preparation assessment with E4D compare software versus traditional methods. *J Dent Educ* 2014, 78(10):1424-1431.

45. Gadbury-Amyot CC, McCracken MS, Woldt JL, Brennan RL: Validity and reliability of portfolio assessment of student competence in two dental school populations: A four-year study. *J Dent Educ* 2014, 78(5):657-667.

46. Morris M, Dillon A: The importance of usability in the establishment of organizational software standards for end user computing. *Int J Hum-Comput Stud* 1996, 45(2):243-258.

47. Beccari MN, Oliveira TL: A philosophical approach about user experience methodology. In: *First International Conference, DUXU 2011, Held as Part of HCI International: 9-14 July 2011; Orlando, FL*: Springer; 2011: 13-22.

48. Zhang D, Adipat B: Challenges, methodologies, and issues in the usability testing of mobile applications. *Int J Hum-Comput Interact* 2005, 18(3):293-308.

49. Masoodian M, Lane N: An empirical study of textual and graphical travel itinerary visualization using mobile phones. In: *Proceedings of the Fourth Australian User Interface Conference (AUIC) on User Interfaces February 2003; Adelaide, South Australia*: Australian Computer Society; 2003: 11-18.

50. Liarokapis F: An augmented reality interface for visualizing and interacting with virtual content. *Virtual Real* 2007, 11:23-43.

51. Buchanan G, Farrant S, Jones M, Thimbleby H, Marsden G, Pazzani MJ: Improving mobile internet usability. In: *Proceedings of the 10th International Conference on World Wide Web: 1-5 May 2001; Hong Kong*: ACM; 2001: 673-680.

52. Proffit WR, White RP, Reinhardt RW: Surgical Orthodontic Treatment. St. Louis, MO: Mosby-Year Book Inc.; 1991.

53. Neumann P, Siebert D, Schulz A, Faulkner G, Krauss M, Tolxdorff T: Using virtual reality techniques in maxillofacial surgery planning. *Virtual Real* 1999, 4(3):213-222.

54. Cevidanes LHC, Tucker S, Styner M, Kim H, Chapuis J, Reyes M, Proffit W, T T, Jaskolka M: Three-dimensional surgical simulation. *Am J Orthod Dentofac Orthop* 2010, 138(3):361-371.

55. Emmel Becker O, Scolari N, Santos Melo MF, Haas Junior OL, Avelar RL, De Menezes LM, De Oliveira RB: Three-dimensional planning in orthognathic surgery using cone-beam computed tomography and computer software. *J Comput Sci Syst Biol* 2013, 6(6):311-316.

56. Xia J, Samman N, Yeung RW, Shen SG, Wang D, Ip HH, Tideman H: Three-dimensional virtual reality surgical planning and simulation workbench for orthognathic surgery. *Int J Adult Orthodon Orthognath Surg* 2000, 15(4):265-282.

57. Gateno J, Xia J, Teichgraeber JF, Rosen A, Hultgren B, Vadnais T: The precision of computer-generated surgical splints. J Oral Maxillofac surg 2003, 61(7), 814-817.

MACHINE LEARNING IN ORTHODONTICS: APPLICATION REVIEW

Ching-Chang Ko, Chihiro Tanikawa, Tai-Hsien Wu, Matthew Pastewait, Christina Bonebreak Jackson, Jane Jungeun Kwon, Yan-Ting Lee, Chunfeng Lian, Li Wang, Dinggang Shen

ABSTRACT

From diagnosing patients using acquired data to developing treatment plans, the current field of orthodontics relies heavily on the experience of the clinician. While orthodontists go through rigorous training, quality control of treatment becomes challenging as the clinicians' performance depends on their amount of experience. To overcome such limitations and streamline the process to prevent errors, artificial intelligence (AI), specifically machine learning (ML), has started to be incorporated into the field. AI is a branch of computer science that has been fruitful in its application in many fields. ML, a subset of AI, is a data analysis method that has been widely utilized in medical and dental image processing. With the development of advanced technologies, it has become feasible to acquire data and feed it to machines for diagnosing and treatment planning using complex algorithms. Since image data includes an abundance of information, ML has become an important tool in image processing in orthodontics because of its efficiency and accuracy. In this paper, we briefly introduce the concept of ML and demonstrate several 2D and 3D ML image processing and natural language processing methods, including the random forest classifier and deep learning neural network, as well as their applications in orthodontics.

KEY WORDS: Machine Learning, Deep Learning, Image Processing, AI in Orthodontics

INTRODUCTION

Artificial Intelligence (AI) is a branch of computer science that has been fruitful in its utilization in many fields ranging from marketing and entertainment to medicine. The general understanding of AI is that machines can work and react like humans. It is a very broad field that covers applications from automatic light timers to a computer program that knows how to play chess. Among such applications, one domain of AI that has been widely discussed recently is machine learning (ML).

ML, a subset of AI, is a data analysis method that allows machines to learn how to accomplish a particular task without being explicitly programmed. Generally, ML can be divided into three major categories: supervised learning, unsupervised learning, and reinforcement learning [1].

Supervised learning is learning from labeled training data. A supervised learning algorithm analyzes the training data based on the label and proposes an inferred model, which can be used to predict the output of new data. Common supervised learning tasks include classification and regression. Cases

such as tumor differentiation, in which the aim is to determine whether a tumor is benign or malignant based on the features of the tumor (e.g., size, shape), are called classification problems. In the field of orthodontics, the decision to extract teeth based on intra-oral findings is another classification example [2]. Conversely, an example of a regression problem is the prediction of the yield in a chemical manufacturing process in which the inputs are the concentrations of reactants, temperature, and pressure, and the output is a continuous, non-discrete value that is produced based on fitting the inputs to an inferred model [1].

Unsupervised learning is finding hidden patterns and structures in unlabeled data. The primary goal of unsupervised learning is clustering, which involves discovering reoccurring patterns and grouping similar examples within the data based on the specific characteristics. This method also determines the distribution of data within the input space, known as density estimation, or projects the data from a high-dimensional space down to two or three dimensions for the purpose of visualization [1]. For instance, a hierarchical agglomerative clustering (HAC) method was used to classify morphological variants of temporomandibular joint osteoarthritis among 169 patients [3].

Reinforcement learning means learning by interacting with an environment and changing behavior to maximize reward (e.g., assign a positive score) [4]. Reinforcement learning involves a series of steps where each step is associated with some reward. The machine develops an algorithm that maximizes the reward. With the development of advanced machines, more involved learning has become feasible. As a result, the machine can utilize more than one learning method to design an algorithm. AlphaGo is a well-known recent example of ML that incorporates both supervised and reinforcement learning to play Go [5]. In medicine, the Probabilistic Roadmap (PRM) method combined with reinforcement learning (RL) has been applied to a surgery robot to perform minimally invasive laparoscopic surgery [6].

Deep learning (DL) is another term that has been popularly discussed in relation to ML. DL is a sub-domain of ML, in which the machine itself calculates specific features of a given input. The precursor of DL is the artificial neural network (ANN), which was developed in the 1900s. Due to its need for extreme computing power to calculate numerous artificial neurons/weights inside the networks, the network structure could only be simple, and the practical applications were limited. However, graphics processing unit (GPU) computing, a very powerful parallel computing technology, has undergone rapid developments since 2010, and it has become possible to fulfill the need of computing power for neural network algorithms. Since then, researchers have been able to design more complicated and “deeper” neural networks to solve more complicated practical problems, and the neural network has become known as “deep learning.”

Although DL is a powerful and accurate tool in many applications, the criteria for such precise output is “big data,” which is difficult to achieve in the field of medicine. Therefore, some conventional ML methods, such as random forest (RF) or support vector machine (SVM), still play an important role in practical problems. Specifically, according to the “No Free Lunch” theorem, there does not exist an ML algorithm that is best for all problems [7]. The selection of algorithm depends on numerous properties of data such as size and structure.

Despite ML and DL’s popularity, there are not many related studies in the field of orthodontics. Nevertheless, those that do exist demonstrate great potential for AI in this area. For example, the research by Lee et al. demonstrates the use of a neural network to automate landmark identification on lateral cephalograms [8]. In this book chapter, we review additional ML orthodontic articles, covering two-dimensional (2D) and three-dimensional (3D) image processing, from object detection to volumetric segmentation, as well as natural language processing. In the first case, AI is used to identify facial traits to aid in orthodontic diagnosis [9]. The second case involves the use of the random forest classifier for volumetric analysis of maxillae with and without impacted canines [10]. In the third case, the PointNet deep learning algorithm is used to automatically segment teeth on maxillary models. The fourth case

involves the use of natural language processing to analyze a patient's clinical findings and develop a prioritized problem list and related treatment plan [11].

CASE I: AN AI SYSTEM FOR THE ORTHODONTIC EXAMINATION OF FACIAL IMAGES

The face plays an important role as a means of nonverbal communication in the transmission of emotions and thoughts during our social lives. Thus, facial topography influences the social acceptability and self-image of individuals. With this in mind, orthodontic diagnosis and treatment planning has been changed from the "Angle" paradigm, which is based on hard tissue relationships, to the "soft-tissue" paradigm, which focuses on the facial outcome. Therefore, when making treatment plans in orthodontics, observing patients' faces in the clinical setting is important. Recently, AI has emerged in the examination of faces using deep learning algorithms. For example, the Face2Gene software can detect genetic problems, which can act as a starting point in cases where a doctor does not know what to make of a patient's symptoms [12]. This shows the efficacy of facial photos in detecting genetic problems. More recently, systems that automatically provide clinical descriptions of oral or facial images for orthodontic diagnostic purposes have been reported [9,13].

In general, there are two traditional models for the deep learning of images. These are called convolutional neural network (CNN) and recurrent neural network (RNN). The CNN is a traditional neural network model that is generally composed of convolutional layers (where filters extract the target features), pooling layers (where the spatial sizes of features and the amount of model parameters are reduced), and fully-connected layers (a linear combination of the features of the previous layer, which makes the next layer). While CNN is a feed forward neural network that is generally used for image recognition and classification, RNN works on the principle of saving the output of a layer and feeding this back to the input to predict the output of the layer, which is particularly useful when a sequence of data is being processed to make a classification decision, such as with time series data. Orthodontic facial diagnosis is also time series examination as orthodontists diagnose a patient comprehensively by looking at the entire face while assessing multiple parts of the face from different angles, rather than by simply targeting one part of the face. For instance, an orthodontist must first look at the frontal face of a patient and examine the patient for asymmetry including inclination of the eyelids and/or distortion of the nose. The orthodontist must also confirm maxillary protrusion and/or prognathism from the side of the face, check the tooth alignment while smiling, and finally give the patient a facial diagnosis. This complex assessment process consequently brings variation in the diagnosis by different orthodontists. To mimic an orthodontist's comprehensive process using an AI system, Murata et al. employed RNN with the attention mechanism detailed below [9].

The developed AI system can provide an objective facial morphological assessment by identifying clinically used facial traits during the orthodontic diagnosis process (e.g., concave profile, upper lip retrusion, presence of scars). This automation considerably reduces the assessment workload for dentists and also prevents variations in diagnosis. We briefly introduce this algorithm below. The detailed implementation can be found in the work [9].

Sample Data

Lateral and frontal facial images of patients who visited the Orthodontic department (352 patients) were employed as the training and evaluation data. An experienced orthodontist examined all the facial images for each patient and identified as many clinically used facial traits during the orthodontic diagnosis process as possible (e.g., deviation of the lips, deviation of the mouth, asymmetry of the face,

concave profile, upper lip retrusion, presence of scars). A sample patient's image, a list of sample assessments (i.e., labels), and the multi-label data used in the work by Murata et al. are shown in Figure 1 [9].

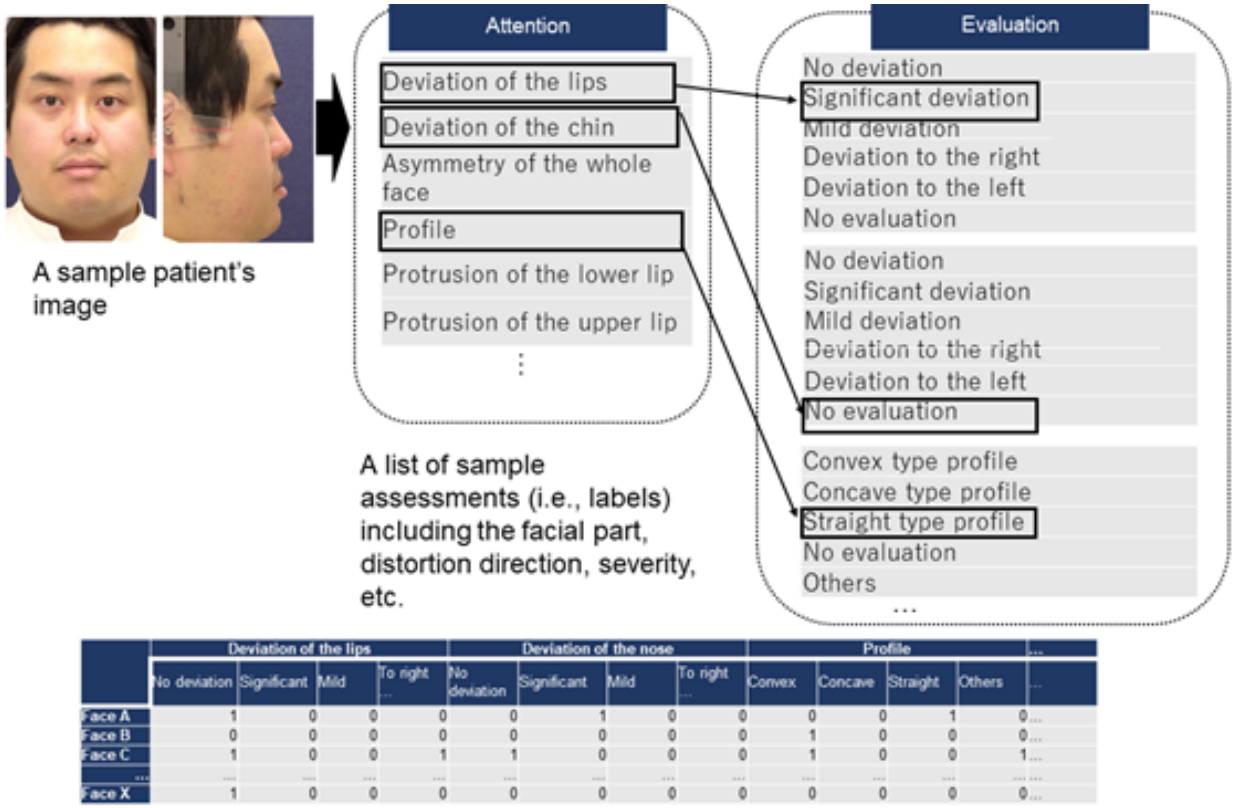

Figure 1. Sample patient's image and a list of sample assessments (i.e., labels) including the region of interest, evaluation, etc. In a previous study by Murata et al., they employed labels representing only the facial part (mouth, chin, and whole face), distorted direction (right and left), and its severity (severe, mild, no deviation).

Model Multi-label Image Classification

In general, medical images may contain multiple regions of interest to be evaluated. An orthodontist diagnoses a patient based on the assessment results of various facial regions from several different facial images. Thus, for automated diagnostic imaging, a typical single-label (binary or multi-class) image classification model was extended to solve the problem of multilabel image classification. Murata et al. proposed a hybrid model using CNN and RNN that sequentially focuses on multiple regions without pre-processing, such as cropping, and for each region, it produces a label (i.e., an assessment) consisting of words, each of which is predicted based on the previously predicted words (at earlier layers in RNN). The model is trained on patients' facial images to predict a set of assessments of facial attention parts such as the eye, nose, lips, chin, and profile. In practice, the assessments of different facial attention parts have mutual dependencies; therefore, they designed a model that learns this dependency. The attention mechanism in RNN tells the network which sub-area of the image impacts the prediction of each

particular label. This helps reduce the computational cost by selecting and learning the most relevant parts of the image for the predicted labels.

Results

Figure 2 shows some patients' facial images with the trained weight. The white regions in the images represent the weight, which corresponds to "attention" described above. Patient A has heavy distortion around his jaw while Patient B has only mild asymmetry. The model was able to predict both of the samples correctly. Patient C has only mild distortions around his mouth and jaw, but the model predicted the wrong labels. Table 1 shows the classification accuracy (%) for each facial part, averaged in a 10-fold cross validation. Although the accuracy itself is still low, the proposed model has mechanisms to mimic an orthodontist's comprehensive process to learn visual attention. In addition, label dependency contributes to an increase in accuracy.

Table 1. The average classification accuracy (%) of the results of a 10-fold cross validation [9]. The numbers in parentheses indicate the standard deviation.

	Traditional model (Multiple CNNs)	**Proposed model [9] (a deep CNN/RNN model with an attention mechanism)**
Lips	**64.0 (±7.5)**	**65.7 (±7.4)**
Chin	**57.9 (±16.5)**	**61.3 (±12.7)**
Whole face	**67.1 (±9.7)**	**67.4 (±9.1)**
Average	**63.0 (±9.6)**	**64.8 (±7.7)**
Worst, Best	**40.0, 74.3**	**49.5, 74.3**

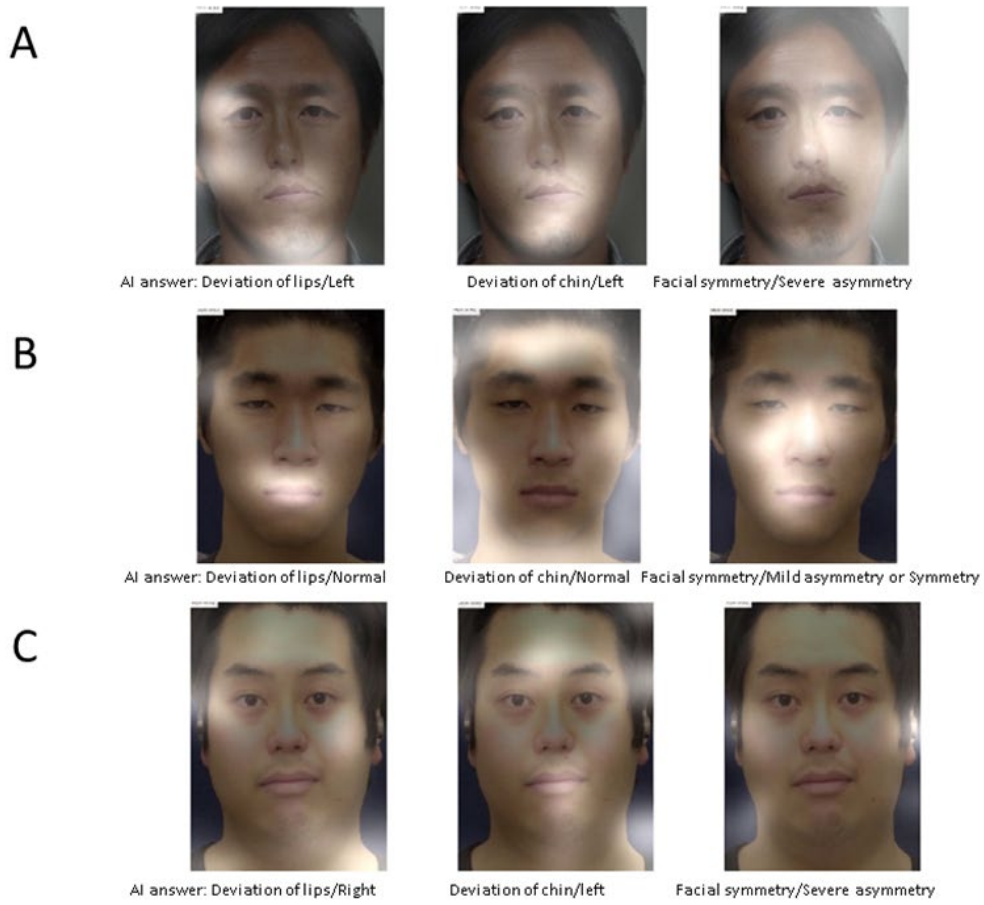

Figure 2. Resultant figures of the AI system. A. Images with visual attention of Patient A who has severe asymmetry around his mouth and chin. The model correctly predicts the labels; B. Images with visual attention of Patient B who does not have any severe problems. The model correctly predicts the labels; C. Images with visual attention of Patient C who has mild distortions around his mouth and chin. The model predicts incorrect labels.

CASE II: AUTOMATED VOLUMETRIC SEGMENTATION OF DENTAL CBCT IMAGE USING PRIOR-GUIDED SEQUENTIAL RANDOM FORESTS

Segmentation of cone-beam computed topographic (CBCT) images has been widely used in orthodontics, which is a crucial step for generating three-dimensional (3D) models for the advanced diagnosis and treatment planning of patients. Since manual segmentation is tedious, several automatic volumetric segmentation methods of CT/CBCT have been presented over the last decade, based on different ML algorithms, like random forest (RF), support vector machine (SVM), and CNN [14,15,16].

In this section, we review the study by Chen et al. in which maxillary constriction in patients with unilaterally impacted canines was assessed using a random forest algorithm (a classical machine learning based on a collection of decision trees) [10]. Their results demonstrated that the maxilla of patients with unilaterally impacted canines had significantly smaller volumes than those without impacted teeth. In

their work, 60 CBCT images were successfully auto-segmented. This many samples would be difficult to segment manually, suggesting an advantage of machine learning in orthodontics, particularly when the number of samples is relatively large.

This machine learning method was first presented by Wang et al. for segmentation of infant brain magnetic resonance (MR) images, and then applied to segmentation of patients with craniomaxillofacial (CMF) deformities [14,17]. Using this method, the volumetric segmentation is formulated as a classification problem, and the random forest serves as the classifier algorithm. We briefly introduce this random forest-based method below. The detailed implementation is referenced in the work by Wang.[14] Since it is a supervised learning problem, there are two stages – training and testing.

Stage 1. Training

The training stage can be divided into the four steps listed below.

Step 1. Estimation of initial probability maps with majority voting

All the expert-segmented CBCT scans are used as training samples and further aligned onto every subject image by affine registration, a function that allows for translation, rotation, and scaling as well as shearing. Then, a majority voting method is employed to count the votes for each label at every voxel for estimating the initial probability maps of all labels. The initial probability maps provide rough localizations of every label, serving as spatial priors that are important for guiding the segmentation.

Step 2. Extraction of CBCT appearance and context features

A Haar-like feature, a digital image feature used in object recognition, is used to define the difference between pixels/voxels inside the area/volume in this method [18]. Superficially, for each voxel x in the original CBCT image or probability maps, its Haar-like features f are computed by

$$f(x, I) = \frac{1}{|R_1|}\sum_{u \in R_1} I(u) - b\frac{1}{|R_2|}\sum_{u \in R_2} I(v),$$

$$R_1 \in R, R_2 \in R, b \in \{0, 1\},$$

where I is the intensity of an original CBCT image or a probability map; R is the patch centered at voxel x; R_1 and R_2 are randomly displaced cubical regions in the patch R, as shown in Figure 3; and the parameter b is either 0 or 1, indicating whether one or two cubical regions are used. The features extracted from the original CBCT images and probability maps are called appearance features and context features, respectively. They are used to coordinate the segmentations in different parts of the CBCT image. These context features have been shown effective in both computer vision and medical image analysis fields [19]. It is important to note that the extraction of context features is recursively conducted on the iteratively updated probability maps, whereas the extraction of appearance features is performed only on the original CBCT images.

Step 3. Training of random-forest-based classifiers

To refine the segmentations (probability maps), a random forest classifier is trained to learn the complex relationship between local appearance/context features and the corresponding manual segmentation labels on all voxels of the training atlases.

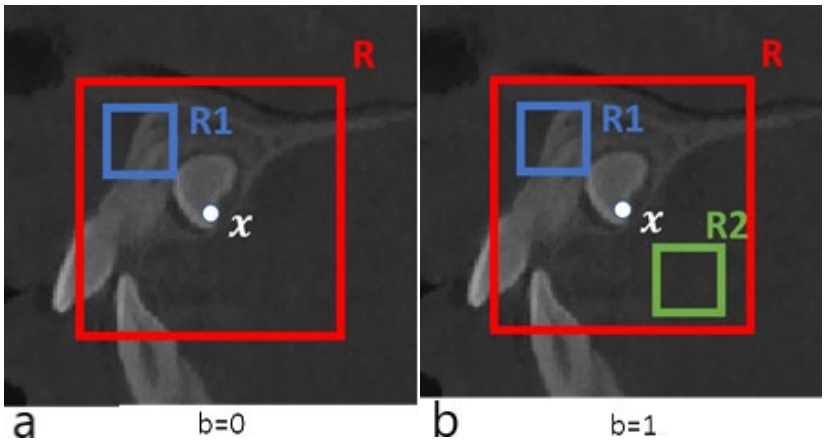

Figure 3. An illustration of how to compute 3D Haar-like features. The red box indicates a patch R centered at x. (a) If b=0, a Haar-like feature is computed as the local mean intensity of a randomly displaced cubical region R_1 (blue box) within the patch R. (b) If b=1, a Haar-like feature is computed as the mean intensity difference over any two randomly displaced, asymmetric cubical regions R_1 and R_2 (blue and green boxes) within the patch R.

Step 4. Repeating Steps 2 and 3 until convergence

In this final step, the classifiers are trained in a sequential manner. Specifically, the segmentation probability maps are updated based on the classifier trained in Step 3. Then, according to Step 2, the context features are extracted from the updated segmentation probability maps and further used with the original CBCT appearance features to train the next classifier. Eventually, a sequence of classifiers is obtained for CBCT segmentation. The flowchart of the entire training stage is shown in Figure 4.

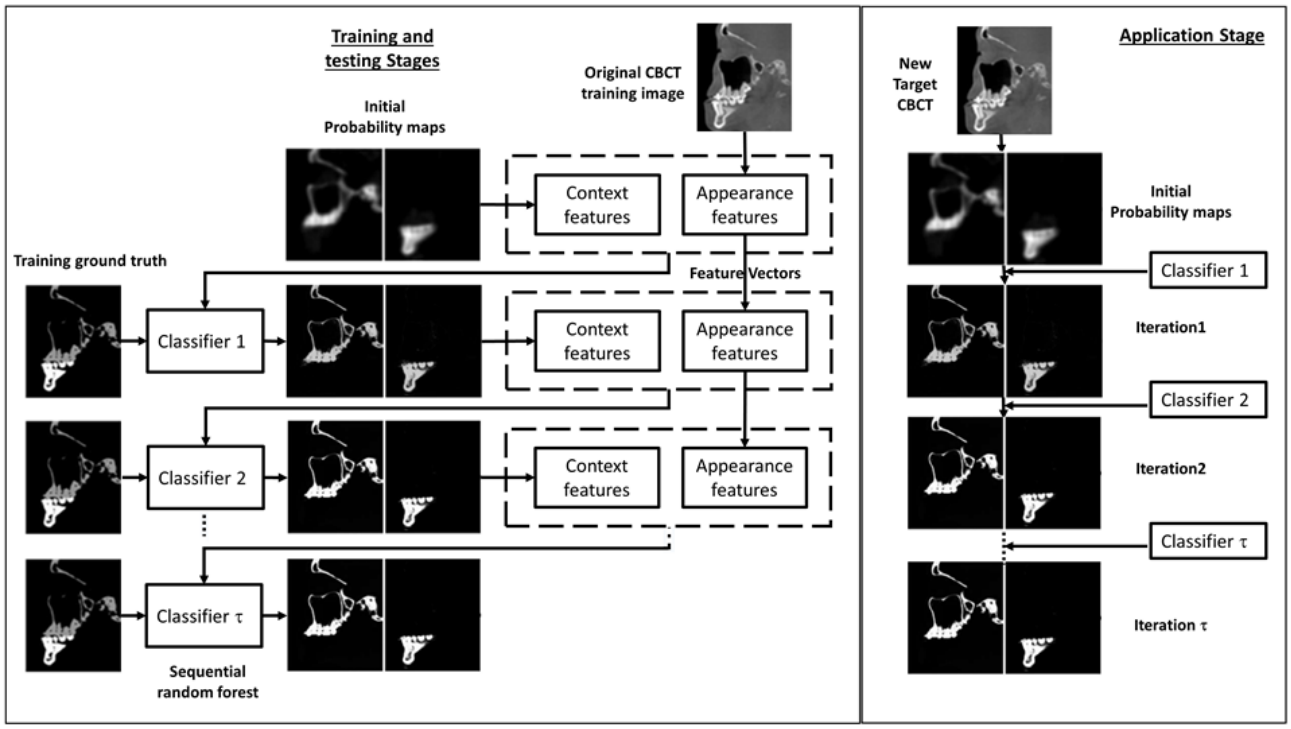

Figure 4. Random Forest classifier flowchart.

Stage 2. Testing

In the testing stage, given a new CBCT image, the initial segmentation probability maps of every label are first estimated using majority voting. Then, based on the estimated probability maps, the context features are extracted and, together with CBCT appearance features, serve as the input to the sequential classifiers for iteratively updating the segmentation probability maps. The refined probability maps, the output of the sequential classifiers, are the final segmentation results.

Results

The accuracy of segmentation classifiers can be evaluated using the Dice Similarity Coefficient (DSC). In the study by Chen et al., the average DSC of the maxillae was 0.800±0.029, ranging from 0.742 to 0.830, based on 30 training and 6 test samples. Then, they utilized this random forest-based method to segment the maxillae of 60 CBCT images, with 30 scans of unilaterally impacted canines, i.e., the Study Group (SG) and 30 scans without impacted teeth, i.e., the Control Group (CG). Their clinical outcomes are listed in Table 2.

Table 2. The clinical outcomes of Study Group and Control Group [10].

	Study Group	**Control Group**
Bone volume **Impacted side for study group** **Left side for control group** **Mean ± SD[1] (10^4 mm³)**	**2.36±0.35**	**2.57±0.30**
Bone volume **Non-impacted side for study group** **Right side for control group** **Mean ± SD[1] (10^4 mm³)**	**2.37±0.34**	**2.65±0.38**
Maxillary width (mm)	**64.3±5.3**	**66.6±3.6**
Maxillary height (mm)	**65.1±3.6**	**67.0±3.5**
Maxillary depth (mm)	**47.7±3.6**	**49.6±3.3**

[1] SD=Standard Deviation

Generally, they found that the difference between SG ($4.73\pm0.67\times10^4$ mm³) and CG ($5.22\pm0.65\times10^4$ mm³) was significant in volume, even after adjusting for gender and age, showing that

the SG tended to have a smaller maxillary volume (roughly 5000 mm^3 less) than the CG. In addition, in the SG, the average volumes of the non-impacted ($(2.36\pm0.35)\times10^4\,mm^3$) and impacted sides ($(2.37\pm0.34)\times10^4\,mm^3$) were not significantly different. Their data might explain O'Neill's finding, in which the use of rapid maxillary expansion (RME) in the early mixed dentition effectively increased the rate of eruption of palatally displaced maxillary canines compared to an untreated control group [20].

In conclusion, the work done by Chen et al. is an excellent example to illustrate the advantages of machine learning in orthodontics. The amount of data is almost impossible to collect manually, particularly the tedious work of volumetric segmentation.

CASE III: AUTOMATIC SEGMENTATION OF DENTAL SURFACE IMAGE USING POINTNET

Computer-aided design/computer-aided manufacturing (CAD/CAM) technology has been widely used in orthodontics. For example, 3D dental surface images could be easily obtained through a 3D intra-oral scanner in clinical orthodontic practices nowadays. As a fundamental part of CAD/CAM-based treatment plans, labeling teeth accurately on 3D dental surfaces is a crucial step for advanced diagnosis. However, automation of this labeling/segmentation task is challenging on the raw dental surface image acquired from the intra-oral scanners for multiple reasons, including large non-tooth and irregular parts (e.g., gingival tissues) in the image.

Since volumetric CNNs have demonstrated their outstanding image processing abilities, many researchers transform the surface images to regular 3D voxel grids and feed them to a CNN-based deep learning network. However, this method is not efficient in terms of computing as well as storage and also results in blurring natural images. For this reason, Qi et al. reported a deep learning architecture, called PointNet, on a point/mesh set for 3D segmentation [21].

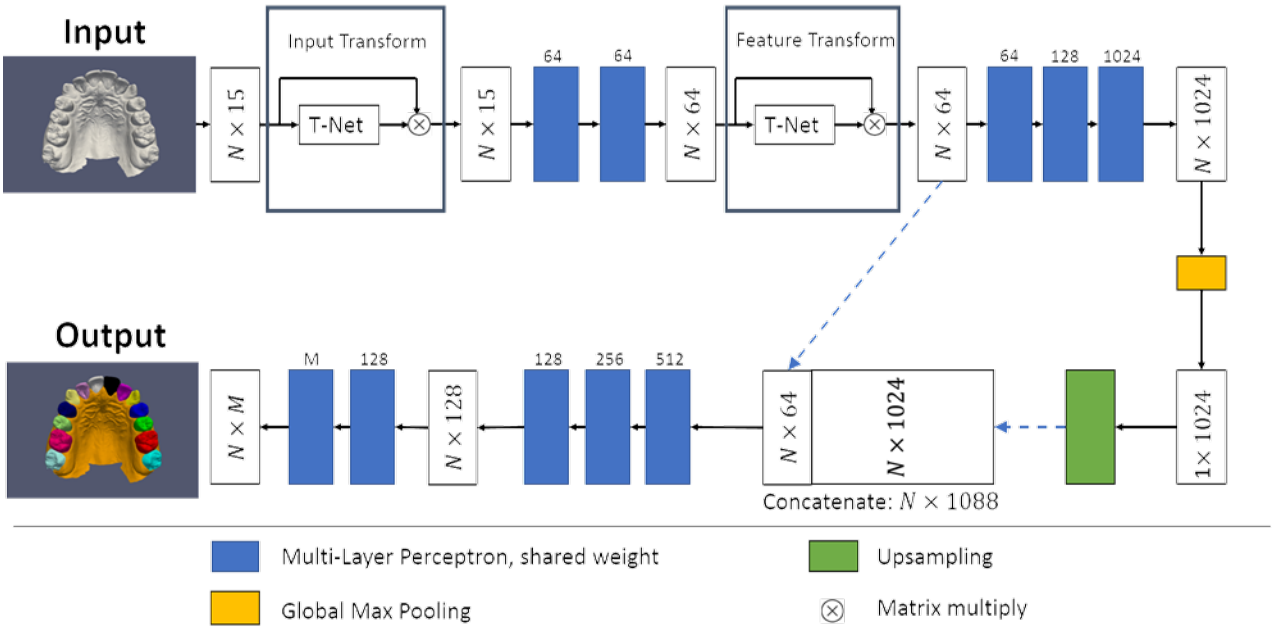

Figure 5. PointNet architecture.

In this section, we demonstrate a tooth-segmentation task using PointNet and discuss its performance. The PointNet architecture shown in Figure 5 is slightly different than the original one, which only takes 3D position (i.e., x, y, and z) of vertices as input features [21]. Instead, we consider N triangles in the surface mesh as input, and a total of 15 features of each triangle are used. The 15 features are 3D positions of three vertices (9 features) and the normal vector (3 features) of each triangle as well as the relative position (3 features) of each triangle with respect to the whole surface. The raw dataset here consists of 20 maxillary dental surfaces from a 3D intra-oral scanner (iTero Element). All surfaces were down-sampled to 10,000 triangles while preserving the original topologies and augmented by random rotation, translation, and rescaling of each surface image in reasonable ranges. The number of categories (M) is 15, including 14 teeth between the left and right second molars as well as the remaining part in the surface image (i.e., background).

The implementation was carried out using Keras [22], a high-level neural network application programming interface (API). Three-fold cross-validation was performed for this demonstration. For each training/validation sample, 6,000 triangles were randomly selected from each surface (10,000 triangles) as the network input data with a 50:50 ratio of triangles from each tooth and gingiva. Specifically, the input array ($N \times 15$) and output array ($N \times M$) are both $6{,}000 \times 15$. The Adam optimizer was used with a mini-batch size of 10; the number of epochs was 100 for the training; and the loss function was generalized Dice loss [23]. The segmentation results were evaluated by three metrics: DSC, sensitivity (SEN), and positive prediction value (PPV).

The segmentation results of DSC, SEN, and PPV (mean$\pm$standard deviation) for all teeth are 0.781$\pm$0.134, 0.828$\pm$0.167, and 0.766$\pm$0.163, respectively, as shown in Table 3. In addition, a screenshot of the results is shown in Figure 6. Although the accuracy still needs to be improved for practical clinical purposes, the results of this demonstration reveal the promise of automatically labeling teeth in the surface image, creating a new path for digesting surface mesh directly instead of converting to 3D voxel grids. A better result could be expected using a more sophisticated deep learning network and a larger dataset in the future.

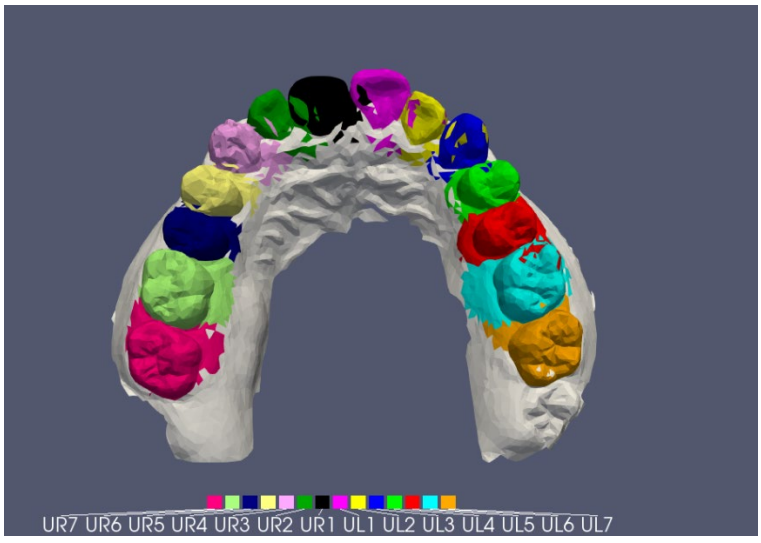

Figure 6. The screenshot of the labeled teeth using PointNet.

Table 3. Results of the labelled teeth using PointNet.

Metric	Mean±SD	Min	Max
DSC	**0.781±0.134**	**0.695**	**0.882**
SEN	**0.828±0.167**	**0.702**	**0.960**
PPV	**0.766±0.163**	**0.575**	**0.855**

To conclude, we have demonstrated a promising path to automatically segment each tooth on a surface image. This task is a critical step for advanced diagnosis and customized treatment planning. It also serves as the first step in a series of orthodontic AI systems to obtain further patient data and information.

CASE IV: USING NATURAL LANGUAGE PROCESSING TO DEVELOP AN AUTOMATED ORTHODONTIC DIAGNOSTIC SYSTEM

An orthodontic diagnosis and treatment plan involves predicting the entire course of action that a dentist should take to obtain the optimal treatment results at the lowest possible risk [24]. Making such an assessment requires years of knowledge and experience. As such, there are cases in which inexperienced dentists make judgment errors or otherwise misunderstand a case's parameters. An AI system that can implement the years of experience of a specialist would be of great significance in providing patients with quick access to experienced treatment planning. In addition, the automatic summarization of orthodontic diagnoses or presentation of necessary examinations in an orthodontic clinic would reduce the heavy workload of dentists, as well as help less experienced dentists in avoiding oversights and judgment errors.

Treatment operates on the logic of "doing the opposite of the problem," and the process of modern orthodontic diagnosis and treatment consists mainly of the following three steps: (1) Collection and itemization of patient information regarding the problem(s); (2) Contemplating solutions for each problem; (3) Determining the course of action and its implementation. A certain regularity is apparent in the logical structure involved in medical diagnosis and treatment planning (as described above). Hence, attempts have been made to automate orthodontic diagnosis and treatment planning, such as the use of expert systems. An orthodontic diagnosis support system using fuzzy logic, a support system for the selection of orthodontic appliances, and a mathematical model that simulates whether or not to extract teeth in optimizing orthodontic treatment outcome, have previously been developed [25, 26, 27]. However, total orthodontic diagnosis and treatment planning support systems for use in clinics have yet to be established.

To put the diagnostic process of a specialist in mathematical terms, if patient information regarding the problem is thought of as a set of feature values, the above step (1) is analogous to representing medical conditions based on the individual weight of each feature value and detecting the degree of similarity between each medical condition. Step (2) can be considered equivalent to learning more about the approach to handle each of the medical conditions, at which point a natural language processing (NLP) AI system could be expected to find a solution (Kajihara et al.) [11]. The aim of the study by Kajihara et al. was to develop an AI system that uses NLP on various clinical text evaluations and their accompanying treatment protocols [11]. Here, we will briefly review the automated process of diagnosis and treatment planning.

Problem Settings

In their study, Kajihara et al. worked on the task of automatically designing a treatment plan from the findings included in the medical certificate written by the dentist. They developed an artificial intelligence system that inputs a document that describes the findings of the patient and outputs a list of problems that the patient has in the order of treatment priority. As findings are free-form descriptions in natural language, the method of feature extraction for machine learning is not obvious. Therefore, the researchers employed a natural language processing approach for feature extraction from text. They developed the following two subtasks to efficiently address the task of generating a treatment plan from clinical findings:

Step 1: List the problems

Step 2: Prioritize treatment

First, Step 1 summarized the findings and listed the orthodontic problems of each patient. Then, Step 2 ranked each problem listed in Step 1 in terms of treatment priority. Solving the above two subtasks, the system automatically created a treatment plan from the findings contained in the medical certificate.

Dataset

Kajihara et al. employed 990 certificates written by dentists for the present experiment. According to the dataset, each patient had an average of 15.4 orthodontic problems. These 990 documents were randomly divided into 810 for training, 90 for validation, and 90 for evaluation.

The researchers developed an NLP system that solved the two subtasks mentioned in the previous section using the dataset. Step 1 was regarded as a text generation task that generated a summary of findings. Compared to the millions to tens of millions of datasets commonly used in text generation tasks, such as machine translation and automatic summarization in natural language processing, their dataset of 990 documents was significantly smaller. Therefore, Kajihara et al. added an annotation (shown in Figure 7(c)) and tackled Step 1 as a multi-label classification problem. In this additional annotation, one dentist classified orthodontic problems into 423 classes. Each patient problem corresponded to one class.

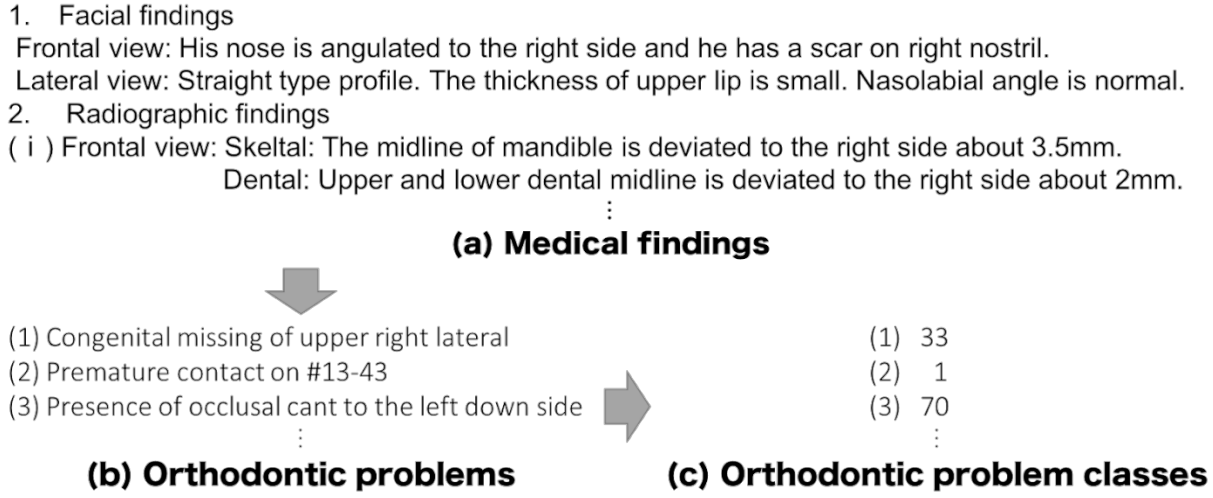

Figure 7. Annotation of orthodontic problem classes to the medical certificate.

Step 1: Multi-label Classification Model for Orthodontic Problems

Proposed Methods

The researchers developed classification models of orthodontic problems on the datasets shown in Figure 7(a) and (c). These models recorded the text of the findings as inputs and generated a list of class labels as outputs (shown in Figure 7(c)). By working as a classification problem rather than a generation problem, it was expected that the small datasets would be less susceptible to linguistic variation.
Kajihara et al. converted each text of findings into vector representation using a natural language processing approach and performed supervised learning of multi-label classification with them as features. The following methods were used to vectorize each document.

- BoW (Bag-of-Words): The BoW representations have dimensions corresponding to the number of vocabulary words in the training dataset, and each dimension has a value of 1 if the corresponding word appears in the input text or 0 if it does not. These are high-dimensional sparse vectors.
- USE (Universal Sentence Encoder): The researchers construct feature vectors from the text using the cross-lingual version of the universal sentence encoder [28]. These are 512-dimensional dense vectors.

Experimental Settings

Each sentence was divided into words using MeCab for the BoW model [29], where MeCab is an open-source text segmentation library for use with text written in the Japanese language. In this experiment, the vocabulary size was 2,075 because only words appearing five or more times in the training dataset were used. In addition, semantically equivalent classes were grouped, and 151 class labels were used.

A multi-layer perceptron (MLP) is a kind of artificial neural network consisting of at least three layers of nodes: an input layer, a hidden layer, and an output layer. In their work, MLP was implemented on an open source deep learning framework (Chainer [30]) for a multi-label classifier [31]. In the output layer, a sigmoid function was used instead of the softmax function in the single-label classification. The research team used a three-layer perceptron for this experiment and examined the hidden layer size as a hyper-parameter from {64, 128, 256, 512, 1024, 2048, 4096} on the validation dataset.

Experimental Results

The performance of each model was automatically evaluated using the F-measure, which is the harmonic average of the precision and the recall. The experimental results showed that the simple BoW model achieved higher performance (0.59) than the USE model (0.54). Unique structures, such as bullets and incomplete sentences, may have had a negative impact on the sentence encoder. On the other hand, BoW models treated documents as a set of words, so they were not affected by the structure of the sentence.

Step 2: Treatment Prioritization Model

Proposed Methods

Kajihara et al. developed a prioritization model of treatment on the datasets shown in Figure 7(b) and (c). This model recorded as input a list of text representing the orthodontic problems or a list of classes

and generated as outputs a list of treatment priority for each problem shown in parentheses in the lower part of Figure 7.

The researchers converted each problem into vector representation using a natural language processing approach and performed learning-to-rank with them as features. The following three methods were used to vectorize each problem.

- BoW (Bag-of-Words): They constructed feature vectors from the text of the problem. These vector representations had dimensions corresponding to the number of vocabulary words in the training dataset, and each dimension had a value of 1 if the corresponding word appeared in the input text, or 0 if it did not.
- OoK (One-of-K): They constructed feature vectors from the labels that represented the problem. These vector representations had dimensions corresponding to numbers of labels appearing in the training dataset, and only one of the dimensions corresponding to the input class had a value of 1 and the other dimensions had a value of 0.
- USE (Universal Sentence Encoder): They constructed feature vectors from the text of the problem using the cross-lingual version of universal sentence encoder [28]. These were 512-dimensional dense vectors.

Experimental Settings

Each sentence was divided into words using MeCab for the BoW model [29]. In this experiment, as the training dataset had 146 vocabulary words and 320 classes, the feature vectors of each model were 146 dimensions for BoW, 320 dimensions for OoK, and 512 dimensions for USE.

For learning-to-rank, the researchers used SVM-rank with a linear kernel, a standard toolkit [32]. For a given set of features, they examined a hyper-parameter among $C \in \{1, 5, 10, 50, 100, 500, 1000, 5000\}$ on the validation dataset.

Spearman's rank correlation coefficient was used to automatically evaluate the performance of each model. When the correlation coefficient between the human ranking and the estimated ranking exceeded 0.4, the estimation result of the model was interpreted as having a positive correlation with human evaluation.

Experimental Results

The experimental results are shown in Figure 8. As each method has Spearman's rank correlation coefficient exceeding 0.4, it can be interpreted that these estimation results have a positive correlation with human evaluation.

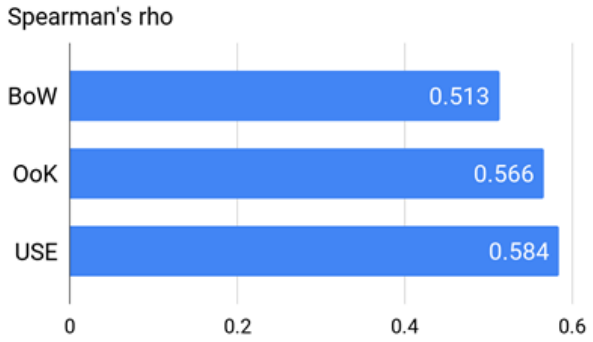

Figure 8. Automatic evaluation of treatment ranking models by Spearman's rho.

Compared to the BoW model, the OoK model is expected to be able to obtain feature vectors that reflect an annotator's expertise, so it is considered that high performance has been achieved. Furthermore, the USE model achieved the highest performance because the dense vectors obtained by deep learning can represent rich information.

Future works

The above algorithm can also be applied to the automated planning of treatment protocols (Figure 9). The system can train a series of transformation models using pairs of relevant treatment protocol summaries and consent form documents. First, relevant sentence pairs would be automatically extracted from the relevant documents using an NLP method of sentence alignment. Next, statistical machine translation or neural machine translation techniques would be used to automatically translate experts' language into simpler language that can be understood by patients easily.

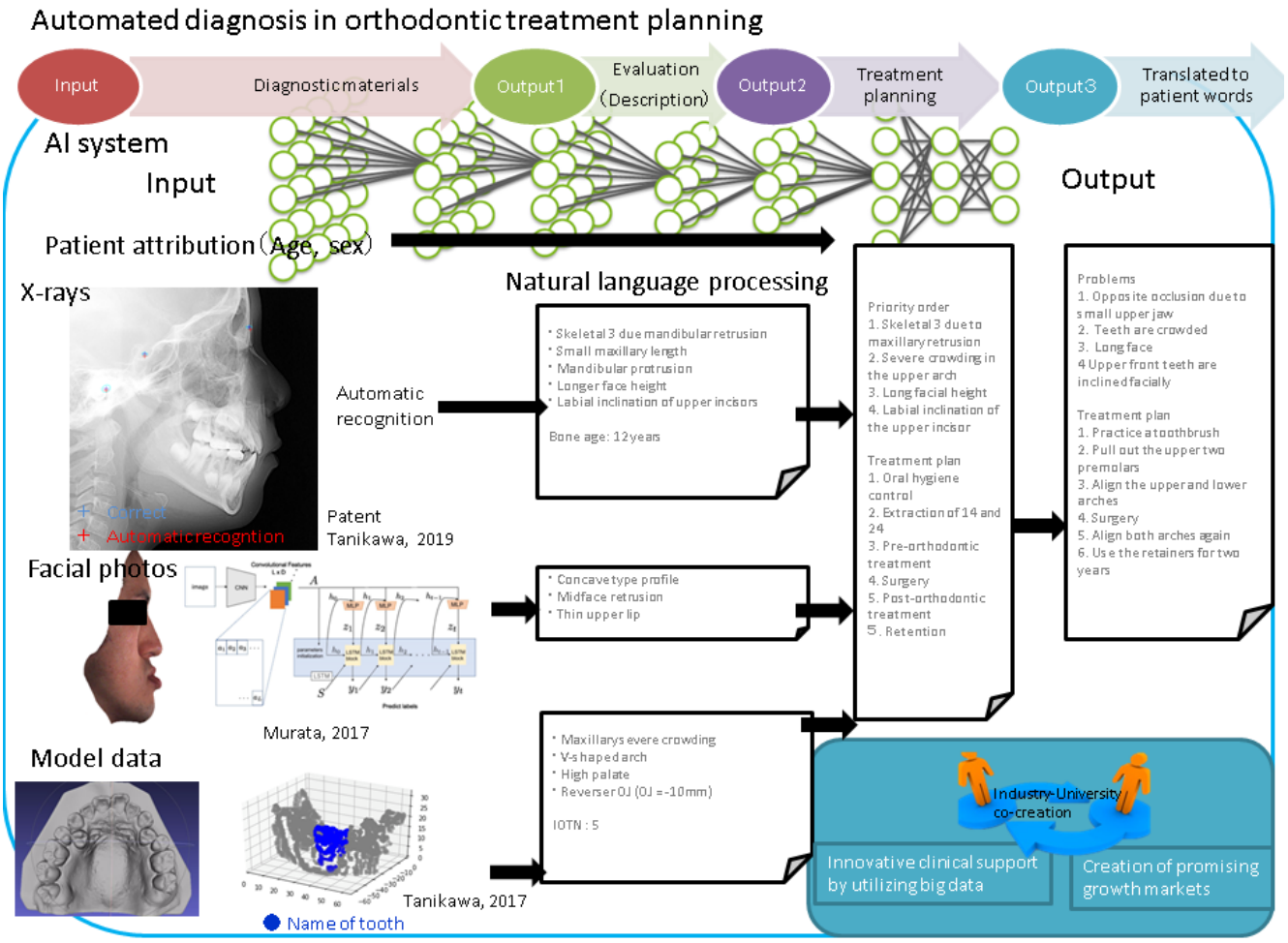

Figure 9. Overview of their fully automated orthodontic diagnosis system.

CONCLUSIONS

Artificial intelligence, including ML and DL, is rapidly expanding into multiple facets of society. Orthodontics may very well be one of the fastest branches of dentistry to adapt AI for three reasons. First, patient encounters during treatment generate many types of data. Cephalometric landmarks, digital photographs, intra-oral and extra-oral features are just a few types of data generated in the dental clinic. AI can perform analytics to decipher this information and aid in efficient diagnosis and treatment planning. Second, the standardization in the field of dentistry is low compared to other areas of healthcare. A range of valid treatment options exists for any given case. Using AI and large datasets (that include diagnostic results, treatments, and outcomes), one can now empirically measure the effectiveness of different treatment modalities given very specific clinical findings and conditions. Third, orthodontics is largely practiced by independent dentists in their own clinics. These dentists have the autonomy to adopt beneficial technologies without the bureaucracy often found in large healthcare organizations. In order to remain competitive in the modern dental market, orthodontists must be proactive in seeking innovation and adopting various technologies. Despite the promise of AI, the volume of orthodontic research in this field is relatively low. Further, the clinical accuracy of AI must be improved with an increased number and variety of cases. Before AI can take on a more important role in making diagnostic recommendations, the volume and quality of research data will need to increase.

ACKNOWLEDGEMENTS

This work is, in part, supported by NIH/NIDCR DE022816 and NSF#1938533.

REFERENCES

1. Bishop CM. *Pattern Recognition and Machine Learning*. New York, NY: Springer; 2006.

2. Jung S-K, Kim T-W. New approach for the diagnosis of extractions with neural network machine learning. *Am J Orthod Dentofac Ortho* 2016;149(1):127-133. doi:https://doi.org/10.1016/j.ajodo.2015.07.030

3. Gomes LR, Gomes M, Jung B, Paniaqua B, Ruellas AC, Goncalves JR, et al. Diagnostic index of 3D osteoarthritic changes in TMJ condylar morphology. in: *Medical Imaging 2015: Computer-Aided Diagnosis* 2015; 9414:941405. https://doi.org/10.1117/12.2082226.

4. Sutton RS, Barto AG. *Reinforcement Learning: An Introduction*. Cambridge, MA: MIT press; 2018.

5. Silver D, Huang A, Maddison CJ, Guez A, Sifre, L, van den Driessche G, et al. Mastering the game of Go with deep neural networks and tree search. *Nature* 2016;529:484. https://doi.org/10.1038/nature16961.

6. Baek D, Hwang M, Kim H, Kwon D. Path Planning for Automation of Surgery Robot based on Probabilistic Roadmap and Reinforcement Learning. In: *2018 15th International Conference on Ubiquitous Robots (UR)*. IEEE 2018:342-347. doi:10.1109/URAI.2018.8441801

7. Wolpert DH, Macready WG. No free lunch theorems for optimization. *IEEE Trans Evol Compu* 1997;1(1):67-82. doi:10.1109/4235.585893

8. Lee C, Tanikawa C, Lim JY, Yamashiro T. Deep Learning Network based Cephalometric Landmark Identification using Multi-scale Patches. Preprint at https://arxiv.org/abs/1906.02961 (2019).

9. Murata S, Lee C, Tanikawa C, Date S. Towards a fully automated diagnostic system for orthodontic treatment in dentistry. In: *2017 IEEE 13th International Conference on E-Science (e-Science)*. IEEE 2017:1-8. doi:10.1109/eScience.2017.12

10. Chen S, Wang L, Li G, Wu T-H, Diachina S, Tejera B, et al. Machine learning in orthodontics: Introducing a 3D auto-segmentation and auto-landmark finder of CBCT images to assess maxillary constriction in unilateral impacted canine patients. *Angle Orthod* 2019;in press.

11. Kajiwara T, Tanikawa C, Shimizu Y, Chu C, Yamashiro T, Nagahara H. Using Natural Language Processing to Develop an Automated Orthodontic Diagnostic System. Prprint at https://arxiv.org/abs/1905.13601 (2019).

12. FACE2GENE. https://www.face2gene.com/.

13. Murata S, Ishigaki K, Lee C, Tanikawa C, Date S, Yoshikawa T. Towards a Smart Dental Healthcare: An Automated Assessment of Orthodontic Treatment Need. *Healthinfo* 2017;(c):35-39.

14. Wang L, Gao Y, Shi F, Gang L, Chen K-C, Tang, Z, et al. Automated segmentation of dental CBCT image with prior-guided sequential random forests. *Med Phys* 2016;43(1):336-346. doi:10.1118/1.4938267

15. Pei Y, Ai X, Zha H, Xu T, Ma G. 3D exemplar-based random walks for tooth segmentation from cone-beam computed tomography images. *Med Phys* 2016;43(9):5040-5050. doi:10.1118/1.4960364

16. Qiu B, Guo J, Kraeima J, Borra RJH, Witjes MJH, van Ooijen PMA. 3D segmentation of mandible from multisectional CT scans by convolutional neural networks. Preprint at https://arxiv.org/abs/1809.06752 (2018).

17. Wang L, Gao Y, Shi F, Li G, Gilmore J, Lin W, et al. LINKS: Learning-based multi-source IntegratioN frameworK for Segmentation of infant brain images. *Neuroimage* 2015;108:160-172. doi:https://doi.org/10.1016/j.neuroimage.2014.12.042

18. Viola P, Jones MJ. Robust Real-Time Face Detection. *Int J Comput Vis* 2004;57(2):137-154. doi:10.1023/B:VISI.0000013087.49260.fb

19. Sutton C, McCallum A, Rohanimanesh K. Dynamic conditional random fields: Factorized probabilistic models for labeling and segmenting sequence data. *J Mach Learn Res* 2007;8(Mar):693-723.

20. O'Neill J. Maxillary expansion as an interceptive treatment for impacted canines. *Evid Based Dent* 2010;11:86. https://doi.org/10.1038/sj.ebd.6400742.

21. Qi CR, Su H, Mo K, Guibas LJ. Pointnet: Deep learning on point sets for 3d classification and segmentation. In: *Proceedings of the IEEE Conference on Computer Vision and Pattern Recognition*. 2017:652-660.

22. Sudre CH, Li W, Vercauteren T, Ourselin S, Cardoso MJ. Generalised dice overlap as a deep learning loss function for highly unbalanced segmentations. In: *Deep Learning in Medical Image Analysis and Multimodal Learning for Clinical Decision Support*. 2017:240-248.

23. Keras. https://keras.io/.

24. Takada K. *Elements of Orthodontics*. I-Cube Co. Ltd; 2017.

25. Sims-Williams JH, Brown ID, Matthewman A, Stephens CD. A computer-controlled expert system for orthodontic advice. *Br Dent J* 1987;163(5):161-166.

26. Stephens CD, Mackin N, Sims-Williams JH. The development and validation of an orthodontic expert system. *Br J Orthod* 1996;23(1):1-9. doi:10.1179/bjo.23.1.1

27. Takada K, Yagi M, Horiguchi E. Computational Formulation of Orthodontic Tooth-Extraction Decisions: Part I: To Extract or Not To Extract. *Angle Orthod* 2009;79(5):885-891. doi:10.2319/081908-436.1

28. Chidambaram M, Yang Y, Cer D, Yuan S, Sung Y-H, Strope B, et al. Learning Cross-Lingual Sentence Representations via a Multi-task Dual-Encoder Model. Preprint at https://arxiv.org/abs/1810.12836 (2018).

29. Kudo T, Yamamoto K, Matsumoto Y. Applying conditional random fields to Japanese morphological analysis. In: *Proceedings of the 2004 Conference on Empirical Methods in Natural Language Processing*. 2004:230-237.

30. Chainer. https://chainer.org/

31. Tokui S, Oono K, Hido S, Clayton J. Chainer: a next-generation open source framework for deep learning. In: *Proceedings of workshop on machine learning systems (LearningSys) in the twenty-ninth annual conference on neural information processing systems (NIPS)*. 2015:5:1-6.

32. Joachims T. Training linear SVMs in linear time. In: *Proceedings of the 12th ACM SIGKDD International Conference on Knowledge Discovery and Data Mining*. 2006:217-226.